Arthur Constantino Scardua

Particle Production in a Bouncing Universe

Brasil

July 2018

Arthur Constantino Scardua

Particle Production in a Bouncing Universe

Thesis for PhD title in Centro Brasileiro de Pesquisas Físicas

Centro Brasileiro de Pesquisas Físicas – CBPF

Coodenação de Astrofísica, Cosmologia e Interações Fundamentais – ICRA

Programa de Pós-Graduação

Supervisor: Nelson Pinto Neto

Brasil

July 2018

Arthur Constantino Scardua
Particle Production in a Bouncing Universe/ Arthur Constantino Scardua. – Brasil, July 2018-
83 p. : il. (algumas color.) ; 30 cm.

Supervisor: Nelson Pinto Neto

Thesis – Centro Brasileiro de Pesquisas Físicas – CBPF
Coodenação de Astrofísica, Cosmologia e Interações Fundamentais – ICRA
Programa de Pós-Graduação, July 2018.

1. Ricochete. 2. Grativy Quantization. 3. Gravitational Waves. 4. Fermions Production I. Nelson Pinto Neto. II. Centro Brasileiro de Pesquisas Físicas. III. Coordenação de Astrofísica, Relavidade e Interações Fundamentais. IV. Particle Production in Bounce Models

Dedico este trabalho aos meus pais, Ediza e Francisco.

Acknowledgements

Estes últimos quatro anos foram difíceis. O doutorado era um prazer de fazer o que eu gosto e um punhado de frustrações. Termino com saudade desses anos que foram.

Nelson é o culpado de muitas das frustrações, e também o responsável por todo o prazer. Às vezes os resultados não são os esperados, mas isso é a ciência.

Os professores Gazeau e Hervé foram responsáveis pela construção de parte deste trabalho. Eu os agradeço.

O resultado desta tese se deve ao suporte de uma multidão de pessoas. Entre elas os meus amigos do CBPF, da UFES, do Guanabara, do Night Ride, da Massa Crítica, do Bike Anjo e de Vitória.

Em especial, algumas pessoas marcaram esse doutorado a qual devo nomear: Adriano Soares, Amanda Borges, Amanda Lima, Amanda Nicotina, Ana Carolina, Arthur Figueiredo, Ayra Poeys, Azucena Towanda, Bernardo Guarisco, Bianca Cecato, Brian Connolly, Brianna Irish, Bruna Cabaleiro, Caio Costa, Camila Bedeschi, Carla Almeida, Carlos Montaña, Carol Massami, Carol Matias, Carolina Cecato, Carolina Cerqueira, Carolina Estevam, Carolina Martins, Caroline Sofiatti, Clayton Vaneli, Clécio De Bom, Cristofher Zuñiga, Daniel Gafanhoto, Daniel Gomes, Daniel Passy, Daniel Reis, Daniel Wagne, Daniela Leite, Danilo Froes, Davi Torobay, David Guarniery, David Marques, Denis Rodrigues, Denise Coutinho, Diego, Diego Noguera, Diego Oliver, Diogo Souza, Eddy, Edgar Ribeiro, Eduardo Bittencourt, Eduardo Tenório, Eduardo Valadão, Elisa Linhales, Elisabete Cecato, Elizabeth Corado, Elmo Brandão, Erick, Estefani Marchiori,Érico Goulart,Érico Novais, Fabrício Borghi, Fausto Júnior, Felipe Aleixo, Felipe Cypriano, Felipe Farjado, Felipe Gonçalves, Felipe Graça, Felipe Lelis, Felipe Monteiro, Felipe Pinheiro, Felipe Santos, Filippe Santos, Flaviano Santos, Florencia Anabella, Frederico Pêgo, Fábio Lucio, Gabriel Freitas, Gabriel Maia, Gabriela, Gabriela Aguiar, Gabrielle Augusto, Gibran Souza, Giuseppe Betini, Grasi Batista, Grecia Gómez, Gregório Rabelo, Guilherme Bremm, Gustavo Dias, Gustavo Vicente, Habib Montoya, Harun Karimpur, Henrique Versilo, Hérisson (Ford), Ian Linhales Cypriano, Ighor Melo, Igor Acácio, Igor Justo, Ingrid Costa, Isaac Torres, Ivan Eugênio da Cunha, Ivan Franklin, Ivana Cavalcanti, Jade Rubi, Jefferson Morais, John Fidélis, Jonatas Nimer, Jonathan Pereira, Josiê Pereira, José Tavares, João Nilo, João Ribeiro, Julia Rafalski, Junior Fonseca, Jão Dabike, Júnior Toniato, Karla Barbosa, Leandro Grisoni, Leonardo Ospedal, Leonardo Vilhagra, Lilian Fabiano, Lilian Grozinger, Liliane Malta, Lorrayne, Lucas Abbud, Lucas Cypriano, Lucas Penteado, Lucas Romano, Luciana Ribeiro, Lucianno Augusto, Luis Armando, Luis Kopp, Luiz Felipe, Luiz Longo, Luiz Quilherme, Marc Casals, Marcel Santos, Marcelo Bertoli, Marcelo Giovani,

Marcelo de Castro, Marcos Alves, Mariana Franzini, Martín Makler, Mauricio Ribeiro, Meigga Juliane, Miguel Peñafiel, Muryel Peres, Mônica Ramalho, Naldinho Tranquilo, Naone Wagner, Nathára Gonzaga, Nicolas Folliet, Nikolai Neves, Nilo, Norton Tavares, Nádia Nogueira, Patrícia Apicelo, Pedro Legey, Philipe Mota, Priscila França, Rayane Sorrentino, Reinaldo Gonçalves, Rhuam Sousa, Ricardo Cappellano, Ricardo Jose, Ricardo Martins, Roberta Dutra, Roberto Dayrell, Rodrigo Lugon, Rodrigo Martins, Rodrigo Turcati, Ruan Couto, Sofiane Faci, Stênio Fafa, Tati Carvalho, Tays, Tays Miranda, Thiago Caramês, Thiago Duro, Thiago Gonçalves, Thiago Moura, Thieberson Gomes, Thássila Deorce, Ubaldo Rodriguez, Vinicius Terra, Vitor Santamini, Vânia Vasconcelos, Wendel Paz, Yuri Plumm.

Agradeço também minha tia Fabiola que me deu muitos conselhos por todo o doutorado e que seu amor foi crucial para estar onde estou.

Tenho muito a agradecer meus amigos e companheiros de sofrimento Gabriel Gantos, Pedro Correia e Jacó Júlio por todo o conhecimento das peculiaridades do ser humano.

Sem Gabriela Devens, José Meira, Katrine Fontes, Nathalia Medeiros, Phercyles Veiga, Eduardo Carvalho, e Eduardo Tenório não teria sobrevivido esses quatro anos. Estavam presentes no meu melhor e no meu pior, e nunca me abandonaram.

Laís Lavra. Pollyana Bruna. Muito obrigado, mesmo. Para xuxu. Muito muito muito mesmo.

Fernanda Poeys, pegou a parte mais pesada, e deu conta.

O final agradecimento vai à Patota feliz de futuras mechas coloridas, que, junto com meus pais, foram os responsáveis por todo meu suporte emocional, físico, intelectual, de planejamento, enfim, de vida. Esse grupo firme, forte de pessoas tão diferentes e tão iguais pertencem as almas mais fodas e ímpares desse Universo que é minha vida: Josephine Rua, Anna Paula Bacalhau, Ana Bárbara Cavalcanti, Cláudia Buss, Cinthya Blois, Maria Elidaiana, Vanessa Pacheco e Jaime Oliveira.

"The cord that tethers ability to success is both loose and elastic. It is easy to see fine qualities in successful books or to see unpublished manuscripts, inexpensive vodkas, or people struggling in any field as somehow lacking. It is easy to believe that ideas that worked were good ideas, that plans that succeeded were well designed, and that ideas and plans that did not were ill conceived. And it is easy to make heroes out of the most successful and to glance with disdain at the least. But ability does not guarantee achievement, nor is achievement proportional to ability. And so it is important to always keep in mind the other term in the equation—the role of chance... What I've learned, above all, is to keep marching forward because the best news is that since chance does play a role, one important factor in success is under our control: the number of at bats, the number of chances taken, the number of opportunities seized."

(The Drunkard's Walk: How Randomness Rules Our Lives, Leonard Mlodinow)

"Inexprimível teto de tênebras; alta obscuridade sem mergulhador possível; luz mesclada à obscuridade, mas uma luz vencida e sombria; claridade reduzida a pó; é semente? É cinza? Milhões de fachos, claridade nula; vasta ignição que não diz o seu segredo, uma difusão de fogo em poeira que parece um bando de faíscas paradas, a desordem do turbilhão e a imobilidade do sepulcro, o problema oferecendo uma abertura de precipício, o enigma desvendando e escondendo a sua face, o infinito mascarado com a escuridão, eis a noite. Pesa no homem esta superposição."

(Os Trabalhadores do Mar, Victor Hugo)

Abstract

This thesis develops the theory of creation of gravitons and fermions for a bounce model whose initial singularity is avoided by quantum phenomena that are interpreted by de Broglie-Bohm theory. Gravitons correspond to primordial gravitational waves and are generated by quantum tensor fluctuations before the bounce. The creation of fermions occurs by the minimum coupling of a fermionic field. In both cases, particle production is small compared to other forms of production.

Palavras-chaves: bounce; particle creation.

Resumo

Esta tese desenvolve a teoria de criação de gravitons e fermions para um modelo de ricochete cuja singularidade inicial é evitada por fenômenos quânticos que são interpretados pela teoria de deBroglie-Bohm. Os gravitons correspondem às ondas gravitacionais primordiais e são geradas por flutuações tensoriais quânticas antes do ricochete. A criação de fermions acontece pelo acoplamento mínimo de um campo fermiônico. Em ambos os casos, a produção de partículas é pequena se comparada a outras formas de produção.

Key-words: Ricochete, criação de partículas.

Contents

Introduction

This thesis develops the theory of creation of gravitons and fermions for a bounce model whose initial singularity is avoided by quantum phenomena that are interpreted by the theory of de Broglie-Bohm [1]. It is part of a set of works which develop the bounce scenario with de Broglie-Bohm which includes the cosmological perturbations [2], evolution analysis [3] and creation of scalar particles [4]. Physics has a standard model of cosmology that has been extensively tested ranging from the formation of the first astrophysical structures to the formation of the first atomic nuclei. Thereafter, there are no experiments that undoubtedly determine which theory should best explain the physics of the first milliseconds after the bounce (or initial singularity). There are numerous theories devoted to what happens before these first milliseconds. Among these theories exist the non-singular quantum ones that have a bounce, so that the scale factor of the Universe is never zero.

In this work, two quantum theories will be presented to avoid the initial singularity: the canonical quantization with the interpretation of de Broglie-Bohm and the Affine Covariant Integral quantization. Affine Covariant Integral quantization associates the quantities of classical phase space with coherent quantum states that have the desired characteristics of the object to be quantized. In this case, quantities that are always positive and never zero, such as the scale factor. By its construction and by being an integral quantization, it constructs self-adjoint and ordered operators from classical quantities, as expected from quantum observables [5]. However, these operators are not unique and depend on the form of construction of coherent states, whose physical interpretation is not yet clear [6]. For this reason, this quantization is developed at the end of Chapter 2 for simple examples, and was not used for particle creation.

Canonical quantization associates quantities of phase space with quantum Hilbert space operators and classical Poisson brackets with quantum commutators (or anti-commutators). This quantization does not generate self-adjoint operators for the scale factor and has ambiguity in the ordering of certain quantized operators, being necessary to choose an ordering and a self-adjoint extension. Result on this topic were published in reference [6]. The classical canonical theory of Hamiltonian formalism and Poisson brackets applied to cosmology with tensor perturbations are presented in Chapter 2. Quantum canonical theory is developed at the beginning of Chapter 2, and will serve as the basis for the particle creation chapters. In Chapter 3, the theory of primordial gravitational waves, generated from a quantum vacuum of tensor perturbations in the context of a bouncing Universe, will be developed. It is an extension of previous works [7] that seeks to detect the main characteristics of these waves and applies in the case of a bounce dominated by

a matter whose sound velocity of the perturbations is close to that of light. Results are published in reference [8].

In Chapter 4, the theory of the creation of fermionic particles for de Broglie-Bohm bounce is developed. The Hamiltonian theory is revisited for the case of spinors, and a numerical prediction is obtained. Unfortunately, the production of primordial gravitational waves due to quantum perturbations and fermionic particles by the minimum coupling are very low. The modeled waves would hardly be detected, having a density far below any current detector. And the production of fermions is much less than expected, requiring another mechanism (or coupling) to generate fermions.

Notation

The follow notation will be used throughout this Thesis.

All greek indices go from 0 to 3, where the 0 coordinate represent the time. Latin indices go from 1 to 3 and represent the spatial coordinates. Capital latin indices between parenthesis are tetrad indices[1], and goes from 0 to 3.

Each four-vector $\mathbf{A}$ can be expressed in the basis $\{\partial_\mu\}$ as $A^\mu\partial_\mu$, where A^μ are their coeficients. In the same way, each one-form $\vec{\mathbf{B}}$ can be expressed in the basis $\{\mathrm{d}x_\mu\}$ as $B_\mu\,\mathrm{d}x^\mu$, where B_μ are their coeficients. For this thesis, A^μ and B_μ will be called vectors and represents a four-vector and a one-form. These basis are dual to each other:

$$(\partial_\mu)^\alpha(\mathrm{d}x^\nu)_\alpha = \delta^\nu_\mu. \tag{1}$$

This thesis uses Einstein summation notation, which equal indices are summed. For instance

$$A_\mu B^\mu = \sum_{\mu=0}^{3} A_\mu B^\mu$$
$$A_i B^i = \sum_{\mu=1}^{3} A_\mu B^\mu.$$

The space-time is a four dimension manifold, with a metric $g_{\mu\nu}$ with signature $(+---)$, and a metric connection

$$\Gamma^\mu_{\nu\alpha} = \frac{g^{\mu\sigma}}{2}(g_{\sigma\nu,\mu} + g_{\sigma\mu,\nu} - g_{\mu\nu,\sigma}), \tag{2}$$

whereby the covariant derivative space-time ∇_μ is defined over a tensor $T^{a_1\ldots a_n}{}_{b_1\ldots b_2}$

$$\begin{aligned}\nabla_\mu T^{a_1\ldots a_n}{}_{b_1\ldots b_2} = {} & \partial_\mu T^{a_1\ldots a_n}{}_{b_1\ldots b_2} + \Gamma^{a_1}_{\lambda\mu} T^{\lambda\ldots a_n}{}_{b_1\ldots b_2} + \ldots + \\ & + \Gamma^{a_1}_{\lambda\mu} T^{a_1\ldots\lambda}{}_{b_1\ldots b_2} - \Gamma^{\lambda}_{b_1\mu} T^{a_1\ldots a_n}{}_{\lambda\ldots b_2} + \\ & - \ldots - \Gamma^{\lambda}_{b_1\mu} T^{a_1\ldots a_n}{}_{b_1\ldots\lambda}\,.\end{aligned} \tag{3}$$

If v^μ is a four-vector and g the metric determinant, then

$$\sqrt{-g}\nabla_\mu v^\mu = \partial_\mu\left(\sqrt{-g}v^\mu\right) \tag{4}$$

is a total divergence.

[1] See Chapter 4

Due to the metric signature, vectors can be separated in respect to its norm. If a vector v^μ is such that

$$v^\mu v^\nu g_{\mu\nu} = v^\mu v_\mu > 0, \quad \text{it is a time-like vector} \tag{5a}$$

$$v^\mu v^\nu g_{\mu\nu} = v^\mu v_\mu < 0, \quad \text{it is a space-like vector} \tag{5b}$$

$$v^\mu v^\nu g_{\mu\nu} = v^\mu v_\mu = 0, \quad \text{it is a null vector.} \tag{5c}$$

1 Hamiltonian Approach

In this chapter, the Space-time separation and the Hamiltonian approach be presented.

"Caio, logo existo."
(Nelson Pinto-Neto)

The Hamiltonian approach is not covariant. It needs a separation of space-time manifold in constant time spatial sections, a foliation, in which a Hamiltonian is responsible for the translation from one spatial hypersurfaces. Not all manifolds can be globally separated in space and time. For instance, the Gödel Universe [9], which allow closed time-like curves, does not allow such foliation [10].

In the follow section (1.1), the space-time action will be separated in space and time. First the space-time will be separated in spatial equal time hypersurfaces, then the configuration space will be constructed with elements that belong to this hypersurface.

1.1 Space and time separation

For a manifold like the Freedmann-Robertson-Lemaître-Walker (FRLW) Universe [11], it is possible to define a continuous function $\tau(x)$ with a non-vanishing continuous time-like gradient[1] $d\tau(x)$. The space-time function $\tau(x)$ defines a set of constant-time non-overlapping space-like hypersurfaces given by $\tau(x) = t$, where t is a constant. The union of all constant-time hypersurfices is igual to the all 4-dimensional space-time. The gradient $d\tau(x)$ is perpendicular to the hypersurfaces. The separation of the space-time in such hypersurfaces is called foliation. If v^μ is a vector tangent to a curve in the hypersurface generated by the foliation τ, then the variation of τ in the tangent v^μ direction is given by

$$v^\mu \partial_\mu \tau = v^\mu \, \mathrm{d}\tau_\mu = 0, \tag{1.1}$$

for all vectors tangent to any curves in the spatial hypersurface. So the metric $g_{\mu\nu}$ can be separated in a spatial hypersurface part, and a τ-like part as

$$g_{\mu\nu} = \gamma_{\mu\nu} + N^2 \, \mathrm{d}\tau_\mu \, \mathrm{d}\tau_\nu = \gamma_{\mu\nu} + n_\mu n_\nu, \tag{1.2}$$

where $\gamma_{\mu\nu}$ is the metric of the hypersurface, $N^2 = (g^{\mu\nu} \, \mathrm{d}\tau_\mu \, \mathrm{d}\tau_\nu)^{-1}$ and $n^\mu = N \, \mathrm{d}\tau^\mu$ is a normalized time-like vector.

The hypersurface has independent geometric properties. It has its own metric, covariant derivative and curvature tensor. The covariant derivative in the hypersurface that acts over hypersurface vectors v^α is

$$D_\mu v^\alpha = \gamma^{\nu\mu} \nabla_\nu v^\alpha. \tag{1.3}$$

The curvature tensor is defined as

$$D_{[\mu} D_{\nu]} v^\alpha = {}^3R^\alpha{}_{\lambda\mu\nu} v^\lambda. \tag{1.4}$$

In order to define how hypersurfaces are embeded in the space-time, it is important to track the variation of their normal vector $\mathrm{d}\tau^\mu$ throughout themselves. It is done by the

[1] Such manifolds are known as globally-hyperbolic manifolds.

extrinsic curvature tensor

$$\mathrm{K}_{\mu}{}^{\nu} = -\gamma^{\alpha}{}_{\mu}\nabla_{\alpha}n^{\nu} = \mathrm{K}^{\nu}{}_{\mu} = \gamma_{\mu}{}^{\sigma}\gamma^{\nu}{}_{\lambda}\mathrm{K}_{\sigma}{}^{\lambda}, \tag{1.5}$$

which is a symmetric tensor that belongs to the spatial hypersurface.

Let $\{\partial_i\}$ be a orthonormal basis of the hypersurface. It means that

$$\begin{aligned} \mathrm{d}\tau_{\mu}\,(\partial_i)^{\mu} &= \mathrm{d}\tau_i = 0 \\ (\partial_i)^{\mu}(\partial_i)^{\nu}g_{\mu\nu} &= -1. \end{aligned} \tag{1.6}$$

Along with ∂_τ, the set $\{\partial_\tau, \partial_i\}$ forms a vector basis for the space-time tangent vector space. Also, the time basis $\partial_0 = \partial_\tau$ is chosen to be dual to the τ gradient[2]

$$\begin{aligned} (\partial_0)^{\mu}\,\mathrm{d}\tau_{\mu} &= 1 \\ (\partial_0)^{\mu} &= N^2 g^{\mu\nu}\,\mathrm{d}\tau_{\nu} + \beta^i, \end{aligned} \tag{1.7}$$

where β^i is the coordenade shift, a hypersurface vector.

The $\mathrm{d}\tau^{\mu}$ and $(\partial_\tau)^{\mu}$ vectors are fundamentally different. The first points to the direction where the time increases more rapidly, while the second points to the direction where the time increases and the other coordinates are constant. Hence, while the vector $\mathrm{d}\tau^{\mu}$ is perpendicular to the hypersurfaces, the vector $(\partial_\tau)^{\mu}$ is not.

The velocities of the configuration space are given by the variation of a variable along a curve of increasing time with constant spatial positions. It means that the velocity of the variable A is given by its Lie derivative along $(\partial_\tau)^{\mu}$

$$\dot{A} = \mathrm{L}_{(\partial_\tau)}A. \tag{1.8}$$

In the basis $\{\partial_\mu\}$, the metric is written as

$$g_{\mu\nu} = g_{\alpha\beta}(\partial_\mu)^{\alpha}(\partial_\nu)^{\beta} \doteq \begin{pmatrix} N^2 + \beta^k\beta_k & \beta_j \\ \beta_i & \gamma_{ij} \end{pmatrix} \tag{1.9a}$$

$$g^{\mu\nu} = (g_{\mu\nu})^{-1} \doteq \begin{pmatrix} N^{-2} & -\frac{\beta^j}{N^2} \\ -\frac{\beta^i}{N^2} & \gamma^{ij} + \frac{\beta^j\beta^i}{N^2} \end{pmatrix} \tag{1.9b}$$

$$\sqrt{-g} = N\sqrt{\gamma}, \tag{1.9c}$$

where the inverse is obtained by the Banachiewicz identity for block matrices, and the determinant can be obtained by the Schur formula [13].

Using the basis $\{\partial_\mu\}$, all spatial quantities will be expressed only with latim indices, representing its lack of the 0th coordenate. It includes the spatial metric γ_{ij}, the extrinsic

[2] For FRLW Universe, but not for all metrics, like Kerr black-hole metric [12], it is possible to choose a basis in which $\beta^i = 0$.

curvature k_{ij} and the shift β_i. In this basis, the velocity of any tensor $T^{\mu_1\cdots\mu_n}{}_{\nu_1\ldots\nu_2}$ is its coeficient partial derivative

$$\dot{T}^{\mu_1\cdots\mu_n}{}_{\nu_1\ldots\nu_2} = \mathrm{L}_{(\partial_\tau)}T^{\mu_1\cdots\mu_n}{}_{\nu_1\ldots\nu_2} = (\partial_\tau)^\alpha\partial_\alpha(T^{\mu_1\cdots\mu_n}{}_{\nu_1\ldots\nu_2}) = \partial_\tau T^{\mu_1\cdots\mu_n}{}_{\nu_1\ldots\nu_2}\,. \tag{1.10}$$

The quantities N, β^i and γ^{ij} with theirs velocities forms configuration space variables. An action written with these quantities is

$$\mathcal{A} = \int_{t_0}^{t}\int_{\Omega_t}\mathcal{L}_g\,\mathrm{d}^3x\,\mathrm{d}t\,, \tag{1.11}$$

where Ω_t is an equal time hypersurface and $\mathcal{L}_g$ is the Lagrangian density, given by

$$\mathcal{L}_g = -\frac{\sqrt{-\gamma}}{6\ell_p}N\Big[{}^3R + \mathrm{K}_{ij}\mathrm{K}^{ij} - \mathrm{K}^2\Big], \tag{1.12}$$

where where $\ell_p = (8\pi\mathrm{G}_N/3)^{1/2}$ is the Planck length ($\hbar = c = 1$), $\mathrm{K} = \mathrm{K}_{ij}\gamma^{ij}$ and

$$\mathrm{K}_{ij} = \frac{1}{2N}\Big[D_{(i}\beta_{j)} - \dot{\gamma}_{ij}\Big]. \tag{1.13}$$

The equation (1.12) is the Lagrangian written in terms of the configuration space variables. However, only the variable γ_{ij} represents true degrees of freedom that will evolve in time. The other variables, N and β^i, will correspond to Lagrange multipliers over the hypersurface. It means that there is no one-to-one correspondence between the velocities and momentum, and constraints will appear in the Hamiltonian.

1.2 The constrained Hamiltonian

The Hamiltonian method is a Legendre transformation that takes the 6 second order differential equations that comes from the extremization of the Lagrangian (1.12) into 12 first order linear equations. It relies in a one-to-one transformation between the velocities and its dependence in the Lagrangian. The function in (1.12) depends only in the spatial metric velocity. Hence, the momenta conjugate to N and β^i are null. These are the conservation in time of constraint equations. The Hamiltonian adds news constraints to support these variables. Therefore, the Hamiltonian density will be

$$\mathcal{H} = \Pi^{ij}\dot{\gamma}_{ij} - \mathcal{L}_g + \lambda^i P_{\beta_i} + \lambda P_N, \tag{1.14}$$

where Π^{ij} is the spatial metric momentum and the last two terms are constraints. The momenta P_{β_i} and P_N are such that $\big(\dot{P}_\beta\big)_i = \dot{P}_N = 0$.

From equation (1.12) and (1.13) we get

$$\Pi^{ij} = \frac{\sqrt{-\gamma}}{6\ell_p}\big(\mathrm{K}^{ij} - \mathrm{K}\gamma^{ij}\big). \tag{1.15}$$

From (1.14), the Hamiltonian density has the form

$$\mathcal{H} = N\mathcal{H}_0 + 2\beta^i\mathcal{H}_i + \lambda^i P_{\beta_i} + \lambda P_N, \tag{1.16}$$

where

$$\mathcal{H}_0 = \frac{\sqrt{-\gamma}}{6\ell_p}\Big({}^3R + \mathrm{K}^2 - \mathrm{K}_{ij}\mathrm{K}^{ij}\Big) = \frac{\sqrt{-\gamma}}{6\ell_p}{}^3R - \frac{6\ell_p}{\gamma}\Big(\frac{1}{2}\gamma_{lp}\gamma_{jk} - \gamma_{lj}\gamma_{pk}\Big)\Pi^{lp}\Pi^{jk} \tag{1.17a}$$

$$\mathcal{H}_i = \frac{1}{6\ell_p}\Big(D_j\mathrm{K}^j{}_i - D_i\mathrm{K}\Big) = \frac{1}{\sqrt{-\gamma}}D_b\Pi_i{}^b. \tag{1.17b}$$

The Hamiltonian is

$$H = \int_{\Omega_t}\mathcal{H}\,\mathrm{d}^3x\,. \tag{1.18}$$

All the dynamic relations can be derived from the Hamiltonian density from the equal time Poisson bracket defined as

$$\frac{\delta f(x)}{\delta f(x')} = \delta(x-x') = \delta(x_1-x_1')\delta(x_2-x_2')\delta(x_3-x_3')$$

$$\begin{aligned}\{A(x),B(x')\} = \int_{\Omega_t}\mathrm{d}^3x''\Bigg(&\frac{\delta A(x)}{\delta\gamma_{ij}(x'')}\frac{\delta B(x')}{\delta\Pi^{ij}(x'')} + \frac{\delta A(x)}{\delta N(x'')}\frac{\delta B(x')}{\delta P_N(x'')} + \\ &+\frac{\delta A(x)}{\delta\beta^i(x'')}\frac{\delta B(x')}{\delta P_{\beta_i}(x'')} - \frac{\delta B(x')}{\delta\gamma_{ij}(x'')}\frac{\delta A(x)}{\delta\Pi^{ij}(x'')} - \frac{\delta B(x')}{\delta N(x'')}\frac{\delta A(x)}{\delta P_N(x'')} + \\ &-\frac{\delta B(x')}{\delta\beta^i(x'')}\frac{\delta A(x)}{\delta P_{\beta_i}(x'')}\Bigg)\end{aligned}$$

Then we get

$$\Big\{\gamma_{ij}(x),\Pi^{kl}(x')\Big\} = \frac{\delta_i^k\delta_j^l + \delta_i^l\delta_j^k}{2}\delta(x-x') \tag{1.19a}$$

So, using the Poisson bracket

$$\{N(x),H\} = \dot{N}(x) = \int_{\Omega_t}\sqrt{-\gamma}\lambda\overbrace{\{N(x),P_N(x')\}}^{\delta^{(3)}(x-x')}\mathrm{d}^3x' = \lambda \tag{1.20a}$$

$$\Big\{\beta^i(x),H\Big\} = \dot{\beta}^i(x) = \int_{\Omega_t}\sqrt{-\gamma}\lambda^j\overbrace{\Big\{\beta^i(x),P_{\beta_j}(x')\Big\}}^{\delta_j^i\delta^{(3)}(x-x')}\mathrm{d}^3x' = \lambda^j \tag{1.20b}$$

$$\begin{aligned}\{\gamma_{ij}(x),H\} = \dot{\gamma}_{ij} &= \int_{\Omega_t}\sqrt{-\gamma}\Big[N\{\gamma_{ij},\mathcal{H}_0\} - 2\beta^k\{\gamma_{ij},\mathcal{H}_k\}\Big]\mathrm{d}^3x' = \\ &= -2N(x)\mathrm{K}_{ij}(x) + D_{(i}\beta_{j)}\end{aligned} \tag{1.20c}$$

$$\Big\{P_{\beta_i}(x),H\Big\} = \int_{\Omega_t}\sqrt{-\gamma}\mathcal{H}_k\overbrace{\Big\{P_{\beta_i},\beta^k\Big\}}^{-\delta^{(3)}(x-x')}\mathrm{d}^3x' = \mathcal{H}_i = \Big(\dot{P}_\beta\Big)_i \equiv 0 \tag{1.20d}$$

$$\{P_N(x),H\} = \int_{\Omega_t}\sqrt{-\gamma}\mathcal{H}_0\overbrace{\{P_N,N\}}^{-\delta^{(3)}(x-x')}\mathrm{d}^3x' = \mathcal{H}_0 = \dot{P}_N \equiv 0 \tag{1.20e}$$

$$\begin{aligned}&\Big\{\Pi^{ij}(x),H\Big\} = \int_{\Omega_t}\sqrt{-\gamma}\Big[N\Big\{\Pi^{ij},\mathcal{H}_0\Big\} + 2\beta^k\Big\{\Pi^{ij},\mathcal{H}_k\Big\}\Big]\mathrm{d}^3x = \dot{\Pi}^{ij} \\ &\Rightarrow (\mathrm{L}_{\partial_0} - \mathrm{L}_\beta)\mathrm{K}_{ij} = -D_iD_jN + N\Big({}^3R_{ij} + \mathrm{K}\mathrm{K}_{ij} - 2\mathrm{K}^l{}_i\mathrm{K}_{lj}\Big).\end{aligned} \tag{1.20f}$$

The equations (1.20a) and (1.20b) show that the evolution of N and β^i are arbitrary: they are Lagrange multipliers. Equation (1.20c) is the inverse transformation of the momentum. equations (1.20e) and (1.20d) are constraints, they do not contain dynamic. The last equation (1.20f) is the true dynamic equation. Equations (1.20) represent the evolution of all degrees of freedom in the space-time metric in vacuum.

1.2.1 The perfect fluid

In this section the perfect fluid representation [14, 15] formalism is developed. This formalism is a four dimensional extension of the potential velocities description of a perfect fluid [14]. A perfect fluid is a continuum which does not conduct heat nor has viscosity. It is a reliable approximation for the large scale content of the Universe like dark matter, baryons, radiation and relativistic particles [16]. It can be described by a normalized four vector field $u^\mu(x)$ which represents its space time flux. In the coordinate system that the fluid is at rest[3], $Nu^\mu = (\partial_\tau)^\mu = N^2\,\mathrm{d}\tau^\mu$, there is no preferred direction, if the Universe is homogeneous and isotropic.

Any time-like continuous four-vector field can be described by 5 dependent scalar potentials: α, β, Φ, S and h [17]. The first two, α and β are related to vorticity, and have no effect in the large scale Universe. The four-vector field can be described as

$$u^\mu = -\frac{g^{\mu\nu}\left(\Phi_{,\nu} + \theta S_{,\nu}\right)}{h}, \tag{1.21}$$

where S is the entropy and h is the enthalpy. The other quantities do not have direct interpretation [18].

The four velocity is normalized, from which the dependence between the scalar potentials can be extracted

$$\begin{aligned} u^\mu u_\mu &= -\frac{(\partial_\tau)^\mu\left(\Phi_{,\mu} + \theta S_{,\mu}\right)}{Nh} = -\frac{\left(\dot{\Phi} + \theta\dot{S}\right)}{Nh} = 1 \\ \Rightarrow h &= -\frac{\left(\dot{\Phi} + \theta\dot{S}\right)}{N}. \end{aligned} \tag{1.22}$$

The Universe can be modeled by non-interacting perfect fluids with constant sound velocity, that follow the state equation $p = \lambda\rho$, where p is the pressure of the fluid, ρ is its energy density, and λ is a constant. The first law of thermodynamics states that

$$\mathcal{T}dS = d\Pi + \rho d(1/\rho_0) = (1+\Pi)d\left[\ln(1+\Pi) - \lambda\ln(\rho_0)\right] \tag{1.23a}$$

$$\Rightarrow \mathcal{T} = 1 + \Pi \tag{1.23b}$$

$$\Rightarrow S = \ln\left(\frac{1+\Pi}{\rho_0^\lambda}\right)$$

$$\therefore p = \lambda\rho_0^{\lambda+1}\exp(s), \tag{1.23c}$$

[3] A particle at rest has no spatial shift in its velocity, i.e., $u^\mu g_{mi} = \beta_i = 0$.

where Π is the specific internal energy, $\mathcal{T}$ is the temperature and ρ_0 is the rest energy density. Using the definition of enthalpy

$$dp = \rho_0 dh - \rho_0 \tau dS \tag{1.24}$$

$$h = \frac{p+\rho}{\rho_0} \tag{1.25}$$

$$\Rightarrow \rho_0 = \left(\frac{he^{-s}}{1+\lambda}\right)^{\frac{1}{\lambda}}. \tag{1.26}$$

The action for the perfect fluid is

$$\mathcal{A}_M = \int p\sqrt{-g}d^4x \tag{1.27}$$

As in the case of the gravitational Hamiltonian, constraints appear. The map between the time variation of the velocity potentials and their momenta are not one-to-one. For instance, the momentum associated to θ, P_θ, is null. The constraints are obtained by the definition of the momenta

$$P_S = \theta P_\Phi \qquad \text{Constraint} \tag{1.28}$$

$$P_\theta = 0 \qquad \text{Constraint} \tag{1.29}$$

$$P_\Phi = \rho_0\sqrt{-\gamma} \tag{1.30}$$

$$\Rightarrow p = \lambda\left(\frac{P_\Phi}{\sqrt{-\gamma}}\right)^{\lambda+1}\exp(S) \tag{1.31}$$

For the quantized fluid it is interesting to use other canonical variables so that we have well determined the time. The transformation of variables

$$\left\{a, P_a, N, P_N, \dot{N}, S, \dot{S}, P_S, \dot{\theta}, \theta, P_\theta, \Phi, P_\Phi\right\} \to \left\{a, P_a, N, P_N, \dot{N}, \dot{S}, \dot{\theta}, \theta, P_\theta, P_T, T, \Phi_N, P_{\Phi_N}\right\} \quad ,$$

where

$$P_T = -\left(\frac{P_\Phi}{\sqrt{\zeta}}\right)^{\lambda+1}\exp(S)\sqrt{\zeta} \tag{1.32a}$$

$$T = P_S\exp(-S)\left(\frac{P_\Phi}{\sqrt{\zeta}}\right)^{-(\lambda+1)}\frac{1}{\sqrt{\zeta}} = -\frac{P_S}{P_T} \tag{1.32b}$$

$$\Phi_N = \Phi(\lambda+1)\frac{P_S}{P_\Phi} \tag{1.32c}$$

$$P_\theta = 0 \tag{1.32d}$$

$$TP_T + \theta P_{\Phi_N} = 0 \tag{1.32e}$$

$$P_{\Phi_N} = P_\Phi \quad , \tag{1.32f}$$

is a canonical transformation, since their Poisson bracket relations are canonical[4] [19].

The Legendre transformation generates the Hamiltonian

$$H_M = \int_{\Omega_t} N \frac{P_T}{a^{3(\lambda-1)}} \sqrt{-\gamma}\, \mathrm{d}^3x \tag{1.33}$$

where

$$\{T, H\} = \dot{T} = \frac{N}{a^{3\lambda}} \tag{1.34a}$$

where, from (1.34a), it is obtained the relation between the time variable τ and the fluid time T[5]

In this section, it was derived the Hamiltonian of a perfect fluid in a homogeneous Universe. In fact, the observable Universe is not homogeneous. The existence of galaxies corroborate the existence of inomogeneities in our Universe. At certain scales much larger than the size of galaxies [16], the inomogeneities are small enough to allow perturbative treatment of the Friedmann model. In the next section, the perturbed FRLW Universe will be derived.

1.2.2 The Full Hamiltonian

The perturbed FRLW metric is given by

$$\gamma_{ij} = a^2(\tau)(\zeta_{ij} + w_{ij}) \tag{1.35a}$$

$$\beta_i = 0, \tag{1.35b}$$

where w_{ij} is the tensor perturbations, and ζ_{ij} is a maximally symmetric metric for tridimensional space.

A maximally symmetric metric as ζ_{ij} has the Riemmann tensor like

$${}^{\zeta}R_{\mu\nu\alpha\beta} = \frac{{}^{\zeta}R}{6}(\zeta_{\mu\alpha}\zeta\nu\beta - \zeta_{\nu\alpha}\zeta_{\mu\beta}), \tag{1.36}$$

where ${}^{\zeta}R = 6C$ is its Ricci scalar, with a constant C.

[4] In fact, it is a canonical transformation

$$\{T, \Phi_N\} = (\lambda+1)\frac{T}{P_\Phi} - (\lambda+1)\frac{T}{P_\Phi} = 0$$
$$\{\Phi_N, P_T\} = \{T, P_{\Phi_N}\} = 0$$
$$\{\Phi_N(t,x'), P_T(t,x)\} = \{\Phi_N(t,x'), P_T(t,x)\} = \delta(x-x')$$

[5] The variable τ is the cosmic time t if $N = 1$, and is the conformal time if $N = a$.

The tensorial perturbation w_{ij} is a traceless tranverse spatial tensor, which indices are raised and lowered by the maximally symmetric metric ζ_{ij}

$$w_{ij}\zeta^{ij} = w^{i}_{\ i} = 0 \tag{1.37a}$$

$$w^{i}_{\ j|i} = 0 \qquad , \tag{1.37b}$$

where $O_{|i}$ is the covariant derivative with respect to ζ_{ij}.

The momentum canonically conjugate to the metric is

$$\Pi^{ij} = \frac{\partial \mathcal{L}_g}{\partial \dot{\gamma}_{ij}} = P_a \frac{\partial \dot{a}}{\partial \dot{\gamma}_{ij}} + P^{ab}\frac{\partial \dot{\omega}_{ab}}{\partial \dot{\gamma}_{ij}} \tag{1.38a}$$

$$P^{ab}\zeta_{ab} = 0 \tag{1.38b}$$

$$\dot{\gamma}_{ij} = 2\frac{\dot{a}}{a}\gamma_{ij} + a^2\omega_{ij} \tag{1.38c}$$

$$\Rightarrow \Pi^{ab} = \frac{P_a\zeta^{ij}}{6a} - \frac{P^{mn}w_{mn}}{3a^4}\zeta^{ij} + \frac{P^{ij}}{a^2}, \tag{1.38d}$$

where P_a is the scale factor momentum, and P^{ij}_w is the tensor perturbation momentum.

Using (1.38) in (1.17a) with (1.33), the full Hamiltonian in second order in tensor perturbation is

$$\begin{aligned} H = \int_{\Sigma_t} N \Bigg\{ \left(6C - Cw^{ab}w_{ab} - \frac{w^{ab//c}w_{ab//c}}{4}\right) a\frac{\sqrt{\zeta}}{6\ell_p} + \\ + \frac{6\ell_p}{\sqrt{\zeta}}\left[\frac{P_a^2}{24a}\left(1 - \frac{5w_{ab}w^{ab}}{12}\right) - \frac{P^{ij}_w w_{ij}P_a}{3a^2} - \frac{P^{ij}_w P_{(w)ij}}{a^3}\right] + \frac{P_T}{a^{3\omega}}\left(1 + \frac{\omega}{4}w_{ab}w^{ab}\right)\Bigg\}\mathrm{d}^3x + \\ + \int_{\Sigma_t}\left[\dot{N}P_N + \dot{\theta}P_\theta - \dot{S}\left(TP_T\left(1 + \frac{\omega}{4}w_{ab}w^{ab}\right) + \theta P_{\Phi_N}\right)\right]\mathrm{d}^3x \qquad . \end{aligned} \tag{1.39}$$

The Hamiltonian can be simplified by the canonical transformation [20]

$$\tilde{a} = ae^{-\frac{w_{ab}w^{ab}}{12}} \simeq a\left(1 - \frac{w_{ab}w^{ab}}{12}\right) \tag{1.40a}$$

$$\tilde{P}_a = P_a e^{\frac{w_{ab}w^{ab}}{12}} \simeq P_a\left(1 + \frac{w_{ab}w^{ab}}{12}\right) \tag{1.40b}$$

$$\tilde{w}_{ij} = w_{ij} \tag{1.40c}$$

$$\tilde{P}^{ij}_w = P^{ij}_w + \frac{aP_a w^{ij}}{6} = P^{ij}_w + \frac{\tilde{a}\tilde{P}_a\tilde{w}^{ij}}{6} \tag{1.40d}$$

which generates the Hamiltonian

$$\begin{aligned} H = \int_{\Sigma_t} N \Bigg\{ \left(6C - \frac{C}{2}w^{ab}w_{ab} - \frac{w^{ab//c}w_{ab//c}}{4}\right)\tilde{a}\frac{\sqrt{\zeta}}{6\ell_p} + \\ + \frac{6\ell_p}{\sqrt{\zeta}}\left[\frac{\tilde{P}_a^2}{24\tilde{a}} - \frac{\tilde{P}^{ij}_w\tilde{P}_{(w)ij}}{\tilde{a}^3}\right] - \frac{P_T}{\tilde{a}^{3\lambda}}\Bigg\}\mathrm{d}^3x + \text{Other variables}, \end{aligned}$$

where, for simplicity, there will be no longer used.

The equations of motions from the Hamiltonian (1.41) are

- for the scale factor

$$\{P_N, H\} = \dot{P}_N \equiv 0 = -\frac{6Ca\sqrt{\zeta}}{6\ell_p} - 6\ell_p \frac{P_a^2}{24\sqrt{\zeta}a} + \rho a^3\sqrt{\zeta} \tag{1.41a}$$

$$\{a, H\} = \dot{a} = 6\ell_p \frac{NP_a}{12a\sqrt{\zeta}} \tag{1.41b}$$

$$\{P_a, H\} = \dot{P}_a = -\frac{6C\sqrt{\zeta}N}{6\ell_p} + 6\ell_p \frac{P_a^2 N}{24a^2\sqrt{\zeta}} - 3pa^2\sqrt{\zeta}N, \tag{1.41c}$$

  which are the Friedmann equations [21]

$$\left(\frac{\dot{a}}{a}\right)^2 = \ell_p \rho N^2 - \frac{CN^2}{a^2} \tag{1.42a}$$

$$\frac{\ddot{a}}{a} - \frac{\dot{a}\dot{N}}{aN} = -\frac{\ell_p N^2(\rho + 3p)}{2} \tag{1.42b}$$

- for the fluid is the same as in (1.34)

- for the tensor perturbations

$$\{w_{ij}(x), H(t)\} = \dot{w}_{ij}(x) = -\frac{12\ell_p N}{\sqrt{\zeta}} \frac{P_{(w)ij}}{a^3} \tag{1.43a}$$

$$\Rightarrow \left\{\frac{12\ell_p N}{\sqrt{\zeta}} \frac{P_{(w)ij}}{a^3}, H\right\} = -\{\dot{w}_{ij}, H\} \frac{\sqrt{\zeta}}{6\ell_p} = -\ddot{w}_{ij} = -w_{ij}{}^{//c}{}_{//c} + 2Cw_{ij} + 2\mathcal{H}\dot{w}_{ij} \tag{1.43b}$$

$$\therefore \ddot{w}_{ij} - w_{ij}{}^{//c}{}_{//c} + 2Cw_{ij} + 2\mathcal{H}\dot{w}_{ij} = 0 \tag{1.43c}$$

The perturbation w_{ij} has only 2 degrees of freedom [6], which are the modes of polarization of the tensor perturbations. For better understanding how the modes evolve, they are divided into their Fourier modes.

$$w_{ij} = \frac{1}{(2\pi)^{3/2}} \sum_{\lambda=1}^{2} \int_{\bar{\Sigma}_t} \varepsilon_{ij}^{(\lambda)} w_k^{(\lambda)}(t) e^{-i\mathbf{k}\cdot\mathbf{x}} dV_k \tag{1.44}$$

The Fourier transform of the equation (1.43c) leads to the evolution of the gravitational wave modes

$$\ddot{\mu}_k + \left(k^2 + 2C - \frac{\ddot{a}}{a}\right)\mu_k = 0 \qquad , \tag{1.45}$$

where $\mu_k = w_k^{(\lambda)} a$ represents the amplitude of the modes of the tensor perturbations.

The equation (1.45) gives the evolution of the Fourier modes as a function of time. Direct gravitational wave detectors[7], measure the energy density of gravitational waves per

[6] The tensor w_{ij} has 9 indices and 7 equations: 3 because of the symmetry $w_{ij} - w_{ji} = 0$; 1 due to the null trace $w^i{}_i = 0$; 3 due to the null divergence$w^{|i}_{ij} = 0$.

[7] It is possible to detect gravitational waves indirectly, as done with CMB polarization measurements [22].

logarithm of frequency $\Omega_{OG}(f)$. It is defined by expanding the gravitational wave energy density[8]

$$\begin{aligned}\Omega_{OG}(\eta) = \frac{\rho_{OG}}{\rho_c} = \frac{\langle T^0{}_0 \rangle}{\rho_c} &= -\left\langle \frac{2}{\rho_c\sqrt{-g^{(0)}}}\frac{\partial \mathcal{L}^{(2)}}{\partial g_{00}^{(0)}} g_{00} \right\rangle \\ &= \frac{1}{12\ell_p^2}\left\langle \frac{1}{a^2} w^{ab'} w_{ab'} - \frac{1}{2} w^{ij,k} w_{ij,k} \right\rangle \end{aligned} \tag{1.46}$$

where $\rho_c = \left(\frac{\mathcal{H}_0}{\ell_p}\right)^2$ is the critical energy density, in Fourier modes

$$\begin{aligned}\Omega_{OG}(\eta) &= \frac{1}{\rho_c a^2}\sum_\lambda \int d(\ln k)\frac{k^3}{4\pi^2}\left[\left|\mu_k^{(\lambda)'}\right|^2 - 2\mathcal{H} Re\left\{\mu_k^{(\lambda)'}\mu_k^{(\lambda)}\right\} + \left(k^2+\mathcal{H}^2\right)\left(\left|\mu_k^{(\lambda)}\right|^2 + \left|\mu_k^{(\lambda)'}\right|^2\right)\right] \\ &= \int d(\ln k)\Omega_{OG}(k,\eta). \end{aligned} \tag{1.47}$$

where $\mu_k^{(\lambda)} = a w_k^{(\lambda)}$.

When the perturbations are inside the curvature scale $k \gg \mathcal{H}$, the energy density of gravitational waves has a simpler form

$$\Omega_{OG}(k,\eta) = \frac{k^5\left|\mu_k^{(\lambda)}\right|^2}{4\pi^2\rho_c a^2} \quad , \tag{1.48}$$

where in this approximation, $\mu(\eta) \propto e^{-ik\eta}$.

[8] The $< \cdot >$ means the spacial mean, in classical regime, and vacuum expected value in quantum regime [58].

2 Quantization methods

In this chapter, the canonical quantization and affine covariant quantization will be developed.

"[...] Starting with a classical system, one often wishes to formulate a quantum theory, which in an appropriate limit, would reduce back to the classical system of departure. In a more general setting, quantization is also understood as a correspondence between a classical and a quantum theory. In this context, one also talks about dequantization, which is a procedure by which one starts with a quantum theory and arrives back at its classical counterpart.[...] "

[23]

In 1922, Friedmann derived from General Relativity equations describing a homogeneous and isotropic Universe, filled with a perfect fluid, which just depend on a scalar time-dependent function: the scale factor $a(t)$ [24]. This proposal contrasted the static and unstable model of Einstein [25], and was a landmark of the dynamic of Universe models. Finding Friedman's equations independently, Lemaître published in 1927 in a French magazine of little impact [26, 27] what would be called afterwards the Hubble law. Two years later, in 1929, at the Mount Wilson Observatory in California, Hubble published the famous article *"A relation between distance and radial velocity among extra-galactic nebulae"* [28] where he proves the ideas suggested by Lemaître. Extending Friedman's model to the past, Tolman published in 1931 the first solution of the Universe with a bounce [29]: a periodic Universe, pointing out the difficulties of finding a fluid with reasonable energy condition which could produce the bounce. This energy condition would be latter named the zero energy condition.

In the following decades, the standard cosmological model was constructed successfully describing an ever expanding Universe. However, the model encountered some problems concerning its initial condition which can be listed as:

- **The problem of the horizon:** Until then there was no explanation for the causality of homogeneous regions of the Universe that in the past were not in causal contact. This problem raised in 1956 by Rindler in an article in which he organized the works of event and particle horizons [30].
- **The flatness problem:** This problem deals with the fact that the energy density of matter has a value very close to the critical density, in which the spacelike hypersurfaces of the Universe would be flat. The problem was proposed by Dicke in lectures he gave in 1969 that are available in the book *"Gravitation and the Universe: Jayne Lectures for 1969"* [31].
- **The initial singularity problem:** The standard model predicts a singularity in the past. It was inevitably that the scale factor go to zero $a(t) = 0$, limiting the validity of the general relativity equations at this point [32, 33].

In order to solve these problems, it was needed a theory of space-time or matter beyond the standard model.

Even though they were not the first to address the initial singularity problem [32], two groups published in 1979 bounce solutions with no singularity: On July 15, two Brazilian physicists proposed a minimal coupling between classical electromagnetism and gravity that produced the necessary effects for the bounce [34]. Four months earlier, on March 19, two Russian physicistsproposed a bounce caused by quantum effects of a scalar field with gravitational interaction [35]. On the other hand, a new paradigm emerged

some years later in other to address the other puzzles: inflation [36]. At that time, bounce solutions responded to the problem of initial singularity, while inflation solved the other problems, and even proposed a way to get the spectrum of initial perturbations [32], necessary to understand the initial conditions of the Universe.

Today it is known that bounce scenarios solve the singularity problem and the all other puzzles of the standard cosmological model, and it also supplies a mechanism to generate primordial cosmological perturbations from quantum vacuum fluctuations, with almost scale invariant spectrum [37, 38, 1], as in inflationary models [39], when the contracting phase is mainly dominated by a matter fluid (a fluid with equation of state $p = \lambda\rho$ with $\lambda \approx 0$)[40, 41]. Hence, they can also be viewed as alternatives to inflation, although they are not necessarily contradictory to it.

There are nowadays many mechanisms to generate the bounce, normally they involve new physics and/or new types of fields. There are also many open questions and issues to be investigated concerning these models [42, 33]. One of them is trough quantum effect, which we will review.

2.1 Canonical quantization and the Bohm interpretation of quantum mechanics

In the canonical quantization, the classical phase space variables are transformed in Hibert space operators. The Poisson brackets of these classical quantities are transformed into quantum commutators (or anti-commutators) of quantum quantities [43]

$$\{A, B\} \to \frac{1}{i\hbar}\left[\hat{A}, \hat{B}\right] \quad , \tag{2.1}$$

where $\hbar$ is the Plank constant divided by 2π. For now on, $\hbar = 1$.

This method is robust enough to handle rectangular coordinates of variables that belong to the entire real axis. However, for situations where you are in a curvilinear coordinate system or the variables are not the real line, this quantization needs more conditions, or it should be abandoned. The case of the scale factor is an example of situations where more information is needed. In a half-line, as the scaling factor, the Hamiltonian operator is not Hermitian[1], needing an extension [44]. One way to obtain this analytical extension is to use the method proposed in [45], presented in 2.2; another way is to impose boundary conditions on quantum states at the edge of the half-line [44]. This imposition limits Hilbert space to states in which the Hamiltonian operator is Hermitian.

The general relativity Hamiltonian in flat FRLW metric with tensorial perturbations filled with a perfect fluid is given by the equation (1.41). It can be quantizated by

[1] In this case, the canonical transformation takes the Hamiltonian into an operator that is not self-adjoint.

transforming the scale factor, fluid parameter, tensor perturbations and its canonical conjugate momentum into operators that satisfies anti-commutation rules in equation (2.1).

$$a \to \hat{a} \tag{2.2a}$$
$$T \to \hat{T} \tag{2.2b}$$
$$w_{ij} \to \hat{w}_{ij} \tag{2.2c}$$
$$P_a \to \hat{P}_a \doteq -i\frac{\partial}{\partial a} \tag{2.2d}$$
$$P_T \to \hat{P}_T \doteq -i\frac{\partial}{\partial T} \tag{2.2e}$$
$$P_w^{ij} \to \hat{P}_w^{ij} \doteq \frac{\delta}{\delta w_{ij}}. \tag{2.2f}$$

The Hamiltonian has a mixed momentum scale factor term in which different ordering are not equivalent. A covariant choice was taken by [46], where the Hamiltonian has the form

$$\begin{aligned}\hat{H} = \int_{\Sigma_t} \hat{N} \Bigg\{ \left(6C - \frac{C}{2}\hat{w}^{ab}\hat{w}_{ab} - \frac{\hat{w}^{ab//c}\hat{w}_{ab//c}}{4}\right)\hat{a}\frac{\sqrt{\zeta}}{6\ell_p} + \\ + \frac{6\ell_p}{\sqrt{\zeta}}\left[\frac{1}{24\hat{a}^{\frac{3\omega+1}{2}}}\hat{P}_a\hat{a}^{\frac{3\omega-1}{2}}\hat{P}_a - \frac{\hat{P}_w^{ij}\hat{P}_{(w)ij}}{\hat{a}^3}\right] - \frac{\hat{P}_T}{\hat{a}^{3\omega}}\Bigg\} \mathrm{d}^3x = 0.\end{aligned} \tag{2.3}$$

The Dirac quantization procedure implies that the wave function should be annihilated by $\hat{H}$

$$\begin{aligned}&\hat{H}\Psi = 0 \\ \Rightarrow\ & i\frac{\partial\Psi}{\partial T} = \left(a^{3\omega+1}\frac{C\sqrt{\zeta}}{12\ell_p}w^{ab}w_{ab} + a^{3\omega+1}\frac{\sqrt{\zeta}}{24\ell_p}w^{ab//c}w_{ab//c} - \frac{6\ell_p}{\sqrt{\zeta}a^{3(1-\omega)}}\frac{\delta^2}{\delta w^{ij}\delta w_{ij}}\right)\Psi + \\ &+ \left[-a^{3\omega+1}\frac{C\sqrt{\zeta}}{\ell_p} + \frac{\ell_p}{\sqrt{\zeta}4}\frac{\partial^2}{\partial\chi^2}\right]\Psi \equiv \hat{H}_T\Psi \qquad ,\end{aligned} \tag{2.4}$$

where $\chi = \frac{2}{3(1-\omega)}a^{\frac{3(1-\omega)}{2}}$.

The notion of time lost by the constraint (1.20e) is recovered by the T fluid parameter that generates the Hamiltonian $\hat{H}_T$. The new Hamiltonian $\hat{H}_T$ is defined on the Hilbert space endowed by the scalar product

$$(\psi,\phi) = \int_0^\infty\int_{\Omega_w}\psi^*\phi d\chi dw = \int_0^\infty\int_{\Omega_w} a^{\frac{1-3\omega}{2}}\psi^*\phi da dw \qquad , \tag{2.5}$$

where the domain $(0,\infty)$ of χ will imply in a necessary boundary condition to be satisfied by Ψ, so that $\hat{H}_T$ is self-adjoint.

The solution wave function of (2.4) can be separated into two parts $\Psi = \varphi\psi$: one referring to the background, $\varphi(\chi, T)$, and another concerning perturbations $\psi[\chi, T, w_{ij}]$.

Applying this separation to (2.4) we get

$$0 = \varphi\left(a^{3\omega+1}\frac{C\sqrt{\zeta}}{12\ell_p}w^{ab}w_{ab} + a^{3\omega+1}\frac{\sqrt{\zeta}}{24\ell_p}w^{ab//c}w_{ab//c} - \frac{6\ell_p}{\sqrt{\zeta}a^{3(1-\omega)}}\frac{\delta^2}{\delta w^{ij}\delta w_{ij}} - i\frac{\partial}{\partial T}\right)\psi + \\ +\psi\left[-a^{3\omega+1}\frac{C\sqrt{\zeta}}{\ell_p} + \frac{\ell_p}{\sqrt{\zeta}4}\frac{\partial^2}{\partial\chi^2} - i\frac{\partial}{\partial T}\right]\varphi + \frac{\ell_p}{4\sqrt{\zeta}}\left(2\frac{\partial\varphi}{\partial\chi}\frac{\partial\psi}{\partial\chi} + \varphi\frac{\partial^2\psi}{\partial\chi^2}\right) \quad , \tag{2.6}$$

To achieve the separation between background and perturbation, it suffices that $\psi[\chi, T, w_{ij}] = \psi_1[T, w_{ij}] + \psi[T, w_{ij}]\int\frac{d\xi}{\varphi^2(\xi)}$. Thus, the last term of (2.6) cancels, and each part of the total wave function must meet

$$i\frac{\partial\psi}{\partial T} = \left(a^{3\omega+1}\frac{C\sqrt{\zeta}}{12\ell_p}w^{ab}w_{ab} + a^{3\omega+1}\frac{\sqrt{\zeta}}{24\ell_p}w^{ab//c}w_{ab//c} - \frac{6\ell_p}{\sqrt{\zeta}a^{3(1-\omega)}}\frac{\delta^2}{\delta w^{ij}\delta w_{ij}}\right)\psi \tag{2.7a}$$

$$i\frac{\partial\varphi}{\partial T} = \frac{\ell_p}{\sqrt{\zeta}4}\frac{\partial^2\varphi}{\partial\chi^2} - a^{3\omega+1}\frac{C\sqrt{\zeta}}{\ell_p}\varphi \tag{2.7b}$$

For the case without spatial curvature $C = 0$[2], the Hamiltonian requirement for $\hat{H}_T$ to be self-adjoint implies that, if two wave functions $\phi(\xi, T)$ and $\sigma(\xi, T)$ belong to the solution set of (2.7b), they must be such that

$$\int_0^\infty \phi^*\frac{\partial^2\sigma}{\partial\chi^2}d\bar{\chi} = \int_0^\infty \sigma\frac{\partial^2\phi^*}{\partial\chi^2}d\bar{\chi}$$

$$\Rightarrow \left(\phi^*\frac{\partial\sigma}{\partial\chi} - \frac{\partial\phi^*}{\partial\chi}\sigma\right)\Big|_{\chi=\infty} = \left(\phi^*\frac{\partial\sigma}{\partial\chi} - \frac{\partial\phi^*}{\partial\chi}\sigma\right)\Big|_{\chi=0}$$

$$\therefore \frac{\partial\phi}{\partial\chi} = \alpha\phi \qquad \frac{\partial\sigma}{\partial\chi} = \alpha\sigma \quad , \tag{2.8}$$

where α is a parameter that will define the boundary conditions of the system, which will limit the solution space of (2.7b) [44].

Equation (2.7b) can be rewritten in the form

$$\frac{\partial\rho}{\partial T} + \frac{\partial j}{\partial a} = 0 \quad , \tag{2.9}$$

where ρ is the quantum density and j is the conserved quantum current, given by

$$\rho = a^{\frac{1-3\omega}{2}}|\psi|^2 \tag{2.10}$$

$$j = \frac{ia^{\frac{3\omega-1}{2}}}{4}\left(\psi^*\partial_a\psi - \psi\partial_a\psi^*\right) \tag{2.11}$$

The equation (2.7b) defines a quantum state for the Universe. In the Copenhagen interpretation, which is the standard one, this wave function defines the probability of a classical observer measuring an observable. For instance, the probability of a classical observer measuring a scale factor a of a quantum universe is $|\Psi(a,t)|^2$. However, there

[2] This means that $\zeta = 1$.

are no classical observers in a quantum Universe. Moreover, the probabilistic idea loses sense, since there is access only to only one realization of the Universe. To solve these two problems, this thesis work with the Bohm-DeBroglie interpretation, where the quantum state is given by a path in configuration space that does not depend on the existence of an observer.

2.1.1 Bohm-DeBroglie Interpretation

When the scale factor was very small, the Universe went through a quantum phase, where everything that exists belongs to the quantum world. In this period, there were no classical observers. This this is not compatible with one of the principles of Copehagen's interpretation of quantum mechanics, where physical reality is only attained by such observers [47]. The interpretation of quantum mechanics proposed by de Broglie and Bohm says that the trajectory of the quantum variables in configuration space does not depend on a classical world, and its probabilistic character comes from the ignorance of the initial position. This interpretation describes Bohmian trajectories, in which every quantum system evolves, and it is obtained when a measurement is made. This interpretation defines Bohmian trajectories for every quantum system, where the positions (or amplitudes of fields) have objective reality. The Bohmian trajectories are deterministic and given by the equation

$$\frac{dq_{tb}}{dt} = \left.\frac{j}{\rho}\right|_{q=q_{tb}} \quad . \tag{2.12}$$

The equation (2.12) is a supplementary equation of quantum mechanics that is in agreement with the other equations. It defines the Bohmian trajectories, which are on the left side of the equation, with the conserved current j and quantum density ρ.

With this quantization, it is possible to define a Bohmian trajectory of the quantum background, i.e., the scale factor, for the cases of particle creation and primordial gravitational waves [48, 49].

In the case of the scale factor presented in (2.10), the equation can be further simplified if one separates the wave function in its amplitude A and its phase S: $\psi(\chi, T) = Ae^{iS}$. In this case, the equation of the Bohmian trajectory can be written as

$$\frac{da_{tb}}{dT} = a^{3\omega-1} \left.\frac{\partial S}{\partial a}\right|_{a=a_{tb}} \quad . \tag{2.13}$$

The equation (2.13) can be solved given the phase of the pilot wave ψ. This wave is the solution of the equation (2.7b) given an initial condition[3]. The initial condition for the Bohmian trajectory, selects one of the possible trajectories.

[3] This initial condition measures the ignorance of the initial Bohmian trajectory.

A simple solution to the equation (2.7b) is the Gaussian[50]

$$A = \left[\frac{8T_b}{\pi(T^2+T_b^2)}\right]^{1/4} \exp\left[\frac{-4T_b a^{3(1-\omega)}}{9(T^2+T_b^2)(1-\omega)^2}\right] \tag{2.14a}$$

$$S = -\left[\frac{4Ta^{3(1-\omega)}}{9(T^2+T_b^2)(1-\omega)^2} + \frac{1}{2}\arctan\left(\frac{T_b}{T}\right) - \frac{\pi}{4}\right] \tag{2.14b}$$

which the solution for the Bohmian trajectory reads

$$a_{tb}(T) = a_b\left[1+\left(\frac{T}{t_b}\right)^2\right]^{\frac{1}{3(1-\omega)}} \tag{2.15}$$

Different S solutions results in different Bohmian trajectories.

The Friedmann equation in terms of the equation (2.15) is

$$H^2 = H_0^2\Omega_\omega \frac{1}{a^{3(\omega+1)}} - H_0^2\Omega_\omega a_b^{-3(\omega+1)}\left(\frac{ab}{a}\right)^6 = H_0^2\Omega_\omega \frac{1}{a^{3(\omega+1)}}\left[1-\left(\frac{a_b}{a}\right)^{3(1-\omega)}\right] \quad , \tag{2.16}$$

where

$$H_0\Omega_\omega = \frac{a_b^{3(1-\omega)}}{9(1-\omega)T_b^2} \tag{2.17}$$

With the Bohmian trajectories are the evolution of the eigen-values of the quantum quantities, in this interpretation. Thus, it is possible to replace the operator $\hat{a}$ by the time function $a(T)$.

2.2 Affine Covariant Integral quantization

Another the solution to the self-adjointness problem in the gravitational Hamiltonian (1.41) induced by the scale factor, is the half-line quantization using Affine Coherent States (ACS). If the operator $\hat{O}$ is self-adjoint, then for any states $|\psi\rangle$ and $|\phi\rangle$

$$\left\langle \psi \middle| \hat{O}\phi \right\rangle = \left\langle \hat{O}\psi \middle| \phi \right\rangle . \tag{2.18}$$

An observable quantity in quantum mechanics is described by self-adjoint operators. It includes the Hamiltonian (1.41).

This section is devoted to present the quantization basisd on ACS. It is an alternative to the canonical quantization presented in the previous subsection 2.1, and it will not be used in the particle creation chapters.

Affine Covariant Integral quantization uses the affine group of symmetries on the half-*plane* combining dilatation and translations which intertwines classical and quantum symmetries through an integral operation. The affine quantization associates coherent quantum states [45] of a overcomplete[4] basis which have the symmetry of a half-line with

[4] A basis of states $\{|\psi_i\rangle\}$ is overcomplete if it still a basis after one removes a states $|\psi_j\rangle$.

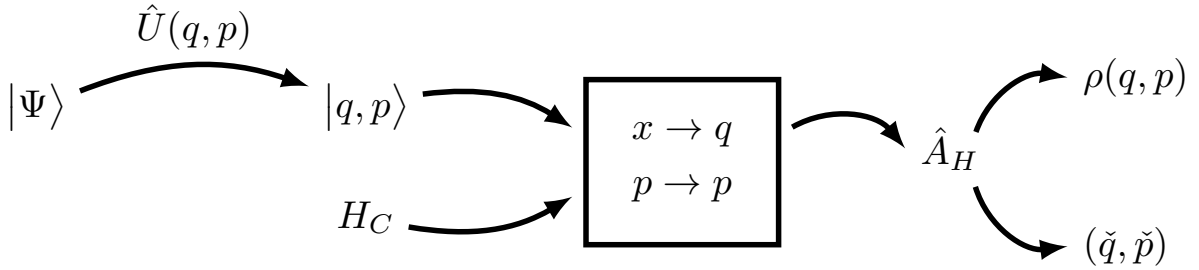

Figure 1 – Affine Covariant Integral quantization associates classical phase space variables with parameters of a overcomplete basis generated by a affine group. With the quantized operator, the semi-classical quantities are generate.

classical quantities, so that the quantum system naturally meets the constraints of a variable that belongs to the half-line, for example, the scale factor. The method is depicted in 1

- First, a overcomplete basis $|p,q\rangle$ is generated by the action of all elements of the two parameter representation of affine group $\hat{U}(p,q)$ in one state $|\Psi\rangle$, called fiducial vector.

$$|p,q\rangle = \hat{U}(p,q)\,|\Psi\rangle\,. \tag{2.19}$$

- Each classical observable $O(p,x)$ from the phase space is mapped in a quantum operator $\hat{A}_O$ in the Hibert space by the integral

$$\hat{A}_O = \int_{\Pi_+} |p,q\rangle\,\langle p,q|\,O(p,q)\frac{\mathrm{d}p\,\mathrm{d}q}{2\pi c_{-1}(\Psi)} \tag{2.20}$$

  where $c_{-1}(\Psi)$ is a function of the fiducial vector

$$c_{-1} = \int_0^\infty |\Psi|^2 \frac{\mathrm{d}x}{x}. \tag{2.21}$$

  The classical momentum p is associated with the translation part of the affine group p, and the classical position x is associated to the dilatation part of the affine group q.

- The evolution of a state $|\psi\rangle$ with the quantized Hamiltonian $\hat{A}_H$

$$-i\hbar\partial_t\,|\psi\rangle = \hat{A}_H\,|\psi\rangle \tag{2.22}$$

- The probability density in the semiclassical space $\rho(p,q,t)$ is constructed with the probability of finding the state $|\psi\rangle$ in the state $|p,q\rangle$

$$\rho(p,q,t) = \frac{|\langle p,q|\psi\rangle|^2}{2\pi c_{-1}} \tag{2.23}$$

- The lower symbol $\check{f}$ of a classical quantity f is the classical behavior from the quantum operator given by the trace of its quantized operator in the $|p,q\rangle$ basis

$$\check{f} = \int_{\Pi_+} \langle p,q|\, \hat{A}_f\, |p,q\rangle \, \frac{\mathrm{d}p\,\mathrm{d}q}{2\pi c_{-1}} \tag{2.24}$$

The examples presented in this chapter [6] correspond to the quantizations of a Hamiltonian in the form

$$H = p^2/2 + V(q) \qquad . \tag{2.25}$$

in the case of a gravitationally collapsing dustball ($V(q) \propto q^2$), an electrically charged sphere ($V(q) \propto -q$) and a simplistic model of Newtonian cosmology ($V(q) \propto 1/q$).

The coherent states are quantum states that form a basis X of linearly dependent quantum states $|x\rangle$ that belong to the space of Hibert that serve two properties:

- For every quantum state $|\psi\rangle$ belonging to the Hilbert space, there exists a representation $\psi(x) = \langle x|\psi\rangle$ in terms of the coherent state basis, where $\langle x|\psi\rangle$ is the scalar product between the states $|x\rangle$ and $|\psi\rangle$;

- The coherent states form a basis: $\int_X |x\rangle\langle x|\, \mathrm{d}\mu\,(x) = \mathbb{1}$, where $\mathbb{1}$ is the identity and $\mathrm{d}\mu\,(x) = g(x)\,\mathrm{d}x$ is a non-zero positive quantity, called measure.

2.2.1 The affine group and its unitary representation

The affine group is a Lie group that is associated with point transformations of a half-line into another half-line. For the one-dimensional case, this group has two parameters that are in the half-plane $\Pi_+ = \{(q,p)|q \in \mathbb{R}^*_+ \text{ e } p \in \mathbb{R}\}$. The factor q is related to a dilatation transformation, and p with a translation with a scale. For example, let x be a point that belongs to the half-line $\mathbb{R}_+$, then the transformation

$$x \to x' = (q,p)\cdot x = \frac{x}{q} + p \qquad ,$$

takes points from one half-line to another half-line.

In this way the sequence of points is always maintained, that is, if $x_1 < x_2 < x_3$, therefore, $x'_1 < x'_2 < x'_3$. Another property is that the ratio between distances is also maintained: $\frac{x_2 - x_1}{x_3 - x_2} = \frac{x'_2 - x'_1}{x'_3 - x'_2}$.

The transformation generates a group whose law of composition and inverse are

$$(q,p)\cdot(q_0,p_0) = \left(qq_0, \frac{p_0}{q} + p\right) \qquad ;$$
$$(q,p)^{-1} = (1/q, -qp) \qquad .$$

This group has a unitary representation $\hat{U}$ given by

$$(\hat{U}(q,p)\psi)(x) = \frac{e^{ipx}}{\sqrt{q}}\psi\left(\frac{x}{q}\right) \quad , \tag{2.26}$$

where $|\psi(x)\rangle$ is a state of the Hilbert space and $\psi(x)$ are the components of this state expanded in the position operator $\hat{X}$.

The transformation of the group generate a two parameters basis of coherent states:

$$e_{q,p}(x) = \left(\hat{U}(q,p)\psi\right)(x) = \frac{e^{ipx}}{\sqrt{q}}\psi\left(\frac{x}{q}\right) \quad , \tag{2.27}$$

where the state $e_{1,0}(x) = \psi(x)$ is called fiducial vector. In the bracket representation

$$|q,p\rangle = \hat{U}|\psi\rangle \quad . \tag{2.28}$$

The great difference of this quantization is to associate the new parameters q and p with classical positions and momentum, with the operator $\hat{Q} = \hat{A}_x \neq \hat{X}$.

The gain of this choice is that the self-adjoint extension of the momentum is resolved naturally, but the cost is the freedom of choice of the fiducial vector that does not yet have a clear physical interpretation.

2.2.2 The basis

From the fiducial vector $\psi(x)$, it is possible to generate a overcomplete basis of states

$$\int_{\Pi_+} |q,p\rangle\langle q,p| d\mu(q,p) = \mathbb{1} \quad , \tag{2.29}$$

where Π_+ is the half-line, and $d\mu(q,p) = \frac{dqdp}{2\pi c_{-1}}$ is the measure. The constant c_{-1} satisfies the equation (2.29)

$$c_\lambda(\psi) = \int_0^\infty \frac{dx}{x^{2+\lambda}} |\psi(x)|^2 \tag{2.30}$$

The quantization of $f(x,p) \to \hat{A}_f(\hat{Q},\hat{P})$ is done through integration

$$\hat{A}_f = \int_{\Pi_+} f(q,p)|q,p\rangle\langle q,p| \frac{dqdp}{2\pi c_{-1}} \quad , \tag{2.31}$$

which associates classic momenta with the variable p and classic positions with the variable q.

The classical behavior of this quantum system is given by the $\check{f}$ function, called the lower symbol, which is the sum of $\hat{A}_f$ in all coherent states

$$\check{f} = \int_{\Pi_+} \langle q,p|A_f|q,p\rangle d\mu \quad . \tag{2.32}$$

The equation (2.32) can not be interpreted as a simple mean since it disregards the overlap between coherent states.

The basis of p and q allows the definition of a *configuration space* for the variables p and q, where it can be defined as a probability density $\rho(q,p,t)$ of the system. This probability density contains the quantum and classical system regimes. It is defined by

$$\rho_\phi(q,p,t) = \frac{1}{2\pi c_{-1}} \left| \langle q,p \left| e^{-i\hat{A}_H t} \right| \phi \rangle \right|^2 \quad . \tag{2.33}$$

The density presented in (2.33) would be an extension of the classical configuration space for quantum regions if the variables q and p can be directly associated with the classic positions and momenta. An example of probability density evolution of the configuration space of the variables q and p and the lower symbol is represented in the figure 6 for the cosmological case.

2.2.3 The quantization of the Dirac Delta

The basis generated by the action of the affine group depend on the fiducial vector. Its relation with the momentum basis $|p\rangle$ and position basis $|x\rangle$ can be seen by quantizing the Dirac delta. For a real ψ, the lower symbol of the quantized version of a Dirac delta localised at (q_0,p_0) is

$$\check{\delta}_{(q_0,p_0)} = \frac{|\langle p,q|p_0,q_0\rangle|^2}{2\pi c_{-1}} = \frac{1}{2\pi c_{-1} q q_0} \left| \int_0^\infty dx\, e^{-i(p-p_0)x}\, \psi\left(\frac{x}{q}\right)\, \psi\left(\frac{x}{q_0}\right) \right|^2 . \tag{2.34}$$

which generates a new probability distribution on the phase space, centered at (q_0,p_0), which regularises the original Dirac probability distribution. In Figure (2) it is shown the shape of this regularized delta at the origin, with the following choice of rapidly decreasing fiducial function

$$\psi_\nu(x) = \left(\frac{\nu}{\pi}\right)^{1/4} \frac{1}{\sqrt{x}} \exp\left[-\frac{\nu}{2}\left(\ln x - \frac{3}{4\nu}\right)^2\right] . \tag{2.35}$$

The above real function, which is nothing but the square root of a Gaussian distribution on the real line with variable $y = \ln x$, centered at $y = 3/4\nu$ ($x = e^{\frac{3}{4\nu}}$), and with variance $1/\nu$, verifies $c_{-2}(\psi_\nu) = 1$, $c_0(\psi_\nu) = c_{-1}(\psi_\nu)$, and more generally

$$c_\gamma(\psi_\nu) = \exp\left[\frac{(\gamma+2)(\gamma-1)}{4\nu}\right] . \tag{2.36}$$

As $\nu \to \infty$, the function (2.35) approaches a Dirac peak. More precisely, it is shown in Fig. (3) that as ν grows, this function smoothly concentrates around $\delta(x-1)$, which is the position eigendistribution for $x = 1$. Conversely, as ν goes to 0, (2.35) tends to 0, which illustrates the total lack of information about the x position. Through these features, one can understand the smoothing effect of ACS quantization on classical functions or distributions.

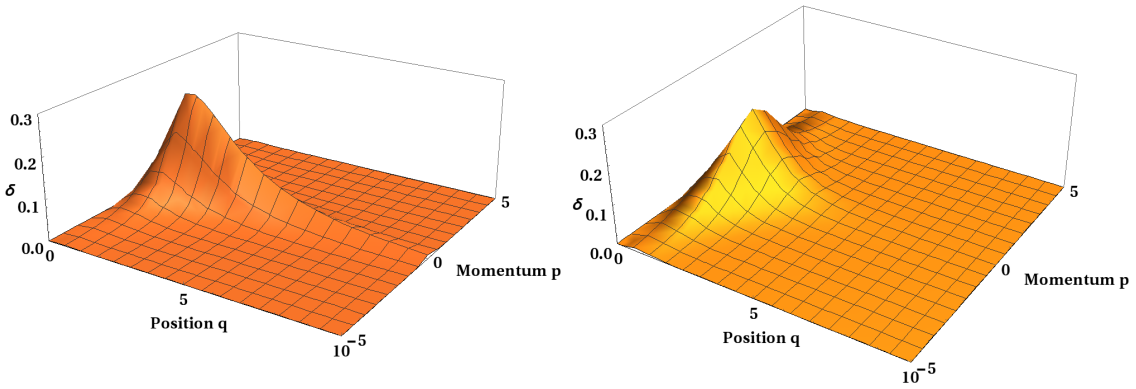

Figure 2 – 3d representation, for different values of ν, of the regularized Dirac δ at the origin with the choice of the rapidly decreasing fiducial function (2.35). The figure on the left is for $\nu = 2$ and the figure on the right is for $\nu = 4$.

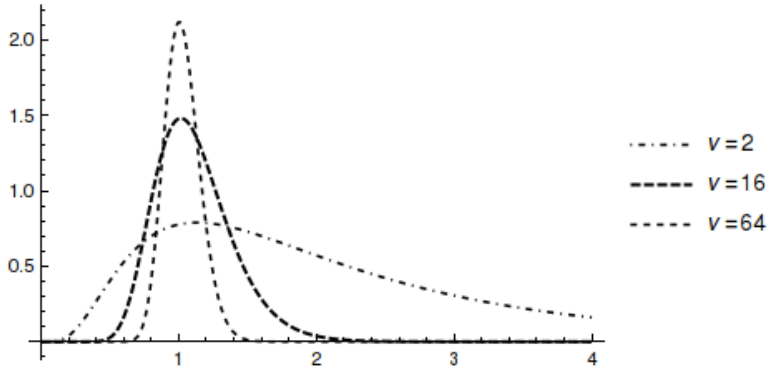

Figure 3 – Fiducial function (2.35) for different ν. As ν grows, it approximates to the Dirac delta.

For a more localized fiducial function, the basis approximates to the positon basis $|x\rangle$. For delocalized fiducial states, it approximates the momentum basis $|p\rangle$.

Lower symbol of powers of q

It is given with the same power up to a constant factor

$$q^\beta \mapsto \check{q^\beta} = \frac{c_{\beta-1}c_{-\beta-2}}{c_{-1}}\, q^\beta \,. \tag{2.37}$$

Lower symbols of momentum, kinetic energy, and product qp

Calculated with real ψ, they read respectively

$$p \mapsto \check{p} = p \,, \tag{2.38}$$

$$p^2 \mapsto \check{p^2} = p^2 + \frac{d(\psi)}{q^2} \,, \tag{2.39}$$

$$qp \mapsto \check{qp} = \frac{c_0 c_{-3}}{c_{-1}} qp\,, \tag{2.40}$$

where

$$d(\psi) = \int_0^\infty (\psi'(x))^2 \left(1 + \frac{c_0}{c_{-1}} x\right) dx = c_{-2}(\psi') + c_0 K_\psi \tag{2.41}$$

where

$$K_\psi = \frac{1}{c_{-1}} \int_0^\infty \mathrm{d}x\, x[\psi'(x)]^2 > 0 \tag{2.42}$$

2.2.4 Classical limit

Dealing with the classical limit imposes to reintroduce the Planck constant by taking into consideration the physical dimensions of the phase space variables (q, p). Consistently, it is replaced in (2.31) by the measure $dq\,dp$ by $dq\,dp/\hbar$. Whatever the choice of a fiducial vector $|\psi\rangle$, one should expect that a certain combination of the limits $\hbar \to 0$ with suitable limits of the parameters of $\psi(x)$ yields the original $f(q, p)$ as

$$\check{f} \to f \tag{2.43}$$

in a certain sense. With the choice (2.35), from (2.36) we get $c_\gamma(\psi_\nu) \to 1$ as $\nu \to \infty$, and the classical limit is trivially obtained for the above expressions (2.37), (2.38) ,(2.39), and (2.40).

2.2.5 ACS quantization of dynamics on half-line

The quantized Hamiltonian (2.25) is

$$A_{\mathrm{H}} = \frac{P^2}{2m} + \frac{K_\psi}{2Q^2} + A_V\,, \tag{2.44}$$

A set of functions that can serve as fiducial vector can be built from a well-known orthonormal composition of Laguerre polynomials [51],

$$e_n^{(\alpha)}(x) := \sqrt{\frac{n!}{\Gamma(n+\alpha+1)}}\, e^{-\frac{x}{2}}\, x^{\frac{\alpha}{2}}\, L_n^{(\alpha)}(x)\,, \quad \int_0^\infty e_n^{(\alpha)}(x)\, e_{n'}^{(\alpha)}(x) dx = \delta_{nn'}\,, \tag{2.45}$$

where $\alpha > 0$ is a free parameter for functions which, with a certain number of their derivatives, vanishes at the origin. On the other hand, for a general n, the expression of the constants c_γ appears quite involved [52]

$$c_\gamma(e_n^{(\alpha)}) = \frac{\Gamma(\alpha-\gamma-1)}{\Gamma(\alpha+1)} \frac{1}{n!} \frac{d^n}{dh^n} \left. \frac{{}_2F_1\left(\frac{\alpha-\gamma-1}{2}, \frac{\alpha-\gamma}{2}; \alpha+1; \frac{4h}{(1+h)^2}\right)}{(1+h)^{\alpha-\gamma-1}(1-h)^{\gamma+2}} \right|_{h=0}. \tag{2.46}$$

This expression is valid for $\alpha > \gamma + 1$.

The second option is the normalized function [53]

$$\psi(x) = \psi^{\nu,\xi}(x) = \frac{1}{\sqrt{2x\, K_0(\nu)}} e^{-\frac{\nu}{4}\left(\xi x + \frac{1}{\xi x}\right)}\,, \tag{2.47}$$

with $\nu > 0$ and $\xi > 0$. Here and in the following, $K_r(z)$ denotes the modified Bessel functions [51], where

$$\xi_{rs} = \xi_{rs}(\nu) = \frac{K_r(\nu)}{K_s(\nu)} = \frac{1}{\xi_{sr}}\,. \tag{2.48}$$

One attractive feature of such a notation is that $\xi_{rs}(\nu) \sim 1$ as $\nu \to \infty$ [5]. The function $\psi^{\nu,\xi}(x)$ falls off with all its derivatives at the origin and at the infinity. The normalization constant and other integrals involving the function $\psi^{\nu,\xi}$ are obtained with the formula [52]

$$\int_0^\infty x^{a-1} e^{-cx-b/x}\, \mathrm{d}x = 2\left(\frac{b}{c}\right)^{a/2} K_a(2\sqrt{bc})\,, \tag{2.49}$$

$\forall\, a, b, c \in \mathbb{C}$, $\mathrm{Re}(b) > 0, \mathrm{Re}(c) > 0$. With such a fiducial vector the integrals c_γ read as

$$c_\gamma\left(\psi^{\nu,\xi}\right) = \xi^{\frac{\gamma}{2}+2}\, \frac{K_{-\gamma-2}(\nu)}{K_0(\nu)} = \xi^{\frac{\gamma}{2}+2}\, \xi_{-\gamma-2,0}\,. \tag{2.50}$$

With these fiducial functions, there are two free parameters ξ and ν (besides the scaling parameter κ). Hence some freedom is left to the ratios $c_\gamma/c_{\gamma'}$.

2.2.6 Some examples

In the following sections, the Affine Covariant Integral quantization will be applied to some simple examples. In such examples, the state where $q = 0$ is not allowed, which is a requirement for the validity of the quantization.

2.2.6.1 Half harmonic oscillator

The system is in a one dimensional oscillatory potential, where the equilibrium is at the origin $q = 0$, but it is limited to the positive axis, $q > 0$. Its Hamiltonian is given by

$$\mathrm{H} = \frac{p^2}{2} + k\frac{q^2}{2}\,, \quad p = \dot{q} \quad q > 0\,. \tag{2.51}$$

An example of a phase space trajectory at constant energy $H = E$, a truncated circle, is given in Figure 4a.

[5] For large argument ν

$$K_r(\nu) \sim e^{-\nu}\sqrt{\pi/(2\nu)},$$

whereas at small $\nu \ll \sqrt{r+1}$

$$K_r(\nu) \sim (1/2)\Gamma(r)(2/\nu)^r$$

for $r > 0$ and

$$K_0(\nu) \sim -\ln(\nu/2) - \gamma$$

.

According to (2.44), the ACS quantization of this classical dynamics yields the quantum Hamiltonian

$$A_{\rm H} = \frac{P^2}{2} + \frac{\widetilde{K}}{Q^2} + \frac{\widetilde{k}}{2}\,Q^2\,, \quad \widetilde{K} = \frac{\hbar^2\,K_\psi}{2}\,, \quad \widetilde{k} = k\,\frac{c_1}{c_{-1}}\,, \tag{2.52}$$

in which the presence of the Planck constant is restored in accordance with the phase space variables (q, p). Passing to the lower symbol of the equation (2.52) through formulas given in (2.37) and (2.39) at constant energy $A_{\rm H} = E$ yields the quantum phase-space correction to (2.51)

$$E = \frac{p^2}{2} + \frac{\hbar^2}{2}\,\frac{d(\psi)}{q^2} + \frac{k}{2}\,\frac{c_1\,c_{-4}}{c_{-1}}q^2 \equiv \frac{p^2}{2} + \frac{\widetilde{\widetilde{K}}}{q^2} + \frac{\widetilde{\widetilde{k}}}{2}q^2\,, \tag{2.53}$$

where $d(\psi)$ is defined in (2.41).

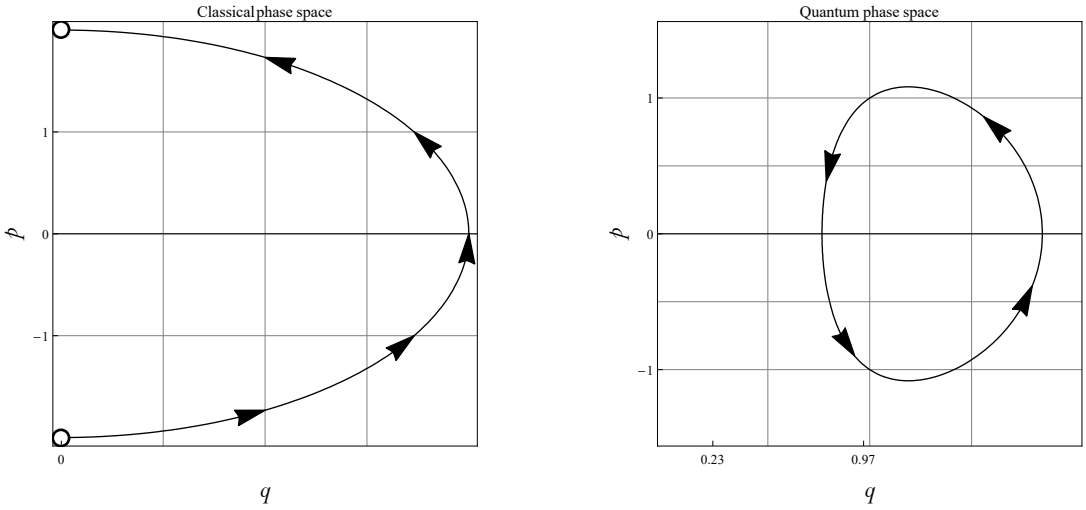

(a) Classical trajectory (b) quantum phase-space trajectory

Figure 4 – **Figure** (4a) is an example of phase space trajectory in the positive half-plane defined by the equation $E = p^2/2 + kq^2/2$ with $E = 2$ and $k = 1$. The reflection at the origin produces the momentum discontinuity $-p_0 \mapsto p_0$. **Figure** (4b) is an example of regularised phase space trajectory in the positive half-plane defined by the equation (2.53) with $E = 2$, $\widetilde{\widetilde{k}} = 1$, and $\widetilde{\widetilde{K}} = 1$, which is the quantum phase space portrait of the classical (2.51). The latter choices for $\widetilde{\widetilde{K}}$ and $\widetilde{\widetilde{k}}$ are easily made possible thanks to a suitable fixing of parameters of the fiducial vector, as was stressed at the end of the previous section. The classical reflection has become a smooth bouncing near the origin.

The presence of the repulsive potential in equation (2.53), of purely quantum origin, allows to eliminate the singularity due to the reflection by creating a smooth bouncing as it is illustrated by Figures (4b).

Note that there is a modification of the oscillator strength k which becomes $\widetilde{k}$ (or $\widetilde{\widetilde{k}}$). If one considers this fact as a problem, the "renormalised" $\widetilde{k}$ or $\widetilde{\widetilde{k}}$ can be made arbitrarily

close to k by choosing in a suitable way the parameters present in the expression of the fiducial ψ. For instance, with the choice of fiducial (2.47), $\widetilde{\widetilde{k}} = \xi^4\, \xi_{30}\, \xi_{2-1}$ and with $\xi = 1$, the product $\xi_{30}\, \xi_{2-1}$ becomes rapidly closer to 1, as shown in the Figure (5). On the other hand, one could decide that what is measured is not k, which belongs to the classical model, but rather the "effective" $\widetilde{k}$ (from which $\widetilde{\widetilde{k}}$ is deduced), viewed as more "realistic" since it is supposed that the quantum model is more fundamental than the classical one. This open a debate analogous to that one arising from the distinction between bare mass and dressed or effective mass in Quantum Field Theory. The same discussion concerns the strength $\widetilde{K}$ of the repulsive potential, which should be adjusted to their observed values if there is any experiment proving the existence of such a regularising effect.

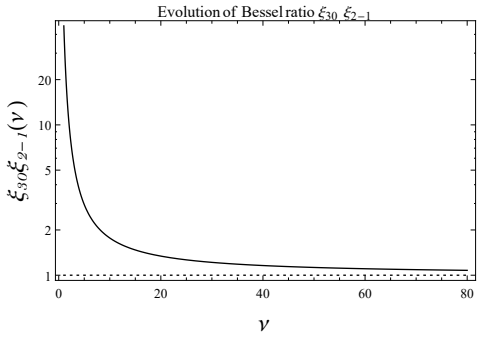

Figure 5 – $\xi_{30}\, \xi_{2-1}$ rapidly becomes closer to 1 for larger ν.

The eigenvalues E_n and eigenfunctions ϕ_n of Equation (2.52) in its operator form are found by solving the eigenvalue equation

$$\frac{1}{2}\left(-\hbar^2\partial_x^2 + \frac{\hbar^2 K_\psi}{x^2} + \widetilde{k}\, x^2\right)\phi_n = E_n\phi_n\,. \tag{2.54}$$

Defining the quantities

$$\mu = \frac{1}{2}\sqrt{1+4K_\psi}\,, \quad \lambda = \frac{1}{2\hbar^2}\left(\frac{k^2}{2}\right)^{\frac{1}{4}}\,, \tag{2.55}$$

the solutions are a combination of exponentials and associated Laguerre polynomials, in

$$\phi_n(x) = 2^{\frac{1}{2}(\mu+1)}x^{(\mu+\frac{1}{2})}e^{-\lambda x^2}L_n^\mu\left(2\lambda x^2\right)\,, \tag{2.56}$$

with $n \in \mathbb{N}$, and the eigenvalues are given by

$$E_n = 2\hbar^3\lambda\,(2n+\mu+2)\,. \tag{2.57}$$

2.2.6.2 Simple dust Universe

This section applies the related quantization on a simplistic model of the Universe, in which the Friedman equations are obtained by means of a Newtonian system.

In this system, the Universe is represented by a sphere of gas of radius q that collapses gravitationally. The dynamics of the q variable is the same as the scale factor for a dust-filled universe. In this system, the Hamiltonian is [21]

$$H = \frac{p^2}{2} - \frac{k}{q} \quad , \tag{2.58}$$

where q represents the scale factor.

The quantization of the Hamiltonian[6] (2.58), associating the scale factor and its classical moment with the transformation variables scale q and translation of scale p, is

$$\hat{A}_H = \frac{\hat{P}^2}{2} + \frac{\hbar^2}{2}\frac{K_\psi}{\hat{Q}^2} - \frac{1}{c_{-1}}\frac{k}{Q} \quad , \tag{2.59}$$

where K_ψ is a constant that depends on the fiducial vector. This quantized Hamiltonian has the last two terms different from the canonical case: the middle term does not appear, and the latter has an extra positive multiplicative constant.

The lower Hamiltonian symbol has an extra term

$$\check{E} = \frac{p^2}{2} + \frac{\tilde{K}_\psi}{q^2} - \frac{k}{q} \quad , \tag{2.60}$$

where $\tilde{K}_\psi$ is a constant that depends on the fiducial vector.

The extra term introduced by quantization causes the dynamics of the scaling factor q to never reach zero, as shown in figure 6

In terms of the scale factor of the Universe, and using the relation $\dot{q} = p$, one gets

$$\left(\frac{\dot{a}}{a}\right)^2 = H^2 = +\frac{k}{q^3} - \frac{\tilde{K}_\psi}{q^4} + \frac{\check{E}}{q^2} \tag{2.61}$$

The quantum effects on the scale factor appear in (2.60) as a phantomic radioactive component, preventing the Universe from collapsing. The energy plays the role of curvature, and the potential the energy density [21].

Although tempting, the figure 6 can not be literally interpreted as a phase space for the quantum case. The variables q and p have no direct relation to the position and momentum when the system is very close to the bounce. In order to have both variables, moment and position, the fiducial function must be distributed over x, so that the Heseiberg inequality holds.

Although simple, this cosmological model avoids the initial singularity as the more realistic model [5]. The difference is that the quantum term is proportional to $1/q^6$, not $1/q^4$. This difference occurs because (2.60) is not the real Hamiltonian of general relativity.

[6] This operator can not be interpreted as a quantization of gravitation, since it is a Newtonian model. The gravitational Hamiltonian follows the equation (1.41).

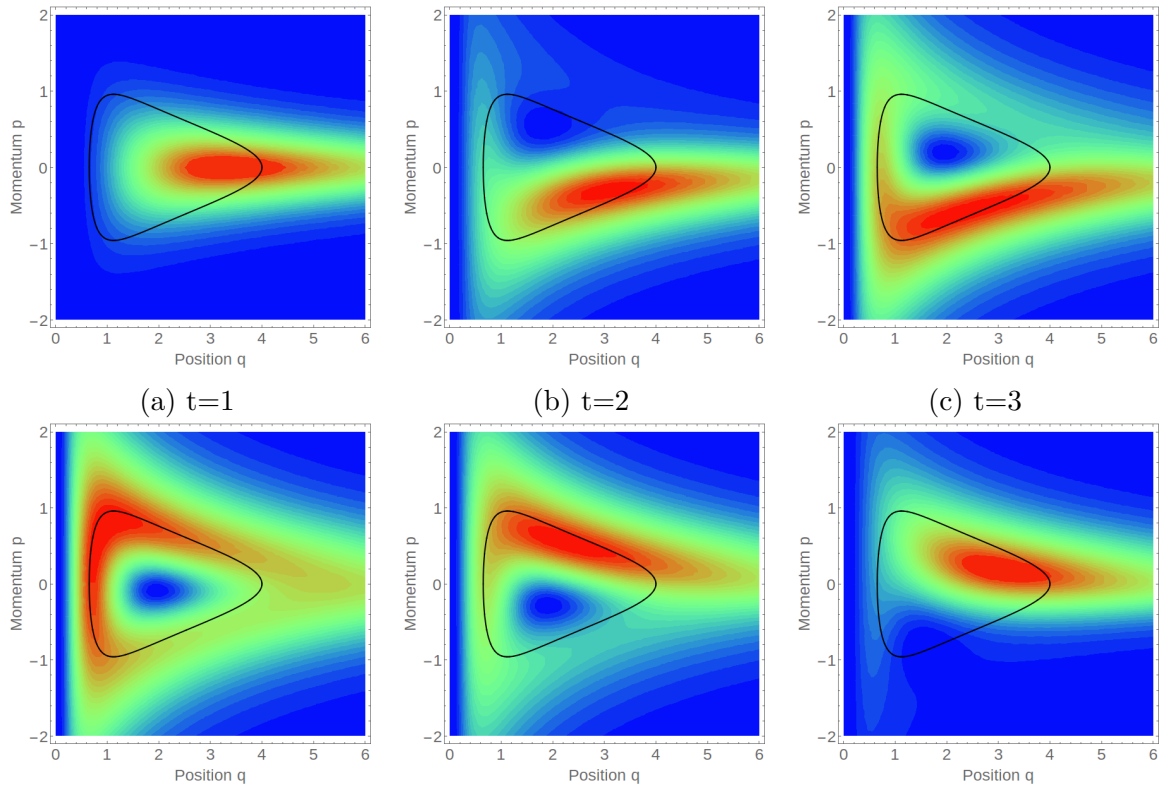

(a) t=1 (b) t=2 (c) t=3

(d) t=4 (e) t=5 (f) t=6

Figure 6 – Evolution of the probability density $\rho(q, p, t)$ and the trajectory defined by the lower symbol (2.60) for a dust-filled Universe. The probability density is defined in the equation (2.33).

The Affine quantization is very practical, since classical systems can be quantized by integrating the classical Hamiltonian. The determination of the fiducial function for the cosmological case would be related to the probability distribution of the scale factor in a certain time; for example, in the bounce. However, the association of the scale factor a with the quantization variable q is not clear. For this reason, this quantization was not considered in the particle creation part of this work.

3 Primordial gravitational waves

In this chapter, the theory of primordial gravitational waves for a bounce Universe will be presented.

"The gravitational-wave detectors record isolated events which are not detected by seismometers, gravimeters, tilt meters, or devices responsive to only electromagnetic fields, of types currently in use. The new limits on gravitational radiation are sufficiently low to be of interest for cosmology.
[54]

One of the big question around the initial Universe concerns the presence of primordial gravitational waves. In the case where the fluid driving the contracting phase is a canonical scalar field, in which the sound velocity of scalar perturbations c_s is equal to the speed of light, $c_s = c = 1$, the production of primordial gravitational waves is usually very high [55], yielding a tensor to scalar perturbation ratio $r = T/S \approx 1$ which is incompatible with observations [56] (T and S are the amplitudes of tensor and scalar perturbations, respectively). On the other hand, for K-essence scalar fields, which mimic hydrodynamical fluids and $c_s = \lambda \approx 0$, the amplitude of primordial gravitational waves produced is very small [7], and they cannot be seen in any band of frequency. This feature is compatible with present cosmological observations, but it does not offer any testable prediction into which this model could be confronted with future observations. As it is well known, the detection of gravitational waves emitted by black holes [57] opened the gravitational waves astronomy era. One of the possible signals to be detected in different frequency ranges in the next decade, away from cosmological scales, are precisely the primordial gravitational waves. Unlike the black hole collision signals recently detected, these primary waves are stochastic and less intense. The detection of such waves will give information about the early Universe [58], e.g., if there was an inflationary era, a bounce, or even both.

The aim of this chapter is to investigate whether high energy modifications of the model described in Ref. [7], a Universe containing radiation and dust which goes through a quantum bounce, can increase the amplitude of primordial gravitational waves in the high frequency regime, the features of such signal and an analytical approximation for the phenomena.

Such regime is the typical frequency region of LISA and LIGO/VIRGO [59, 60] detectors (around 10^{-2}Hz and 10^{3}Hz, respectively), much bigger than the typical frequencies relevant for the Cosmic Microwave Background (CMB) observations of primordial gravitational waves, around 10^{-18}Hz [61][1]. In fact, the energy density of gravitational waves has a spectrum proportional to $f^{\frac{2(9w_c-1)}{1+3w_c}}$, where f is the frequency and w_c is the equation of state parameter of the fluid which is dominating the background when the mode is leaving the Hubble radius. Hence, for modes leaving the Hubble radius at the dust dominated phase, it decreases with frequency as f^{-2}, and it increases as f^2 for modes leaving the Hubble radius at the radiation dominated phase. If one adds to the model a stiff fluid with $w \approx 1$, which should dominate its densest phase, so dense that that the sound velocity of the fluid becomes comparable with the speed of light [62], then for modes leaving the Hubble radius at the stiff matter dominated phase, the energy density of gravitational waves would increase with frequency as f^4. The goal of this chapter is to evaluate whether adding this stiff fluid to the model can sufficiently increase the energy

[1] This convention was already used in [61].

density of gravitational waves in the high frequency regime in a way that they could be detected by future observations, without spoiling the good features of the model (scale invariant spectrum of scalar cosmological perturbations, standard nucleosynthesis phase, etc)[2].

3.1 The full background model

The present model contains three non-interacting perfect fluids: dust, radiation, and a fluid satisfying $p = w\rho$, with $1/3 < w < 1$, usually with $w \approx 1$, an almost stiff matter (asm). The dust fluid controls the dynamics of the Universe when it is large, and the asm dominates its dynamics near the bounce, when the curvature scalar reaches its highest values[3], and the Universe moves from the contracting to the expanding phase. The radiation fluid dominates in between these two fluids. When the curvature scale approaches the Planck length scale, the scale factor gets near its smallest value a_b, and quantum effects realize the transition between contraction to expansion, the bounce. This quantum phase is dominated by the asm fluid.

The radiation and dust fluid model massless or ultra-relativistic massive fields, and cold massive fields, respectively. The asm fluid can represent the content of the Universe when it was so dense that the sound velocity of the fluid becomes comparable with the speed of light [62].

In order to satisfy cosmological observations and the model hypotheses, there are some constraints the asm fluid must fulfill[4]:

- The quantum effects must be restricted to the asm dominated phase;
- Radiation must dominate during nucleosynthesis;
- There must be a classical region between asm and radiation.

As shown in figure 7, the Universe had a contracting phase in the past, when it was almost flat and very homogeneous. The inhomogeneities were generated by quantum vacuum fluctuations at this phase, and amplified afterwards. The tensorial quantum stochastic fluctuations generated in this contracting past were the sources of the primordial stochastic gravitational waves which could be observed today[5].

[2] Only very small scales, around $10^{-20}R_H$, where R_H is the Hubble radius today, could cross the curvature scale in the period where the w fluid is dominant. Since this are very small scales, they do not affect neither CMB observations nor large scale structure formation.

[3] The curvature scale is proportional to the inverse of the square root of the curvature scalar.

[4] Imposing these constraints will limit the amplification of gravitational waves in the asm era, as we will see.

[5] As they are stochastic, there is no coherent time-dependent signal that could be detected using a match-filtering method as used in the first direct detection of gravitational waves [57]

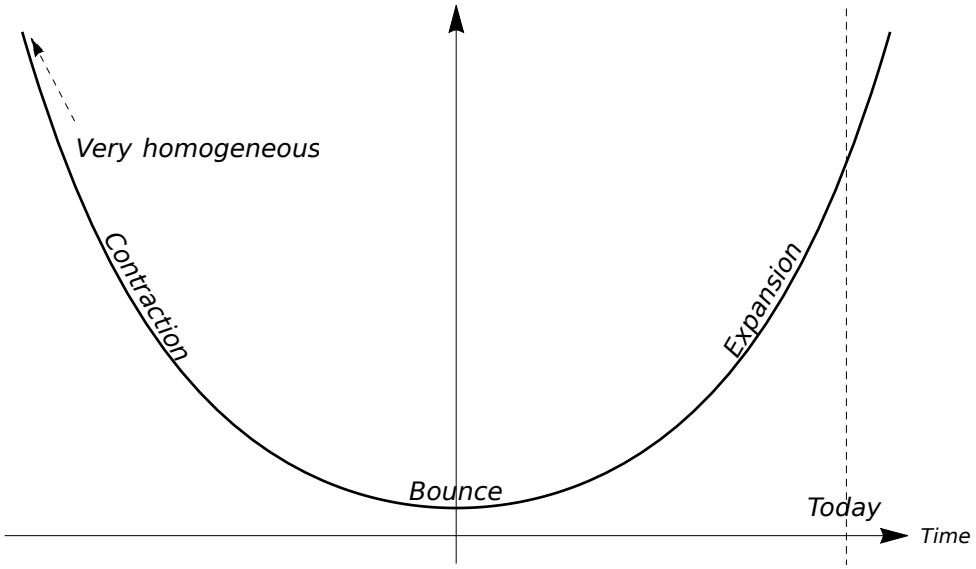

Figure 7 – Evolution of the scale factor in parametric time.

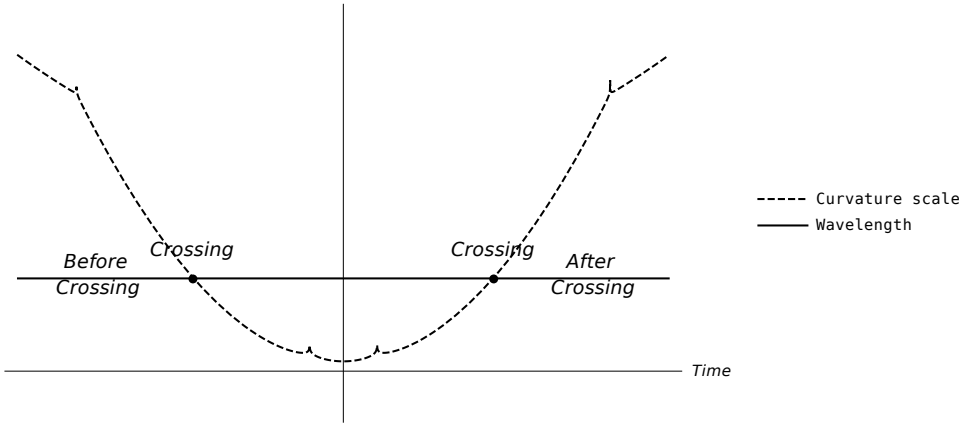

Figure 8 – Crossing the curvature scale. The co-moving wavelength $\lambda = 1/k$, the horizontal line, is smaller than the co-moving curvature scale $|a/(a'')|^{1/2}$, the dashed line, in the far past and in the far future of the history of the Universe, when the tensor mode oscillates, and it becomes bigger around the bounce, when the tensor mode gets amplified.

Waves with different frequencies will have different amplifications, depending when their wavelengths becomes bigger than the Universe curvature scale. When they are smaller, they do not feel the curvature of the Universe and they oscillate as free fields in flat space-time. When their wavelengths become bigger than the curvature scale, they are pumped by the gravitational field, and they get amplified. figure 8 shows a comparison between the co-moving wavelength $\lambda = 1/k$ and the co-moving curvature scale $|a/(a'')|^{1/2}$ along the history of the Universe.

This amplification changes according to which fluid dominates the dynamics of the background when the crossing occurs. Hence, we expect to obtain different dependence of amplitude with frequency for each different fluid domination. The background model have two regimes. A classical and a quantum regime. The quantum regime has a classical limit

which must match with the usual classical evolution. Therefore, there must be a matching period where both regimes become very close to each other.

In the classical one, the Friedmann equation relates the scale factor a and the conformal time η through the equation

$$a' = \text{Sign}(\eta) H_0 \sqrt{\Omega_r + \Omega_d a + \Omega_w a^{(1-3w)}}, \tag{3.1}$$

where $\Omega_i \equiv \rho_i/\rho_c$, $i = r, d, w$ and ρ_c is the critical density today; H_0 is the Hubble factor today; and w is the fluid parameter of asm, i.e., $p_{asm} = w\rho_{asm}$. We set $a_{today} \equiv a_0 = 1$.

The critical densities must satisfy the constraints of observation: the equality between radiation and dust must occur in the redshift 2740, and asm must dominate earlier than the nucleosynthesis era, which occurs at redshift 10^9 [21]:

$$\Omega_r = \Omega_d \frac{1}{1+z_e} \tag{3.2}$$

$$\Omega_r > \Omega_w \left(\frac{1}{1+z_n}\right). \tag{3.3}$$

In the quantum regime,

$$a' = \text{Sign}(\eta) H_0 \sqrt{\Omega_w a^{1-3w} \left[1 - \left(\frac{a_b}{a}\right)^{3(1-w)}\right]}, \tag{3.4}$$

which in terms of the Hubble parameter reads

$$\frac{H^2}{H_0^2} = \frac{\Omega_\omega}{a^{3(1+\omega)}} - \frac{\Omega_\omega a_b^{3(1-\omega)}}{a^6}. \tag{3.5}$$

The equation (3.5) presents an effective negative energy of a stiff matter fluid on its right-hand-side besides the usual classical ams fluid, but this effective negative energy fluid is not really there. It comes from the quantum correction of the classical Friedmann equation. It is similar to what happens in Loop Quantum Cosmology, where the right-hand-side of their Friedmann equation can be effectibelly written as $\left(\rho - \frac{\rho^2}{\rho_c^2}\right)$, but the negative term comes from the quantum amend [63, 64, 65].

There is a period when both (3.1)) and (3.4) are valid, dominated by a classical asm, which happens when

$$\left(\frac{a_b}{a}\right)^{3(1-w)} \ll 1.$$

Let us take

$$\left(\frac{a_b}{a}\right)^{3(1-w)} < \frac{1}{100} \ll 1 \tag{3.6}$$

This choice will not affect the main results. Equality between asm and radiation happens for the scale factor

$$\left(\frac{\Omega_w}{\Omega_r}\right)^{\frac{1}{3w-1}}.$$

Then,

$$a_b 10^{\frac{2}{3(1-w)}} < a < \left(\frac{\Omega_w}{\Omega_r}\right)^{\frac{1}{3w-1}} < a_n, \tag{3.7}$$

where a_n is the scale factor at the nucleosynthesis era. Equation (3.7) constrains Ω_w with respect to the scale factor in the bounce a_b, and the fluid parameter w. Because of this equation, the stiffness of the fluid is limited to

$$w < 1 - \frac{2}{3\mathrm{Log}_{10}\left(\frac{a_n}{a_b}\right)}. \tag{3.8}$$

While the nucleosynthesis scale factor is $a_n \sim 10^{-11}$, the bounce scale factor has the value $a_b > 10^{-31}$ (we are using the Wheeler-DeWitt approach for the quantum phase, which is not expected to be valid at scales very close to the Planck energy scale [4]). Hence, for the more realistic models, where the bounce does not happen very close to the nucleosynthesis era, $10^{10} < a_n/a_b < 10^{20}$, which implies that the ratio a_n/a_b is a large number. Therefore, another choice in (3.6) will not affect significantly the inequality (3.8).

The amplitude of gravitational waves satisfies the wave equation (1.43c)

$$v_k^{''} + \left(k^2 - \frac{a''}{a}\right) v_k = 0, \tag{3.9}$$

where the potential takes the form

$$\frac{a''}{a} = \frac{H_0^2}{2}\left[\frac{\Omega_d}{a} - (3w-1)\frac{\Omega_w}{a^{3w+1}}\right] \text{Classical} \tag{3.10a}$$

$$\frac{a''}{a} = \alpha^2 \left(\frac{a_b}{a}\right)^4 \left[1 - \frac{3w-1}{2}\left(\frac{a_b}{a}\right)^{3(w-1)}\right] \text{Quantum}, \tag{3.10b}$$

where

$$\alpha^2 \equiv \frac{H_0^2 \Omega_w}{a_b^{1+3w}}$$

For $1 \gg a \gg a_b$ in the equations (3.10) the classical and quantum regimes approach each other.

The behavior of the potential is shown in figure 9. Two maxima are classical due to the transition radiation-asm, one in each bounce side. The two minima come from the quantum regime, and the highest peak happens in the bounce.

3.2 Numerical solutions and analytical approximations

For a better understanding on how the different fluids present in the model control the amplitude of gravitational waves, it is necessary a semi-analytical approach. Such approximation can be done separating the evolution in three regions, as shown in figure (10).

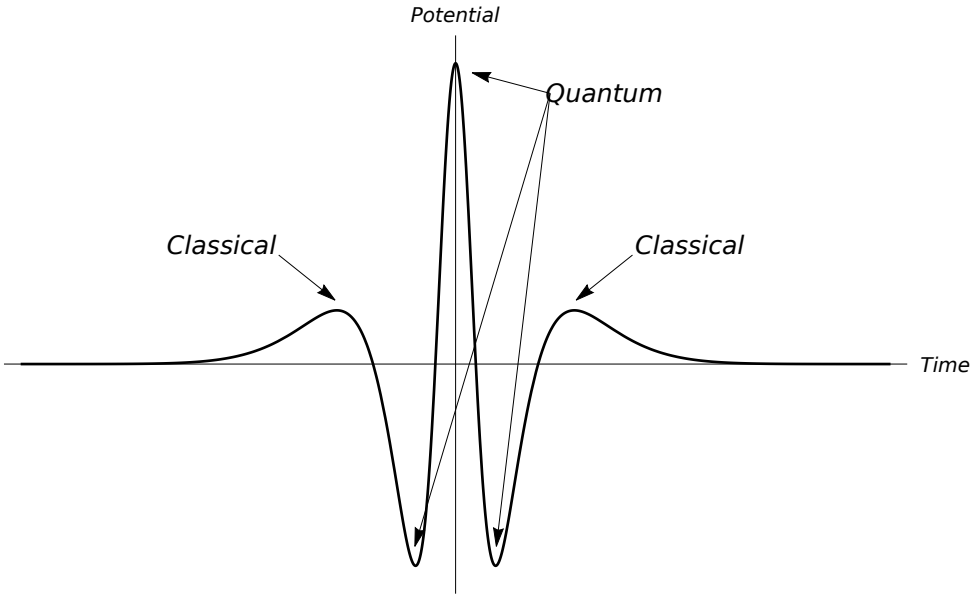

Figure 9 – Structure of the potential a''/a (not in scale).

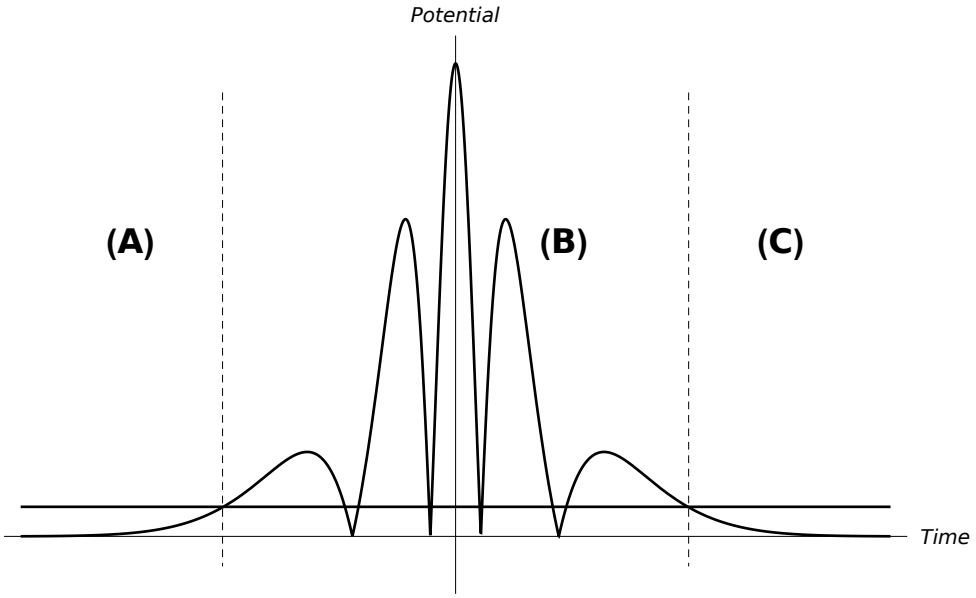

Figure 10 – Crossing the potential a''/a (it is not in scale).

(A) Outside the potential, or inside the curvature scale: $k \gg \frac{a''}{a}$

(B) Inside the potential, or outside the curvature scale: $k \ll \frac{a''}{a}$

(C) Outside the potential again, or re-entering the curvature scale: $k \gg \frac{a''}{a}$

There are regions in B where $k > \frac{a''}{a}$, but they are negligible.

In A and C, the solutions are oscillatory. Using the quantum initial condition

$$v(\eta) = \frac{e^{-ik\eta}}{\sqrt{2k}}, \qquad \text{in (A)} \tag{3.11}$$

$$v(\eta) = C_1 e^{-ik\eta} + C_2 e^{ik\eta}, \qquad \text{in (C).} \tag{3.12}$$

In (B), the zero order term neglecting k reads

$$v(\eta) = a(\eta)\left[B_1 + B_2 \int_{-\eta_c}^{\eta} \frac{d\bar{\eta}}{a^2(\bar{\eta})}\right], \tag{3.13}$$

where $-\eta_c$ denotes the conformal time when $k^2 = \left|\frac{a''}{a}\right|$ in the contracting phase, $\eta = 0$ is the bounce conformal time, and η_c is the conformal time when the solution exits the potential again (the potential a''/a is symmetric). The constants can be obtained through matching conditions, and read,

$$B_2 = (av' - va')|_{-\eta_c} \tag{3.14a}$$

$$B_1 = \frac{v(-\eta_c)}{a(-\eta_c)}. \tag{3.14b}$$

From now on, $a_c = a(\eta_c) = a(-\eta_c)$ and $a'_c = |a'(\eta_c)| = a'(\eta_c) = -a'(-\eta_c)$.

The constants in equations (3.14) are, using equation (3.11)

$$B_1 = \frac{e^{-ik\eta_c}}{a_c\sqrt{2k}} \tag{3.15}$$

$$B_2 = \frac{e^{ik\eta_c}}{a_c\sqrt{2k}}\left(a'_c a_c - ika_c^2\right). \tag{3.16}$$

Therefore, equation (3.13)) can be expressed as

$$v(\eta_c) = \frac{e^{ik\eta_c}}{\sqrt{2k}}\left[1 + \left(a'_c a_c - ika_c^2\right) I(a_c)\right], \tag{3.17}$$

where

$$I(a_c) = \int_{-\eta_c}^{\eta_c} \frac{d\eta}{a^2(\eta)} = 2\int_{a_b}^{a_c} \frac{da}{a^2|a'(a)|}. \tag{3.18}$$

Using the fact that B_2 is constant, the derivative in the region B can be expressed as

$$v' = \frac{B_2}{a} + v\frac{a'}{a}$$

$$\Rightarrow v'(\eta_c) = \frac{e^{ik\eta_c}}{\sqrt{2k}}\left[\frac{a'_c}{a_c}\left(2 + a'_c a_c I(a_c)\right) - ik\left(1 + a'_c a_c I(a_c)\right)\right]. \tag{3.19}$$

With the functions v and v' in region B determined, the constants present in the function in region C are

$$C_1 = \left[v(\eta_c) + \frac{v'(\eta_c)}{-ik}\right]\frac{e^{ik\eta_c}}{2} \tag{3.20}$$

$$C_2 = \left[v(\eta_c) - \frac{v'(\eta_c)}{-ik}\right]\frac{e^{-ik\eta_c}}{2}. \tag{3.21}$$

The critical energy of gravitational waves [58] when the waves reenter the curvature scale is then given by,

$$\begin{aligned}\Omega_g &\simeq \frac{k^5 l_p^2}{3\pi^2 H_0^2}\left(|v|^2 + \left|\frac{v'}{k}\right|^2\right) = \frac{2k^5 l_p^2}{3\pi^2 H_0^2}(|C_1|^2 + |C_2|^2) \\ &= \frac{k^4 l_p^2}{3\pi^2 H_0^2}\left[2 + 4a_c' a_c I(a_c) + a_c'^2 a_c^2 I^2(a_c) + k^2 a_c^4 I^2(a_c) + \right. \\ &\left. + \frac{a_c'^2}{a_c^2 k^2}\left(4 + 4a_c' a_c I(a_c) + a_c'^2 a_c^2 I^2(a_c)\right)\right].\end{aligned} \tag{3.22}$$

The peak of the potential, which happens at the bounce, leads to a maximum k

$$k_M^2 = \frac{3(1-w)}{2}\alpha^2 \Rightarrow \frac{k_M^2}{H_0^2} = \frac{3(1-w)\Omega_w}{2a_b^{1+3w}}. \tag{3.23}$$

As $10^{-31} < a_b \ll 10^{-11}$ [4], this is a huge physical frequency, and implies a minimum physical wavelength many orders of magnitude smaller than the Hubble radius today. For frequencies smaller than this huge maximum frequency, the term $I^2(a_c)$ dominates in equation (3.22). In fact, as the integrand in equation (3.18) is a decreasing function of a, one has

$$a_c|a_c'|I(a_c) = 2a_c|a_c'|\int_{a_b}^{a_c}\frac{da}{a^2|a'|} \gg 2a_c|a_c'|\frac{(a_c - a_b)}{a_c^2|a_c'|} \simeq 2, \tag{3.24}$$

when $a_c \gg a_b$, which is the case for $k \ll k_M$. As in the crossing $a_c''/a_c \simeq (a_c'/a_c)^2 \simeq k^2$, and as

$$I(a_c) = 2\int_{a_b}^{a_c}\frac{da}{a^2|a'|} \simeq 2\int_{a_b}^{a_q}\frac{da}{a^2|a'|} \equiv I_q, \tag{3.25}$$

because the integrand in $I(a_c)$ is dominated by small values of a (a_q denotes the scale factor in the beginning of the quantum phase), the energy density can be expressed as

$$\Omega_g \propto \frac{k^6 l_p^2}{3\pi^2 H_0^2} I_q^2 a_c^4, \tag{3.26}$$

where I_q does not depend on a_c. As

$$a_c \approx \left(\frac{H_0^2\Omega_w}{k^2}\right)^{\frac{1}{1+3w_c}},$$

$$\begin{aligned}\Omega_g &\propto \frac{l_p^2}{3\pi^2} I_q^2 \left(\frac{\Omega_{w_c}}{2}\right)^{\frac{4}{1+3w_c}} \left(\frac{k}{H_0}\right)^{\frac{2(9w_c-1)}{1+3w_c}} \\ &\propto k^{\frac{2(9w_c-1)}{1+3w_c}},\end{aligned} \tag{3.27}$$

where w_c is the equation of state parameter of the fluid which is dominating the background when the mode is leaving the Hubble radius[6].

The equation (3.27) shows that frequencies that crosses the potential in the dust era ($\lambda = 0$) have energy density decaying with f^{-2}; the ones entering the potential in the radiation era have energy density growing with f^2; and frequencies that crosses the potential in the asm era have energy density growing with f^4. For frequencies $k \geq k_M$, the integral I_c is zero, since the waves never crosses the curvature scale. In this case, Eq. (3.22) is dominated by the first term inside the braces, and hence the energy density grows also as f^4. It is the usual flat spacetime ultraviolet divergence. These behaviors are shown in figures 12, 14 and 13 below.

Concerning the amplitudes, the term which contributes mostly to the energy density is the quantum part of the integral equation (3.19):

$$\begin{aligned}I_q &= \int_{a_b}^{a_q} \frac{da}{a^2|a'|} = \frac{1}{\alpha}\int_{a_b}^{a_q} \frac{da}{a^2\sqrt{\left(\frac{a_b}{a}\right)^{3w-1} - \left(\frac{a_b}{a}\right)^2}} \\ &= \frac{2}{H_0\sqrt{\Omega_w a_b^{3(1-w)}}} \frac{\arctan\left(\sqrt{\left(\frac{a_q}{a_b}\right)^{3(1-w)} - 1}\right)}{3(1-w)}.\end{aligned} \tag{3.28}$$

Its dependency on w shows that it decreases until $w \approx 1 + \frac{2}{3\ln(a_b)}$, when it reaches its minimum value, then it increases rapidly to infinity, when $w = 1$, as shown in Fig 11.

However, w is limited to the constraint equation (3.8), which is also indicated in figure (11). It shows that, although the energy density increases more in frequency for higher values of w as shown in equation (3.27), the value of I_q decreases significantly with w in its physical allowed region, as shown in figure 11. The combination of these two behaviors implies a net decreasing in the amplitude with respect to the case without the asm fluid, as shown in of figure 12.

The usual increasing in the energy density due to the depth of the bounce is quite suppressed due to the presence of the asm fluid. Indeed, the ratio between different gravitational waves energy densities for two different bouncing models with different scale

[6] In a cosmological model described by general relativity with single fluid domination, leaving the Hubble radius is the same as leaving the curvature scale and as crossing the potential

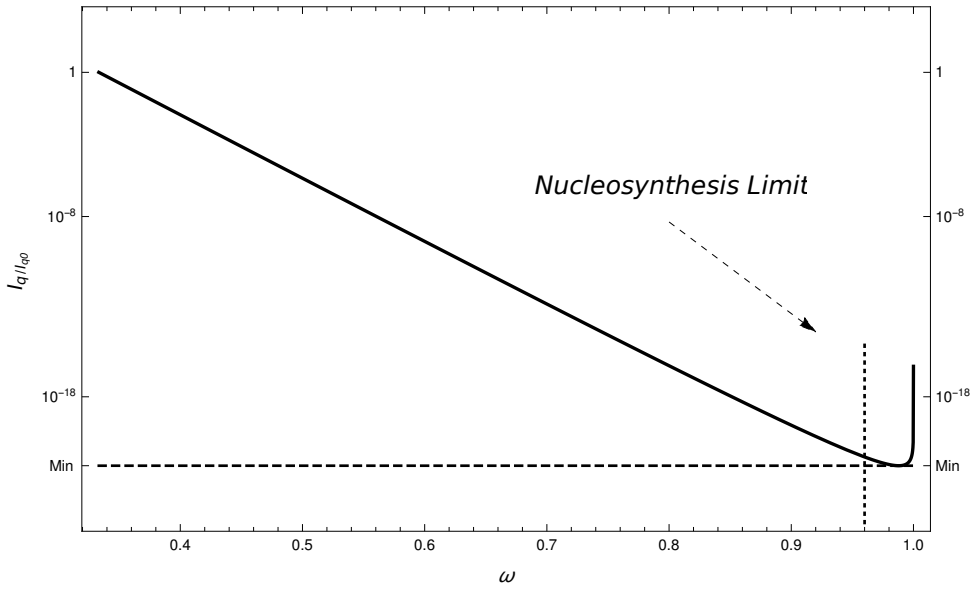

Figure 11 – The ratio between the integral equation (3.28)) and its value for $w = 1/3$ for different w, considering $a_b = 10^{-24}$ and $(a_q/a_b)^{3(1-w)} = 100$. The minimum value is when $w \approx 0.99$. However, due to the constraint equation (3.8), w is limited to $w \approx 0.96$.

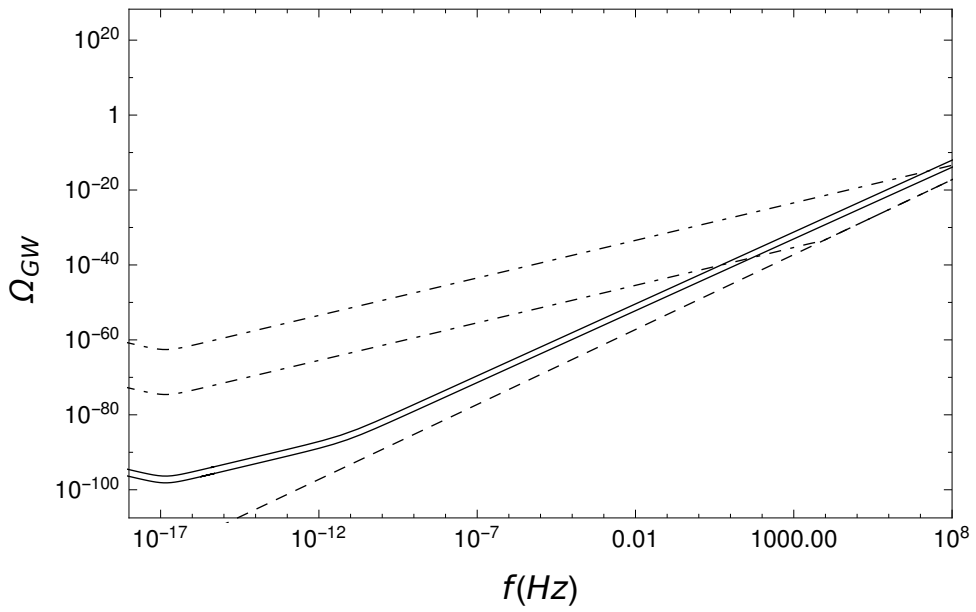

Figure 12 – The energy density of gravitational waves with state parameter $w = 1/3$ and minimum scale factors $a_b = 10^{-24}, 10^{-18}$, represented by dot-dashed curves, and state parameter $w = 0.9$ with minimum scale factors $a_b = 10^{-24}, 10^{-30}$, represented by continuous curves. The higher energy densities correspond to smaller a_b, respectively. The dashed curve corresponds to the limit where the frequency never enters the potential. The different inclinations of the curves are in accordance with the discussion after equation (3.27).

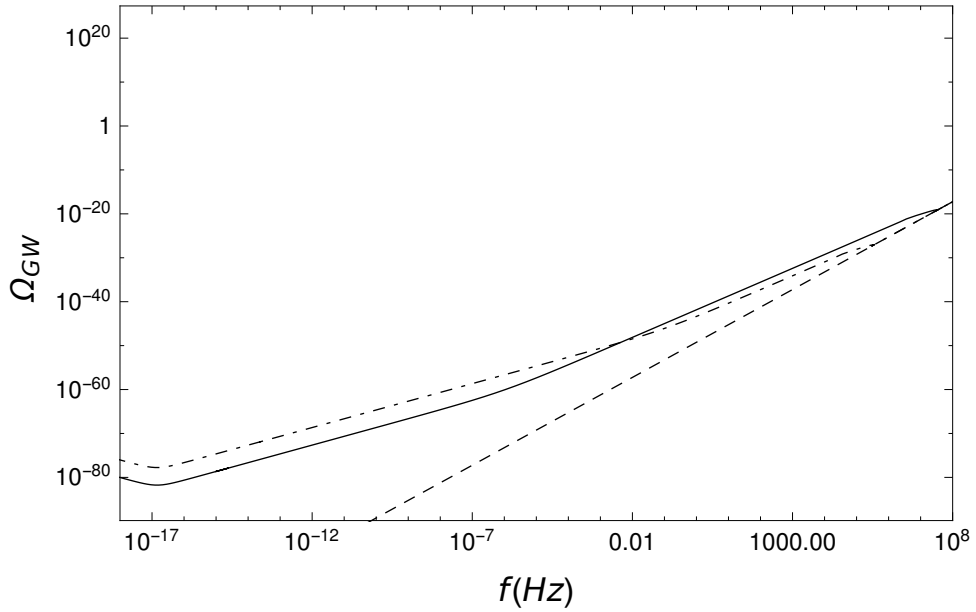

Figure 13 – Gravitational waves energy density dependence on Ω_w for minimum scale factor $a_b = 10^{-24}$, and ams fluid parameter $w = 0.6$. The dot-dashed curve corresponds to $\Omega_w = 10^{-19}$, while the continuous curve corresponds to $\Omega_w = 10^{-15}$. The dashed curve corresponds to the limit where the frequency never enters in the potential. Again, the different inclinations of the curves are in accordance with the discussion after equation (3.27).

factors at the bounce, a_{b1} and a_{b2}, reads, using equation (3.28),

$$\frac{\Omega_{g1}}{\Omega_{g2}} = \left(\frac{a_{b2}}{a_{b1}}\right)^{3(1-w)} \frac{\arctan\left(\sqrt{\left(\frac{a_q}{a_{b1}}\right)^{3(1-w)} - 1}\right)}{\arctan\left(\sqrt{\left(\frac{a_q}{a_{b_2}}\right)^{3(1-w)} - 1}\right)}. \tag{3.29}$$

Hence, for fluids with state parameter close to 1 dominating during the bounce, the increase in intensity due to the bounce depth is exponentially suppressed, as shown in figure 11.

The summary of the results are:

- The energy density of primordial gravitational waves decreases with the energy density of the fluid which dominates at the bounce. Shown is equations in equations (3.27)) and (3.28), together with the figure 13.

- The increasing of the energy density of primordial gravitational waves in frequency for increasing w with $1/3 < w < 1$ does not usually compensate the decreasing of its intensity due to the decreasing of I_q with w presented in figure 11. This compensation usually happens only for very high frequencies, inaccessible by nowadays experiments, shown in figure 14.

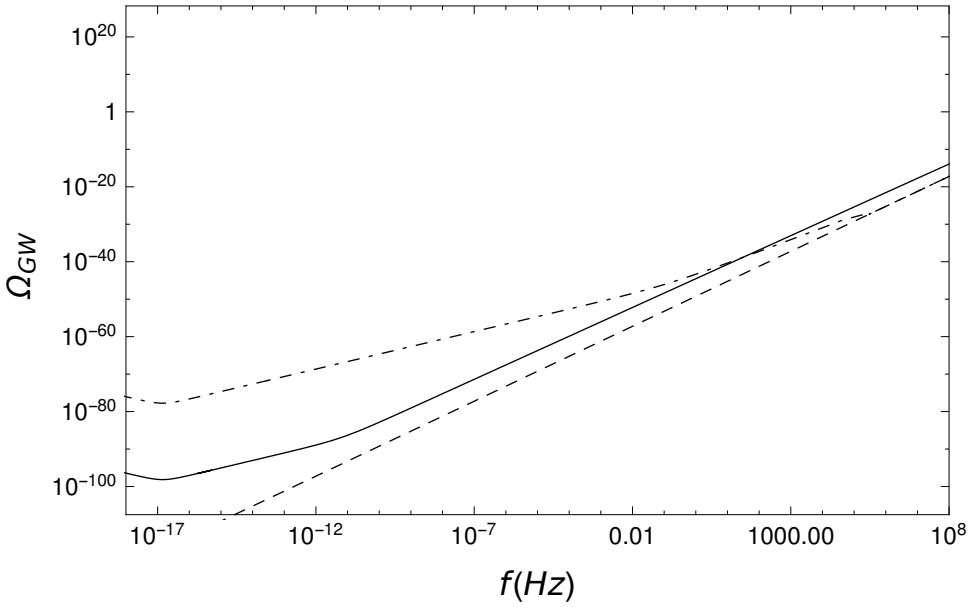

Figure 14 – Behavior of the energy density of primordial gravitational waves with respect to the equation of state parameter w for minimum scale factor $a_b = 10^{-24}$, and ams energy density today given by $\Omega_w = 10^{-19}$. The fluid parameter $w = 0.9$ corresponds to the continuous line, and $w = 0.6$, corresponds to the dot-dashed line. The dashed curve correspond to the limit where the frequency never enters in the potential. Once again, the different inclinations of the curves are in accordance with the discussion after equation (3.27).

- The energy density of primordial gravitational waves is more sensitive to the depth of the bounce for lower equation of state parameters w, as shown in the equation (3.29). This sensitivity is shown in figure 12.

- Finally, Fig. 15 presents one of the highest energy densities of primordial gravitational waves we found for one particular bouncing model, comparing it with results from inflation and present observational bounds. Note that the amplitude is still far below possible observations. In these frequencies, there is also the astrophysical background, proportional do f^3. The LIGO detectors can separate between different grow behaviors [60].

3.3 Conclusion

In bouncing models containing K-essence scalar fields simulating hydrodynamical fluids with $c_s^2 = w$, the amplitude of primordial gravitational waves produced is usually very small [7] for cosmological scales, or low frequencies, but it can grow significantly at high frequencies if the fluid which dominates the background dynamics at the bounce is as close to stiff matter as possible. In this chapter it was shown that this can indeed be true, described in equation (3.27), but the amplitude of gravitational waves does also depend on I_q defined on equation (3.25), which gets smaller when the bounce fluid approaches

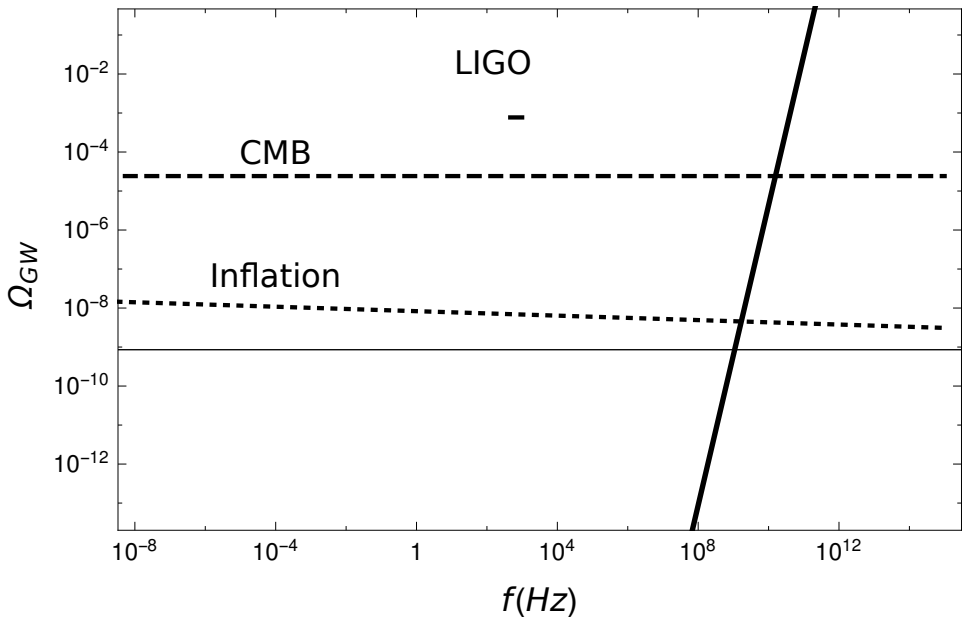

Figure 15 – Amplitude of gravitational waves energy density for high frequencies. The amplitude refers to a model with $a_b = 10^{-30}$, and $w = 0.9$. The inflation amplitude corresponds to a slow-roll model with $r = T/S = 0.6$ [39]; the CMB line refers to the imprints we should expect in CMB [66]; the LIGO limit is the lower sensitivity for scale-invariant perturbations [60]. Note that the usual flat spacetime ultra-violet divergences were not subtracted in this figure.

stiff matter. The compromise between these two effects makes the amplitude of primordial gravitational waves not sufficiently big at high frequencies in order to be detected by present day or near future observations for background models being symmetric around the bounce, and satisfying the nucleosynthesis bounds. These conclusions are corroborated by figures 13, 14, 12 and 15, based on numerical calculations, and understood through analytical considerations. Hence, it seems that bouncing models where the background is dominated by hydrodynamical fluids do not present any significant amount of primordial gravitational waves at any frequency range compatible with observations. Any detection of such waves will then rule out this kind of models.

An alternative would be to consider bouncing models which are not symmetric around the bounce due, e.g., to particle production near the bounce [4]. In this case, one could suppose that radiation was created after the bounce, and the nucleosynthesis bounds originating constraint equation (3.8) could be relaxed, because in the contracting phase there would be almost no radiation. It would be a bouncing model with some sort of reheating. In this case, one could have w as close to 1 as necessary, yielding a sufficiently big I_q as indicated by the $w \approx 1$ part of figure (11). In this case, the model could produce a sufficient amount of relic gravitational waves that could be detected.

4 Fermions creation

In this chapter, the fermions production in the bounce model will be presented.

"(...) the spinor ψ (...) provides a realization of an irreducible representation of the Lorentz group(...)"
[67]

The Universe may have started with the same amount of particles we see today, or they may have been created along their evolution. Whatever the origin of the particles that fill the Universe, a number of them are needed in the expansion phase to explain the formation of the first atomic nuclei and the subsequent formation of all the astronomical objects that are observed today. Without having a special reason for choosing initial conditions for particle density, arises the hypothesis that they were created throughout the evolution of the Universe. This hypothesis is addressed in inflation theories which, due to an exponential expansion of the Universe, the density of particles is much lower than the value necessary for the formation of the first atomic nuclei. The main theories of inflation solve this problem by proposing a phase called reheating where there is still controversy as to how these particles are generated [68].

In this chapter, the initial particles have been generated by the evolving gravitational field of the Universe . A phenomenon similar to the Unruh effect and the Hawking radiation [69, 70]. The treatment of uncharged spin 1/2 fermions is an extension to earlier works that dealt with the creation of scalar fields in the bounce [4]. In the worked models, the very homogeneous, isotropic, large and contracting initial condition of the Universe presents quantum fields in a vacuum state. During the evolution of this Universe, the definition of quantum vacuum changes, generating particles.

When the Universe had a very large scale factor and was in the era of contraction of a bouncing model, there were no fermionic particles. The field of fermionic particles was in the vacuum state, and as the Universe evolved, the definition of vacuum state changed through Bogoliubov's transformations. After the bounce, the state of the fermionic field is in the vacuum of the contraction era, which was not equivalent to the vacuum defined by the observer. This difference gives rise to fermionic particles that inhabit the whole Universe. In this chapter, it is shown that the creation of fermionic particles has a very characteristic spectrum and differs from other theories like [71]. In the case of articles following the line of [72, 73], the particles are created by a transition effect of the mass of fermionic particles at the end of inflation. During creation, the article [71] argues that the scale factor is practically constant, and the particles undergo successive transitions. In the present case, the creation of particles occurs over a longer period, and is given only by the dynamics of the scale factor.

4.1 Classical fermions

In this section, the theory classical of fermionic fields is derived. The aim is to define a Hamiltonian H and a momentum Π canonically conjugate to the spinor field $\Psi(x,t)$ that will be quantized in the next section.

The fermionic field Lagrangian for curved space-times is given by [74]

$$\mathcal{L}_f = \frac{i}{2}\Big[\overline{\Psi}\gamma^\mu\mathcal{D}_\mu\Psi - \Big(\mathcal{D}_\mu\overline{\Psi}\Big)\gamma^\mu\Psi - m\overline{\Psi}\Psi\Big]. \tag{4.1}$$

The 4 Dirac matrices γ^μ satisfy the anti-commutation relation

$$\{\gamma^\mu, \gamma^\nu\} = 2g^{\mu\nu}\mathbb{1}, \tag{4.2}$$

where $g^{\mu\nu}$ is the space-time metric and $\mathbb{1}$ is the identity matrix.

The spin metric h_s is a matrix that relates the spinor field Ψ with its dual $\overline{\Psi}$

$$\overline{\Psi} = \Psi^\dagger h_s, \tag{4.3}$$

and relates the Dirac matrices to its transpose complex,

$$\gamma^{\mu\dagger} = h_s\gamma^\mu h_s^{-1}, \tag{4.4}$$

a crucial property for the invariance of the Lagrangian (4.1) under spinor point transformations [74].

The differential operator $\mathcal{D}_\mu$ is the covariant derivative that has the properties

$$\mathcal{D}_\mu\Psi = \partial_\mu\Psi + \Gamma_\mu\Psi; \tag{4.5a}$$
$$\mathcal{D}_\mu\overline{\Psi} = \partial_\mu\overline{\Psi} - \overline{\Psi}\Gamma_\mu; \tag{4.5b}$$
$$\mathcal{D}_\mu\gamma^\alpha = \nabla_\mu\gamma^\alpha + [\Gamma_\mu, \gamma^\alpha] = 0, \tag{4.5c}$$

where ∇_μ is the space-time covariant derivative, and Γ_μ is the spin connection.

Without loss of generality, the Dirac matrices can be written as[1]

$$\gamma^\mu = e^\mu{}_{(A)}\gamma^{(A)}, \tag{4.6}$$

where $e^\mu{}_{(A)}$ are a tetrad coordinate, and $\gamma^{(A)}$ are any constant set of Dirac matrices that satisfies

$$\left\{\gamma^{(A)}, \gamma^{(B)}\right\} = 2\eta^{(A)(B)}, \tag{4.7}$$

where $\eta^{(A)(B)}$ is the Minkowski metric. All the tetrad indices are depicted by latin capital indices in parenthesis, like (A).

The tetrad basis has the properties

$$e_{\nu(A)}e_\mu{}^{(A)} = g_{\nu\mu}; \tag{4.8a}$$
$$e^\mu{}_{(A)}e_{\mu(B)} = \eta_{(A)(B)}, \tag{4.8b}$$

[1] There is always a spin transformation S such that, for any set of γ^μ, [74]

$$\tilde{\gamma}^\mu = S\gamma^\mu S^{-1} = e^\mu{}_{(A)}\gamma^{(A)}.$$

where $\eta_{(A)(B)}$ is the Minkowski metric.

In terms of the tetrad basis choice in equation (4.6), the spin connection is

$$\Gamma_\mu = \frac{1}{8} e^\nu{}_{(C)} e_{\nu(D);\mu} \left[\gamma^{(C)}, \gamma^{(D)}\right] = \frac{1}{8}[\gamma^\nu, \gamma_{\nu;\mu}] \tag{4.9}$$

The dynamics of the fermionic field can be obtained by the Hamilton equations. The space-time is divided in space-time hyper-surface given by $\tau(x,t)$ constant is space-like, perpendicular to $\mathrm{d}\tau_\mu$. The gradient $\mathrm{d}\tau_\mu$ points to direction where τ increases. For different foliations $\tau(x,t)$, there are different Hamiltonians.

First, it will be defined the time variation $\dot{\Psi}$ with respect to the foliation τ. Then the Lagrangian will be expressed in terms of $\dot{\Psi}$, whereby the momentum will be defined. At last, the Hamiltonian will be constructed and the Hamilton equations will be derived.

The variation of the spinor field along a time line is given by the Lie derivative [67, 75]

$$\dot{\Psi} = \mathfrak{L}_{\partial_\tau} \Psi = (\partial_\tau)^\mu \mathcal{D}_\mu \Psi; \tag{4.10a}$$

$$\dot{\overline{\Psi}} = \mathfrak{L}_{\partial_\tau} \overline{\Psi} = (\partial_\tau)^\mu \mathcal{D}_\mu \overline{\Psi}. \tag{4.10b}$$

The vector $(\partial_\tau)^\mu$ is the direction where τ increases, but the coordinates over the spatial surface are still the same. Explicitly,

$$\mathrm{d}\tau^\mu = g^{\mu\nu}\partial_\nu \tau \qquad (\partial_\tau)^\mu = \partial_\tau x^\mu, \tag{4.11}$$

where these two vectors satisfy the relation

$$\mathrm{d}\tau_\mu \, (\partial_\tau)^\mu = \frac{\partial \tau}{\partial x^\mu} \frac{\partial x^\mu}{\partial \tau} = \frac{\partial \tau}{\partial \tau} = 1. \tag{4.12}$$

Due to the relation (4.12), the vector ∂_τ can be expressed in terms of the gradient

$$(\partial_\tau)^\mu = N^2 \, \mathrm{d}\tau^\mu + \beta^\mu, \tag{4.13}$$

where β^μ is a vector over the spatial surface[2], and $N^{-2} = \mathrm{d}\tau^\mu \, \mathrm{d}\tau_\mu$. Different from the gradient, ∂_τ is not perpendicular to the spatial surface.

Using the equation (4.13), it is possible to construct the relation

$$\delta^\mu_\nu = P^\mu{}_\nu + L_\nu (\partial_\tau)^\mu, \tag{4.14}$$

where $P^\mu{}_\nu \, (\partial_\tau)_\mu = 0$, and $L_\nu = \frac{(\partial_\tau)_\nu}{(\partial_\tau)^\alpha (\partial_\tau)_\alpha}$. Using the (1.9) coordinates for the FRLW metric, $P^\mu{}_\nu$ is the projector in the spatial indices and L_ν in the temporal indices. It is important to notice that the equation (4.14) does not separate the manifold in space and time sections, because (∂_τ) is not perpendicular to the spatial surface.

[2] It means that $\beta^\mu \, \mathrm{d}\tau_\mu = 0$.

Using the equation (4.14) and the definition (4.10), the Lagrangian can be expressed as

$$\begin{aligned}\mathcal{L}_f &= \frac{i}{2}\Big[\overline{\Psi}\gamma^\mu P^\alpha{}_\mu \mathcal{D}_\alpha\Psi + \overline{\Psi}\gamma^\mu L_\mu\dot{\Psi} - \big(\mathcal{D}_\alpha\overline{\Psi}\big)\gamma^\mu P^\alpha{}_\mu\Psi - \dot{\overline{\Psi}}\gamma^\mu L_\mu\Psi\Big] - m\overline{\Psi}\Psi = \\ &= i\Big(\overline{\Psi}\gamma^\mu P^\alpha{}_\mu \mathcal{D}_\alpha\Psi + \overline{\Psi}\gamma^\mu L_\mu\dot{\Psi}\Big) - m\overline{\Psi}\Psi - \frac{1}{\sqrt{-g}}\partial_\mu\Big(\sqrt{-g}\overline{\Psi}\gamma^\mu\Psi\Big) = \\ &= -i\Big[\big(\mathcal{D}_\alpha\overline{\Psi}\big)\gamma^\mu P^\alpha{}_\mu\Psi + \dot{\overline{\Psi}}\gamma^\mu L_\mu\Psi\Big] - m\overline{\Psi}\Psi + \frac{1}{\sqrt{-g}}\partial_\mu\Big(\sqrt{-g}\overline{\Psi}\gamma^\mu\Psi\Big),\end{aligned} \tag{4.15}$$

where the last term $\frac{1}{\sqrt{-g}}\partial_\mu\Big(\sqrt{-g}\overline{\Psi}\gamma^\mu\Psi\Big)$ is a total divergence[3].

From (4.15), the momentum is defined by

$$\Pi_1(x,t) = \int \mathrm{d}^4x'\,\sqrt{-g}\frac{\delta\mathcal{L}(x',t')}{\delta\Psi(x)} = i\overline{\Psi}(x,t)\gamma^\mu(x,t)L_\mu(x,t); \tag{4.16a}$$

$$\Pi_2(x,t) = -i\gamma^\mu(x,t)L_\mu(x,t)\Psi(x,t). \tag{4.16b}$$

From equations (4.16), the Hamiltonian density is defined as

$$\begin{aligned}\mathcal{H} &= \Pi_1\dot{\Psi} + \dot{\overline{\Psi}}\Pi_2 - \mathcal{L} = \\ &= -\frac{i}{2}\Big[\overline{\Psi}\gamma^\mu P^\alpha{}_\mu \mathcal{D}_\alpha\Psi - \big(\mathcal{D}_\alpha\overline{\Psi}\big)\gamma^\mu P^\alpha{}_\mu\Psi\Big] + m\overline{\Psi}\Psi = \\ &= -i\overline{\Psi}\gamma^\mu P^\alpha{}_\mu \mathcal{D}_\alpha\Psi + m\overline{\Psi}\Psi + \frac{1}{\sqrt{-\gamma}}\partial_\alpha\Big(\sqrt{-\gamma}\overline{\Psi}\gamma^\mu P^\alpha{}_\mu\Psi\Big) = \\ &= i\big(\mathcal{D}_\alpha\overline{\Psi}\big)\gamma^\mu P^\alpha{}_\mu\Psi + m\overline{\Psi}\Psi - \frac{1}{\sqrt{-\gamma}}\partial_\alpha\Big(\sqrt{-\gamma}\overline{\Psi}\gamma^\mu P^\alpha{}_\mu\Psi\Big),\end{aligned} \tag{4.17}$$

where the last term $\frac{1}{\sqrt{-\gamma}}\partial_\alpha\Big(\sqrt{-\gamma}\overline{\Psi}\gamma^\mu P^\alpha{}_\mu\Psi\Big)$ is a total divergent over the spatial surface[4], and γ is the determinant of the metric of the spatial surface[5].

The Poisson bracket relations are defined as

$$\{A,B\} = \int_{\Omega_\tau}\mathrm{d}^3x\,\sqrt{-\gamma}\left(\frac{\delta A}{\delta\Psi}\frac{\delta B}{\delta\Pi_1} + \frac{\delta A}{\delta\overline{\Psi}}\frac{\delta B}{\delta\Pi_2} - \frac{\delta B}{\delta\Psi}\frac{\delta A}{\delta\Pi_1} - \frac{\delta B}{\delta\overline{\Psi}}\frac{\delta A}{\delta\Pi_2}\right), \tag{4.18}$$

[3] It was used the relation

$$(\mathcal{D}_\mu\overline{\Psi})\gamma^\mu\Psi = \frac{\sqrt{-g}}{\sqrt{-g}}\mathcal{D}_\mu(\overline{\Psi}\gamma^\mu\Psi) - \overline{\Psi}\gamma^\mu\mathcal{D}_\mu\Psi = \frac{1}{\sqrt{-g}}\partial_\mu(\sqrt{-g}\overline{\Psi}\gamma^\mu\Psi) - \overline{\Psi}\gamma^\mu\mathcal{D}_\mu\Psi,$$

paying attention to the relation $\mathcal{D}_\mu\big(\overline{\Psi}\gamma^\mu\Psi\big) = \nabla_\mu\big(\overline{\Psi}\gamma^\mu\Psi\big)$,because $\overline{\Psi}\gamma^\mu\Psi$ is a vector.

[4] It was used the relation

$$(\mathcal{D}_\alpha\overline{\Psi})\gamma^\mu P^\alpha{}_\mu\Psi = \frac{\sqrt{-\gamma}}{\sqrt{-\gamma}}\mathcal{D}_\alpha(\overline{\Psi}\gamma^\mu P^\alpha{}_\mu\Psi) - \overline{\Psi}\gamma^\mu P^\alpha{}_\mu\mathcal{D}_\alpha\Psi = \frac{1}{\sqrt{-\gamma}}\partial_\alpha(\sqrt{-\gamma}\overline{\Psi}\gamma^\mu P^\alpha{}_\mu\Psi) - \overline{\Psi}\gamma^\mu P^\alpha{}_\mu\mathcal{D}_\alpha\Psi,$$

paying attention to the relation $\mathcal{D}_\alpha\big(\overline{\Psi}\gamma^\mu P^\alpha{}_\mu\Psi\big) = \nabla^3_\alpha\big(\overline{\Psi}\gamma^\mu P^\alpha{}_\mu\Psi\big)$,because $\overline{\Psi}\gamma^\mu P^\alpha{}_\mu\Psi$ is a vector over the space surface; where ∇^3_μ is the covariant derivative over the spatial surface.

[5] The metric in the spatial surface is defined by

$$g^3{}_{\mu\nu} = g_{\mu\nu} - N^2\,\mathrm{d}\tau_\mu\,\mathrm{d}\tau_\mu$$

.

where Ω_τ is the spatial equal time τ surface, and whereby

$$\{\Psi(x,t),\Psi(x',t')\} = 0; \tag{4.19a}$$
$$\left\{\overline{\Psi}(x,t),\Psi(x',t')\right\} = 0; \tag{4.19b}$$
$$\{\Psi(x,t),\Pi_1(x',t')\} = \delta^{(3)}(x,t,x',t'); \tag{4.19c}$$
$$\left\{\overline{\Psi}(x,t),\Pi_2(x',t')\right\} = \delta^{(3)}(x,t,x',t'). \tag{4.19d}$$

where $\tau(x,t) = \tau(x',t')$ and

$$\int_{\Omega_\tau} \mathrm{d}^3x\,\sqrt{-\gamma}\delta^{(3)}(x,t,x',t')f(x,t) = f(x',t'). \tag{4.20}$$

With the Hamiltonian density defined in (4.17), the momentum in (4.16) and the Poisson bracket (4.18), the Hamilton equations of motion for Ψ is

$$\begin{aligned}\{\Pi_2,\mathcal{H}\} = \dot{\Pi}_2 &= -i(\partial_\tau)^\mu\mathcal{D}_\mu(\gamma^\alpha L_\alpha\Psi) = -i\gamma^\alpha L_\alpha(\partial_\tau)^\mu\mathcal{D}_\mu\Psi = \\ &= -i\gamma^\alpha L_\alpha\dot{\Psi} = i\gamma^\mu P^\alpha{}_\mu\,\mathcal{D}_\alpha\Psi - m\Psi \\ \Rightarrow &i\gamma^\mu\Big[P^\alpha{}_\mu + L_\mu(\partial_\tau)^\alpha\Big]\mathcal{D}_\alpha\Psi - m\Psi = i\gamma^\mu\mathcal{D}_\mu\Psi - m\Psi = 0\end{aligned} \tag{4.21a}$$

and for $\overline{\Psi}$ reads

$$\begin{aligned}\{\Pi_1,\mathcal{H}\} = \dot{\Pi}_1 &= \Big(\mathcal{D}_\mu\overline{\Psi}\Big)i\gamma^\alpha L_\alpha(\partial_\tau)^\mu = i\dot{\overline{\Psi}}\gamma^\alpha L_\alpha = -i\Big(\mathcal{D}_\alpha\overline{\Psi}\Big)\gamma^\mu P^\alpha{}_\mu - m\Psi \\ \Rightarrow &i\Big(\mathcal{D}_\alpha\overline{\Psi}\Big)\gamma^\mu\Big[P^\alpha{}_\mu + L_\mu(\partial_\tau)^\alpha\Big] + m\overline{\Psi} = i\Big(\mathcal{D}_\mu\overline{\Psi}\Big)\gamma^\mu + m\overline{\Psi} = 0\end{aligned} \tag{4.21b}$$

The fermions are described by the field $\Psi(x,t)$ which carries its degrees of freedom. Such field is a solution of the Dirac equation for curved space-times[6] that comes from Hamilton equations (4.21).

The full Hamiltonian of the fermionic field with respect to τ is, using the equations of motion (4.21), and the Hamiltonian density (4.17),

$$\begin{aligned}\mathrm{H} &= \int_{\Omega_\tau}\mathrm{d}^3x\,\sqrt{-\gamma}\mathcal{H} = \\ &= \int_{\Omega_\tau}\mathrm{d}^3x\,\sqrt{-\gamma}\Big\{-\frac{i}{2}\Big[\overline{\Psi}\gamma^\mu P^\alpha{}_\mu\,\mathcal{D}_\alpha\Psi - \Big(\mathcal{D}_\alpha\overline{\Psi}\Big)\gamma^\mu P^\alpha{}_\mu\,\Psi\Big] + m\overline{\Psi}\Psi\Big\} = \\ &= \frac{i}{2}\int_{\Omega_\tau}\mathrm{d}^3x\,\sqrt{-\gamma}L_\alpha\Big(\overline{\Psi}\gamma^\alpha\dot{\Psi} - \dot{\overline{\Psi}}\gamma^\alpha\Psi\Big) \\ &= \frac{i}{2}\int_{\Omega_\tau}\mathrm{d}^3x\,\sqrt{-\gamma}L_\alpha\left(\overline{\Psi}\gamma^\alpha\frac{\partial}{\partial\tau}(\Psi) - \frac{\partial}{\partial\tau}\Big(\overline{\Psi}\Big)\gamma^\alpha\Psi + (\partial_\tau)^\mu\overline{\Psi}(\gamma^\alpha\Gamma_\mu + \Gamma_\mu\gamma^\alpha)\Psi\right)\end{aligned} \tag{4.22}$$

[6] There is more than one Dirac equation for curved space-times [76]. The equations (4.21) uses Dirac-Fock-Weyl development [77, 78], which is the standard equation for fermions in curved space-times.

4.1.1 Dirac equation in a homogeneous and isotropic Universe

In the FRLW Universe, in terms of the conformal time, the metric is given by

$$g_{\mu\nu} = a^2(\eta)\eta_{\mu\nu} \doteq a^2(\eta)\begin{pmatrix} 1 & 0 & 0 & 0 \\ 0 & -1 & 0 & 0 \\ 0 & 0 & -1 & 0 \\ 0 & 0 & 0 & -1 \end{pmatrix}, \tag{4.23}$$

From (4.8), the tetrad read

$$e_{\mu}{}^{(A)} = \delta_{\mu}^{(A)} a(\eta); \tag{4.24a}$$
$$e^{\mu}{}_{(A)} = \delta^{\mu}_{(A)} a^{-1}(\eta), \tag{4.24b}$$

where the tetrad indice is a capital latin label. It means that $e_{\nu(D)}$ is a one form, not a tensor of rank 2. From equations (4.24), the quantity

$$e_{\nu(D);\mu} = e_{\nu(D),\mu} - \Gamma^{\alpha}_{\nu\mu} e_{\alpha(D)} = g_{\alpha\nu}\delta^{\alpha}_{(D)}\left(a^{-1}\right)_{,\mu} + a'\left(\eta_{\nu\mu}\delta^{0}_{(D)} + \eta_{\nu(D)}\delta^{0}_{\mu} - \delta^{0}_{\nu}\eta_{\mu(D)}\right), \tag{4.25}$$

is a tensor of rank 2.

Equation (4.24) applied to (4.6) yields

$$\gamma^{\mu} = \frac{\gamma^{(A)}\delta^{\mu}_{(A)}}{a(\eta)}. \tag{4.26}$$

Applying equation (4.25), equations (4.24) and equation (4.9) give

$$\Gamma_{\mu} = \frac{aH}{2}\left(\gamma_{(A)}\gamma^{(0)} - \delta^{(0)}_{(A)}\right)\delta^{(C)}_{\mu} = -\frac{aH}{2}\left(\gamma^{(0)}\gamma_{(A)} - \delta^{(0)}_{(A)}\right)\delta^{(C)}_{\mu}; \tag{4.27a}$$
$$\gamma^{\mu}\Gamma_{\mu} = \frac{3}{2}H\gamma^{(0)}; \tag{4.27b}$$
$$\Gamma_{\mu}\gamma^{\mu} = -\frac{3}{2}H\gamma^{(0)}, \tag{4.27c}$$

where $H = \frac{a'}{a^2}$ is the Hubble function.

Hence the Dirac equations (4.21), using (4.27), becomes

$$\left(i\frac{\gamma^{(A)}\delta^{\mu}_{(A)}}{a}\partial_{\mu} + i\frac{3}{2}H\gamma^{(0)} - ma\right)\Psi = 0; \tag{4.28a}$$
$$i\partial_{\mu}\overline{\Psi}\frac{\gamma^{(A)}\delta^{\mu}_{(A)}}{a} + i\frac{3}{2}H\overline{\Psi}\gamma^{(0)} + ma\overline{\Psi} = 0. \tag{4.28b}$$

Using (4.7), without lost of generality, it is choosen a set of constant Dirac matrices such that

$$\begin{aligned} h_s &= \gamma^{(0)} \\ \Rightarrow h_s \neq \gamma^0 &= \frac{\gamma^{(0)}}{a} \\ \Rightarrow {\gamma^{(A)}}^\dagger &= \gamma^{(0)}\gamma^{(A)}{\gamma^{(0)}}^{-1}; \\ \Rightarrow {\gamma^{(0)}}^\dagger &= \gamma^{(0)} = {\gamma^{(0)}}^{-1}; \\ \Rightarrow {\gamma^{(A)}}^\dagger &= -\gamma^{(A)} = {\gamma^{(A)}}^{-1} \quad \text{for} \quad A \neq 0. \end{aligned} \tag{4.29}$$

There are two possible standard foliations of the FRLW Universe: The cosmic time t and the conformal time η, where $\mathrm{d}t = a\,\mathrm{d}\eta$. For cosmic time foliation one gets

$$(\partial_t)^\mu = \frac{\partial x^\mu}{\partial t} = \frac{\partial \eta}{\partial t}\delta_0^\mu = a^{-1}\delta_0^\mu \tag{4.30a}$$

$$(\partial_t)_\alpha(\partial_t)^\alpha = a^{-1}\delta_0^\mu a^{-1}\delta_0^\beta g_{\alpha\beta} = 1 \tag{4.30b}$$

$$L_\nu^{(t)} = \frac{(\partial_t)^\mu}{(\partial_t)_\alpha(\partial_t)^\alpha} g_{\mu\nu} = a\delta_\nu^0 \tag{4.30c}$$

$$P^{(t)\mu}{}_\nu = \delta_\nu^\mu - \delta_\nu^0\delta_0^\mu \tag{4.30d}$$

$$L_\nu^{(t)}\gamma^\nu = a\delta_\nu^0\frac{\delta^\nu_{(A)}}{a}\gamma^{(A)} = \gamma^{(0)} \tag{4.30e}$$

$$(\partial_t)^\mu\Gamma_\mu = \frac{Ha}{2}\left(\gamma^{(0)}\gamma_{(A)} - \delta^{(0)}_{(A)}\right)\delta^{(A)}_\mu a^{-1}\delta_0^\mu = 0 \tag{4.30f}$$

$$\mathrm{d}t^\mu\,\mathrm{d}t_\mu = N^{-2} = \frac{\partial t}{\partial x^\mu}\frac{\partial t}{\partial x^\nu}g^{\mu\nu} = 1 \tag{4.30g}$$

$$\gamma_{\mu\nu} = g_{\mu\nu} - N^2\,\mathrm{d}t_\mu\,\mathrm{d}t_\nu \doteq \begin{pmatrix} 0 & 0 & 0 & 0 \\ 0 & -a^2 & 0 & 0 \\ 0 & 0 & -a^2 & 0 \\ 0 & 0 & 0 & -a^2 \end{pmatrix} \tag{4.30h}$$

$$\sqrt{-\gamma} = a^3 \tag{4.30i}$$

$$\delta^{(3)}(x,\eta,x',\eta') = \frac{1}{a^3}\delta(x-x') \tag{4.30j}$$

$$\Pi_1 = i\overline{\Psi}\gamma^{(0)} = i\Psi^\dagger \tag{4.30k}$$

$$\Pi_2 = -i\gamma^{(0)}\Psi \tag{4.30l}$$

Using the (4.30) and (4.22), the hamiltonian for cosmic time foliation is

$$\begin{aligned}
\mathrm{H}^{(t)} &= -a^3 \int_{\Omega_t} \mathrm{d}^3x \left(i\overline{\Psi}\gamma^i\partial_i\Psi + \frac{3}{2}H\overline{\Psi}\gamma^{(0)}\Psi - m\overline{\Psi}\Psi \right) + \text{Const} = \\
&= a^3 \int_{\Omega_t} \mathrm{d}^3x \left[i\big(\partial_i\overline{\Psi}\big)\gamma^i\Psi - \frac{3}{2}H\overline{\Psi}\gamma^{(0)}\Psi + m\overline{\Psi}\Psi \right] - \text{Const} = \\
&= \frac{ia^3}{2} \int_{\Omega_t} \mathrm{d}^3x \left[\overline{\Psi}\gamma^{(0)}\partial_t\Psi - \big(\partial_t\overline{\Psi}\big)\gamma^{(0)}\Psi \right] = \\
&= \frac{ia^2}{2} \int_{\Omega_t} \mathrm{d}^3x \left[\overline{\Psi}\gamma^{(0)}\partial_\eta\Psi - \big(\partial_\eta\overline{\Psi}\big)\gamma^{(0)}\Psi \right] = \\
&= \frac{ia^2}{2} \int_{\Omega_t} \mathrm{d}^3x \left[\Psi^\dagger\partial_\eta\Psi - \big(\partial_\eta\Psi^\dagger\big)\Psi \right] = \\
&= \frac{i}{2a} \int_{\Omega_t} \mathrm{d}^3x \left[\big(a^{3/2}\Psi^\dagger\big)\partial_\eta\big(a^{3/2}\Psi\big) - \big(\partial_\eta a^{3/2}\Psi^\dagger\big)\big(a^{3/2}\Psi\big) \right] = \\
&= \frac{i}{2a} \int_{\Omega_t} \mathrm{d}^3x \left[\chi^\dagger\partial_\eta\chi^\dagger - \big(\partial_\eta\chi^\dagger\big)\chi \right],
\end{aligned} \tag{4.31}$$

where $\chi = a^{3/2}\Psi$. The "Const" term comes from a spatial divergence, given in the equation (4.17), and the summation over i goes from 1 to 3.

For the conformal time foliation

$$(\partial_\eta)^\mu = \frac{\partial x^\mu}{\partial\eta} = \frac{\partial\eta}{\partial\eta}\delta_0^\mu = \delta_0^\mu \tag{4.32a}$$

$$(\partial_\eta)_\alpha(\partial_\eta)^\alpha = \delta_0^\mu\delta_0^\beta g_{\alpha\beta} = a^2 \tag{4.32b}$$

$$L_\nu^{(\eta)} = \frac{(\partial_\eta)^\mu}{(\partial_\eta)_\alpha(\partial_\eta)^\alpha} g_{\mu\nu} = \delta_\nu^0 \tag{4.32c}$$

$$P^{(\eta)\mu}{}_\nu = \delta_\nu^\mu - \delta_\nu^0\delta_0^\mu \tag{4.32d}$$

$$L_\nu^{(\eta)}\gamma^\nu = \delta_\nu^0\frac{\delta_{(A)}^\nu}{a}\gamma^{(A)} = \frac{\gamma^{(0)}}{a} \tag{4.32e}$$

$$(\partial_\eta)^\mu\Gamma_\mu = \frac{Ha}{2}\big(\gamma^{(0)}\gamma_{(A)} - \delta_{(A)}^{(0)}\big)\delta_\mu^{(A)}\delta_0^\mu = 0 \tag{4.32f}$$

$$\mathrm{d}\eta^\mu\,\mathrm{d}\eta_\mu = N^{-2} = \frac{\partial\eta}{\partial x^\mu}\frac{\partial\eta}{\partial x^\nu}g^{\mu\nu} = a^{-2} \tag{4.32g}$$

$$\gamma_{\mu\nu} = g_{\mu\nu} - N^2\,\mathrm{d}\eta_\mu\,\mathrm{d}\eta_\nu \doteq \begin{pmatrix} 0 & 0 & 0 & 0 \\ 0 & -a^2 & 0 & 0 \\ 0 & 0 & -a^2 & 0 \\ 0 & 0 & 0 & -a^2 \end{pmatrix} \tag{4.32h}$$

$$\sqrt{-\gamma} = a^3 \tag{4.32i}$$

$$\delta^{(3)}(x,\eta,x',\eta') = \frac{1}{a^3}\delta(x-x') \tag{4.32j}$$

$$\Pi_1 = \frac{i}{a}\overline{\Psi}\gamma^{(0)} = i\Psi^\dagger \tag{4.32k}$$

$$\Pi_2 = -\frac{i}{a}\gamma^{(0)}\Psi \tag{4.32l}$$

Using the (4.30) and (4.22), the hamiltonian for cosmic time foliation is

$$\mathrm{H}^{(\eta)} = \frac{ia^2}{2}\int_{\Omega_t} \mathrm{d}^3x \left[\overline{\Psi}\partial_\eta\Psi - \left(\partial_\eta\overline{\Psi}\right)\Psi\right] = \mathrm{H}^{(t)} \equiv \mathrm{H}. \tag{4.33}$$

4.2 Creation of particles

In the previous section , it was obtained in equation (4.28) for the classical Dirac equation in a FLRW Universe. In this section the theory of creation of particles will be developed for the Unvierse, in which the scale factor is given by (2.15).

In this section, the fields are quantized by replacing the functions Ψ and $\overline{\Psi}$ by the operators $\hat{\Psi}$ and $\hat{\overline{\Psi}}$, that satisfy the equal time anti-commutation rules [43]

$$\left\{\hat{\Psi}(x,\eta), \hat{\Psi}^\dagger(x',\eta)\right\} = \delta^{(3)}(x-x') = \frac{\delta(x-x')}{a^3} \tag{4.34a}$$

$$\left\{\hat{\Psi}(x,\eta), \hat{\Psi}(x',\eta)\right\} = 0. \tag{4.34b}$$

The quantized hamiltinan is, from (4.31)

$$\begin{aligned}\hat{\mathrm{H}} &= -a^3\int_{\Omega_t}\mathrm{d}^3x\left(i\hat{\overline{\Psi}}\gamma^i\partial_i\hat{\Psi} + \frac{3}{2}H\hat{\overline{\Psi}}\gamma^{(0)}\hat{\Psi} - m\hat{\overline{\Psi}}\hat{\Psi}\right) + \hat{\mathrm{Const}} = \\ &= a^3\int_{\Omega_t}\mathrm{d}^3x\left[i\left(\partial_i\hat{\overline{\Psi}}\right)\gamma^i\hat{\Psi} - \frac{3}{2}H\hat{\overline{\Psi}}\gamma^{(0)}\hat{\Psi} + m\hat{\overline{\Psi}}\hat{\Psi}\right] - \hat{\mathrm{Const}}.\end{aligned} \tag{4.35}$$

The Heisenberg equations of motion are

$$\begin{aligned}\dot{\Psi} = \frac{1}{a}\partial_\eta\Psi &= -i\left[\hat{\Psi}, \hat{\mathrm{H}}\right] = \\ &= -a^3\int_{\Omega_t}\mathrm{d}^3x\left(i\left\{\hat{\Psi}, \hat{\Psi}^\dagger\right\}\gamma^{(0)}\gamma^i\partial_i\hat{\Psi} - i\left\{\hat{\Psi}, \partial_i\hat{\Psi}\right\}\overline{\Psi}\gamma^i + \right. \\ &\quad + \frac{3}{2}H\left\{\hat{\Psi}, \hat{\Psi}^\dagger\right\}\hat{\Psi} - \frac{3}{2}H\left\{\hat{\Psi}, \hat{\Psi}\right\}\hat{\Psi}^\dagger + \\ &\quad \left. - m\left\{\hat{\Psi}, \hat{\Psi}^\dagger\right\}\gamma^{(0)}\hat{\Psi} + m\left\{\hat{\Psi}, \hat{\Psi}\right\}\overline{\Psi}\right) = \\ &= -i\gamma^{(0)}\gamma^i\partial_i\hat{\Psi} - \frac{3}{2}H\hat{\Psi} + m\gamma^{(0)}\hat{\Psi} \\ \Rightarrow 0 &= \left(\frac{i}{a}\gamma^{(A)}\delta^\mu_{(A)}\partial_\mu + i\frac{3}{2}H\gamma^{(0)} - m\right)\hat{\Psi}.\end{aligned} \tag{4.36}$$

The quantum non-charged fermionic field operator that describe the degrees of freedom in a homogeneous and isotropic Universe obeys the Dirac equation (4.36)

$$\left(i\frac{\gamma^{(A)}}{a}\delta^\mu_{(A)}\partial_\mu + i\frac{3}{2}H\gamma^{(0)} - m\right)\hat{\Psi}(x) = 0, \tag{4.37}$$

where H is the Hubble rate given by $H = \frac{a'}{a^2}$.

The differential equation (4.37) commutes with spatial translations and rotations. Therefore the spinor operator $\hat{\Psi}$ can be separated in spatial translation and rotation basis

with time independent indices. It means that each Fourier mode of the field can evolve independently and does not depend on the direction.

The same does not happen with time translations. The differential equation in (4.37) does not commute with temporal translations, therefore coefficients of the temporal translations basis do not evolves independently. In practice this means that the spinor operator cannot be expanded in independent temporal frequency modes. In fact, the time dependency will be described by functions with mixed time-frequencies.

The equation (4.37) can be simplified by using $\hat{\chi}(x) = a^{\frac{3}{2}}\hat{\Psi}(x)$

$$\Big(i\gamma^{(A)}\delta^{\mu}_{(A)}\partial_{\mu} - ma(\eta)\Big)\hat{\chi}(x,\eta) = 0. \tag{4.38}$$

The equation (4.38) is a variable mass Dirac equation, which one of its properties is the non conservation of particle number.

In the momentum representation, the spinor operator $\hat{\chi}(x,\eta)$ is divided in Fourier modes

$$\hat{\chi}(x,\eta) = \frac{1}{(2\pi)^{\frac{3}{2}}}\int \mathrm{d}^3\vec{\mathbf{k}}\, e^{-i\vec{\mathbf{k}}\cdot\vec{\mathbf{x}}}\hat{\chi}(\vec{\mathbf{k}},\eta), \tag{4.39}$$

which satisfies the equation

$$\Big(i\gamma^{(0)}\partial_{\eta} + \vec{\gamma}\cdot\vec{\mathbf{k}} - ma(\eta)\Big)\hat{\chi}(\vec{\mathbf{k}},\eta) = 0. \tag{4.40}$$

The spinor part of the field in momentum representation can also be separated in a basis generated by the eigen-vectors of the helicity h and $\gamma^{(0)}$. These two matrices commute and their eigen-vectors form a basis $S_{l,j}$ for the 4-dim spinor, where l is for $\gamma^{(0)}$ eigen-values and j for h. Explicitly

$$\hat{\chi}(\vec{\mathbf{k}},\eta) = \sum_{l,j} S_{l,j}(\vec{\mathbf{k}})\hat{O}_{l,j}(\vec{\mathbf{k}},\eta), \tag{4.41}$$

where $\hat{O}$ are the coefficients of the expansion.

The helicity can be expressed by [79]

$$h = \gamma^{(0)}\vec{\gamma}\gamma 5\cdot\hat{\mathbf{k}}, \tag{4.42}$$

where

$$\gamma 5 = -i\frac{\sqrt{-g}}{4}\epsilon_{\alpha\beta\sigma\theta}\gamma^{\alpha}\gamma^{\beta}\gamma^{\sigma}\gamma^{\theta} = i\gamma^{(0)}\gamma^{(1)}\gamma^{(2)}\gamma^{(3)}, \tag{4.43}$$

where the final equality was only possible due to (4.6). In general coordinates, $\gamma 5$ is not constant.

Without loss of generality, it is chosen a basis $S_{l,j}$ that has the following properties:

$$\mathrm{h}S_{l,j} = jS_{l,j}; \tag{4.44a}$$
$$\gamma^{(0)}S_{l,j} = lS_{l,j}; \tag{4.44b}$$
$$\gamma 5 S_{l,j} = -jS_{-l,j}. \tag{4.44c}$$
$$S^{\dagger}_{l,j}S_{m,n} = \frac{1}{2}\delta_{lm}\delta_{jn} \tag{4.44d}$$

Equations (4.44) define a basis uniquely, including its phase (4.44c).

Applying the $\gamma 5\gamma^{(0)}$ operator to the equation (4.40), one obtains

$$\begin{aligned}
\gamma 5\gamma^{(0)}\left(i\gamma^{(0)}\partial_\eta + \vec{\gamma}\cdot\vec{\mathbf{k}} - ma(\eta)\right)\hat{\chi}(\vec{\mathbf{k}},\eta) = 0 = \\
= \left(i\gamma 5\partial_0 + \left(\gamma^{(0)}\vec{\gamma}\gamma 5\cdot\hat{\mathbf{k}}\right)k - ma(\eta)\gamma 5\gamma^{(0)}\right)\sum_{l,j} S_{l,j}(\vec{\mathbf{k}})\hat{O}_{l,j}(\vec{\mathbf{k}},\eta) = \\
\left(i\gamma 5\partial_0 + \mathrm{h}k - ma(\eta)\gamma 5\gamma^{(0)}\right)\sum_{l,j} S_{l,j}(\vec{\mathbf{k}})\hat{O}_{l,j}(\vec{\mathbf{k}},\eta) = \\
\sum_{l,j}\left(i(-jS_{-l,j})\partial_0\hat{O}_{l,j} + jkS_{l,j}\hat{O}_{l,j} + jlma(\eta)S_{-l,j}\hat{O}_{l,j}\right) = 0 \\
\therefore i\partial_0\hat{O}_{l,j}(\vec{\mathbf{k}},\eta) - k\hat{O}_{-l,j}(\vec{\mathbf{k}},\eta) - lma(\eta)\hat{O}_{l,j}(\vec{\mathbf{k}},\eta) = 0,
\end{aligned} \tag{4.45}$$

where $k = \left\|\vec{\mathbf{k}}\right\|$ is the norm of the $\vec{\mathbf{k}}$ vector.

Explicitly, equation (4.45) has the form

$$i\partial_0\hat{O}_{1,j}(\vec{\mathbf{k}},\eta) - k\hat{O}_{-1,j}(\vec{\mathbf{k}},\eta) - ma(\eta)\hat{O}_{1,j}(\vec{\mathbf{k}},\eta) = 0 \tag{4.46a}$$
$$i\partial_0\hat{O}_{-1,j}(\vec{\mathbf{k}},\eta) - k\hat{O}_{1,j}(\vec{\mathbf{k}},\eta) + ma(\eta)\hat{O}_{-1,j}(\vec{\mathbf{k}},\eta) = 0 \tag{4.46b}$$

which can be joined to a second order l independent equation

$$\hat{O}''_{\pm 1,j}(\vec{\mathbf{k}},\eta) + \left(\omega^2 \pm ima'(\eta)\right)\hat{O}_{\pm 1,\eta}(\vec{\mathbf{k}},\eta) = 0, \tag{4.47}$$

where $\omega^2 = k^2 + m^2a^2(\eta)$. The equation (4.47) has two linearly independent solutions. One is associated to particles ($u_\pm$) and the other to anti-particles ($v_\pm$)

$$\hat{O}_{\pm 1,j}(\vec{\mathbf{k}},\eta) = u_\pm(\vec{\mathbf{k}},\eta)\hat{a}_j(\vec{\mathbf{k}}) + v_\pm(\vec{\mathbf{k}},\eta)\hat{b}^{\dagger}(-\vec{\mathbf{k}}), \tag{4.48}$$

where $\hat{a}_j(\vec{\mathbf{k}})$ ($\hat{b}^{\dagger}_j(-\vec{\mathbf{k}})$) is the annihilation (creation) operator for a particle (anti-particle) with momentum $\vec{\mathbf{k}}$ ($-\vec{\mathbf{k}}$) and helicity j.

The particle and anti-particle association with the linearly independent solutions of equation (4.47) depends on the existence of a period of time where it is possible to separate the solution in positive (particles) and negative (anti-particles) frequencies. For the analyzed model, it happens in $\eta \to -\infty$ and $\eta \to \infty$. For other times, equation

(4.47) mixes positive and negative frequencies, losing a unique description of particle and anti-particle. This happens in de-Sitter Universes.

The relation between u_+ (v_+) and u_- (v_-) is obtained by applying the equation (4.48) to the equations (4.46)

$$u'_+(\vec{\mathbf{k}},\eta) = iku_-(\vec{\mathbf{k}},\eta) - ima(\eta)u_+(\vec{\mathbf{k}},\eta) \tag{4.49a}$$
$$u'_-(\vec{\mathbf{k}},\eta) = iku_+(\vec{\mathbf{k}},\eta) + ima(\eta)u_-(\vec{\mathbf{k}},\eta) \tag{4.49b}$$

where $v_\pm$ satisfy the same equations. Equation (4.49) preserves the quantity

$$|u_+|^2 + |u_-|^2 = 2, \tag{4.50}$$

and the same is valid for $v_\pm$[7].

Similarly to the (4.47), $u_\pm$ has a second order equation

$$u''_\pm(\vec{\mathbf{k}},\eta) + \Big(\omega^2 \pm ima(\eta)\Big)u_\pm(\vec{\mathbf{k}},\eta) = 0. \tag{4.51}$$

If $u_+(\vec{\mathbf{k}},\eta)$ is a solution of the equation (4.51), then the function $u^*_-(k,\eta)$ is a linear independent solution of the same equation[8]. It implies that, with a choice of phase,

$$v_\pm = \mp u^*_\mp. \tag{4.52}$$

So the functions u_+ and v_+ (u_- and v_-) are linear independent solutions of equation (4.47) that represents particles ($u_\pm$) and anti-particles ($v_\pm$). $\hat{\chi}(\vec{\mathbf{k}},\eta)$ can be rewritten in terms of particle and anti-particle representation

$$\hat{\chi}(\vec{\mathbf{k}},\eta) = \sum_j U_j(\vec{\mathbf{k}},\eta)\hat{a}_j(\vec{\mathbf{k}}) + V_j(\vec{\mathbf{k}},\eta)\hat{b}^\dagger_j(-\vec{\mathbf{k}}), \tag{4.53}$$

where V_j and U_j are spinors given by

$$U_j(\vec{\mathbf{k}},\eta) = u_+(\vec{\mathbf{k}},\eta)S_{1,j}(\vec{\mathbf{k}}) + u_-(\vec{\mathbf{k}},\eta)S_{-1,j}(\vec{\mathbf{k}}) \tag{4.54a}$$
$$V_j(\vec{\mathbf{k}},\eta) = v_+(\vec{\mathbf{k}},\eta)S_{1,j}(\vec{\mathbf{k}}) + v_-(\vec{\mathbf{k}},\eta)S_{-1,j}(\vec{\mathbf{k}}) = \tag{4.54b}$$
$$= -u^*_-(\vec{\mathbf{k}},\eta)S_{1,j} + u^*_+(\vec{\mathbf{k}},\eta)S_{-1,j}(\vec{\mathbf{k}}) \tag{4.54c}$$

By the definitions of U_l and V_l in (4.54), one obtains the following important properties:

$$U^\dagger_j V_m = 0, \quad \frac{\partial}{\partial\eta}(U^\dagger_j V_m) = 0, \quad \bar{U}_j\frac{\partial}{\partial\eta}V_j - \left(\frac{\partial}{\partial\eta}\bar{U}_j\right)V_j = 0, \quad U^\dagger_j U_m = V^\dagger_j V_m = \delta_{jm} \quad .$$

[7] It was chosen, without any loss of generality, the value 1 for the sum in the equation (4.50).

[8] The Wronskian of u_+ and u^*_- is constant, which makes then linearly independent. In fact, from (4.49)

$$W(u_+,u^*_-) = u'_+u^*_- - u_+u'^*_- = ik(|u_+|^2 + |u_-|^2) = ik$$

Therefore, the field operator $\hat{\Psi}(x)$ in terms of the defined quantities above reads

$$\hat{\chi}(x) = \frac{1}{(2\pi)^{3/2}} \sum_j \int \mathrm{d}^3\vec{\mathbf{k}}\, e^{-i\vec{\mathbf{k}}\cdot\vec{\mathbf{x}}} \Big(U_j(\vec{\mathbf{k}},\eta)\hat{\mathbf{a}}_j(\vec{\mathbf{k}}) + V_j(\vec{\mathbf{k}},\eta)\hat{\mathbf{b}}_j^\dagger(-\vec{\mathbf{k}},\eta) \Big) \tag{4.55}$$

From (4.31), the Hamiltonian of the fermionic particles is given by

$$\hat{\mathrm{H}} = \frac{i}{2a} \int_{\Omega_t} \mathrm{d}^3x \left[\hat{\chi}^\dagger \partial_\eta \hat{\chi}^\dagger - \left(\partial_\eta \hat{\chi}^\dagger \right) \hat{\chi} \right] \tag{4.56}$$

From the canonical anti-commutation relations (4.34), one gets

$$\{\hat{a}_j(\vec{\mathbf{k}}), \hat{a}_m^\dagger(\vec{\mathbf{k}}')\} = \{\hat{b}_j(\vec{\mathbf{k}}), \hat{b}_m^\dagger(\vec{\mathbf{k}}')\} = \delta_{jm}\delta(\vec{\mathbf{k}} - \vec{\mathbf{k}}') \quad , \tag{4.57}$$

and null for the other combinations.

Substituting Eqs. (4.54) and (4.55) into the Hamiltonian, quations (4.56) one obtains

$$\begin{aligned} H = \int d^3\vec{k} \sum_j \Big\{ & E_k(\eta) \left[\hat{a}_j^\dagger(\vec{\mathbf{k}})\hat{a}_j(\vec{\mathbf{k}}) - \hat{b}_j(-k)\hat{b}_j^\dagger(-\vec{\mathbf{k}}) \right] + \\ & + F_k(\eta)\hat{b}_j(-\vec{\mathbf{k}})\hat{a}_j(\vec{\mathbf{k}}) + F_k^*(\eta)\hat{a}_j^\dagger(\vec{\mathbf{k}})\hat{b}_j^\dagger(-\vec{\mathbf{k}}) \Big\} \quad , \end{aligned} \tag{4.58}$$

where

$$\omega_k(\eta) = \sqrt{k^2 + m^2a^2(\eta)} \quad , \tag{4.59}$$

$$E_k(\eta) = -\Big(kRe\left(u_+^* u_- \right) + ma(\eta)\left(1 - |u_+|^2 \right) \Big) \quad , \tag{4.60}$$

$$F_k(\eta) = -\left(\frac{k}{2}\left(u_+^2 - u_-^2 \right) + ma(\eta)u_+u_- \right) \quad , \tag{4.61}$$

$$E_k^2 + |F_k|^2 = \omega_k^2 \quad , \quad -\omega_k \leq E_k \leq \omega_k \quad . \tag{4.62}$$

One can diagonalize the Hamiltonian (4.58) through the Bogoliubov transformation [80]:

$$\hat{\hat{a}}_j(\vec{\mathbf{k}}) = \alpha_k(\eta)\hat{a}_j(\vec{\mathbf{k}}) + \beta_k(\eta)\hat{b}_l^\dagger(-\vec{\mathbf{k}}) \quad , \tag{4.63a}$$

$$\hat{\hat{b}}_j(\vec{\mathbf{k}}) = -\beta_k^*(\eta)\hat{a}_j(\vec{\mathbf{k}}) + \alpha_k^*(\eta)\hat{b}_l^\dagger(-\vec{\mathbf{k}}) \quad , \tag{4.63b}$$

where $\alpha_k(\eta)$ and $\beta_k(\eta)$ satisfy

$$\alpha_k(\eta) = \beta_k(\eta)\left(\frac{E_k(\eta) + \omega}{F_k^*(\eta)} \right) \quad , \quad \beta_k(\eta) = \frac{F_k^*(\eta)}{2w(\eta)\alpha_k^*(\eta)} \quad , \tag{4.64}$$

$$|\beta_k(\eta)|^2 = \frac{|F_k(\eta)|^2}{2\omega(\omega + E_k(\eta))} = \frac{\omega - E_k(\eta)}{2\omega} \quad , \tag{4.65}$$

$$|\alpha_k(\eta)|^2 + |\beta_k(\eta)|^2 = 1 \quad , \quad |\alpha_k(\eta)|^2 - |\beta_k(\eta)|^2 = \frac{E_k(\eta)}{w(\eta)} \quad . \tag{4.66}$$

In terms of the new creation and annihilation operators, Eqs (4.63), the normal ordered Hamiltonian operator then reads

$$\hat{\mathrm{H}} = \frac{1}{a}\int d^3\vec{k}\sum_j \omega(\eta)\left[\hat{\bar{a}}_j^\dagger(\vec{\mathbf{k}})\hat{\bar{a}}_j(\vec{\mathbf{k}}) + \hat{\bar{b}}_j^\dagger(\vec{\mathbf{k}})\hat{\bar{b}}_j(\vec{\mathbf{k}})\right] \quad . \tag{4.67}$$

From the Hamiltonian (4.67), an observer will naturally define the vacuum state in some conformal time η as $\hat{\bar{a}}_j(\vec{\mathbf{k}})(\eta)\,|0_\eta\rangle = \hat{\bar{b}}_j(\vec{\mathbf{k}})(\eta)\,|0_\eta\rangle = 0$. In order to obtain the number of particles created, it is necessary to compare the different vacua in different times. This evolution is dictated by the dynamics of $u_+(\eta)$ and $u_-(\eta)$ through equations (4.49).

4.2.1 Convenient description of $u_\pm$

The equations for $u_\pm$ will be rewritten in a more convenient way.

The number of particles is related with the functions $u_\pm$. The differential equations for these functions can be written in matrix form

$$\mathbf{u}' = \mathbf{M}\mathbf{u}, \tag{4.68}$$

where

$$\mathbf{u} = \begin{pmatrix} u_+ \\ u_- \end{pmatrix} \tag{4.69}$$

$$\mathbf{M} = \begin{pmatrix} -ima(\eta) & ik \\ ik & ima(\eta) \end{pmatrix} = -\mathbf{M}^\dagger \tag{4.70}$$

The derivative of the norm, using the equation (4.70), reads

$$\left(\mathbf{u}^\dagger\mathbf{u}\right)' = \mathbf{u}^\dagger\mathbf{M}\mathbf{u} + \mathbf{u}^\dagger\mathbf{M}^\dagger\mathbf{u} = 0, \tag{4.71}$$

This is the property stated in the equation (4.50).

It is possible to rewrite the matrix equation (4.69) in a clear way diagonalizing the matrix $\mathbf{M}$ through a transformation $\mathbf{T}_r$.

$$\mathbf{T}_r\mathbf{M}\mathbf{T}_r^{-1} = \begin{pmatrix} \lambda & 0 \\ 0 & -\lambda \end{pmatrix} \tag{4.72}$$

$$\mathbf{z} = \mathbf{T}_r\mathbf{u} \tag{4.73}$$

$$\mathbf{u}' = (\mathbf{T}_r^{-1}\mathbf{z})' = \left(\mathbf{T}_r^{-1}\right)'\mathbf{z} + \mathbf{T}_r^{-1}\mathbf{u}' = \mathbf{M}\mathbf{T}_r^{-1}\mathbf{z} \tag{4.74}$$

$$\mathbf{z}' = \begin{pmatrix} \lambda & 0 \\ 0 & -\lambda \end{pmatrix}\mathbf{z} - \mathbf{T}_r'\mathbf{T}_r^{-1}\mathbf{z} \tag{4.75}$$

$$\mathbf{Z} = \begin{pmatrix} e^{-i\int\omega\mathrm{d}\eta} & 0 \\ 0 & e^{i\int\omega\mathrm{d}\eta} \end{pmatrix}\mathbf{z} = \begin{pmatrix} \alpha(\vec{\mathbf{k}},\eta) \\ \beta(\vec{\mathbf{k}},\eta) \end{pmatrix} \tag{4.76}$$

$$\therefore \mathbf{Z}' = -\begin{pmatrix} e^{i\int\omega\mathrm{d}\eta} & 0 \\ 0 & e^{-i\int\omega\mathrm{d}\eta} \end{pmatrix}\mathbf{T}_r'\mathbf{T}_r^{-1}\begin{pmatrix} e^{+i\int\omega\mathrm{d}\eta} & 0 \\ 0 & e^{-i\int\omega\mathrm{d}\eta} \end{pmatrix}\mathbf{Z} \tag{4.77}$$

where $\pm\lambda$ are the eigen-values[9] of $\mathbf{M}$. The $\mathbf{T}_r$ matrix can be constructed with the two eigen-vectors of $\mathbf{M}$ of norm 2

$$\mathbf{e}_+ = \begin{pmatrix} \sqrt{1-\frac{ma}{w}} \\ \sqrt{1+\frac{ma}{w}} \end{pmatrix} \tag{4.78}$$

$$\mathbf{e}_- = \begin{pmatrix} \sqrt{1+\frac{ma}{w}} \\ -\sqrt{1+\frac{ma}{w}} \end{pmatrix} \tag{4.79}$$

where

$$\mathbf{M}\mathbf{e}_\pm = \pm i\omega \mathbf{e}_\pm \tag{4.80}$$

So $\mathbf{T}_r$ is formed by a matrix which its lines are the eigen-vectors $\mathbf{e}_\pm^\dagger$, and its inverse is a matrix whose columns are the eigen-vectors $\mathbf{e}_\pm$

$$\mathbf{T}_r = \begin{pmatrix} \mathbf{e}_+^\dagger \\ \mathbf{e}_-^\dagger \end{pmatrix} \tag{4.81}$$

$$\mathbf{T}_r^{-1} = \begin{pmatrix} \mathbf{e}_+ & \mathbf{e}_- \end{pmatrix} \tag{4.82}$$

$$\mathbf{T}_r\mathbf{T}_r^{-1} = \begin{pmatrix} \mathbf{e}_+^\dagger\mathbf{e}_+ & \mathbf{e}_+^\dagger\mathbf{e}_- \\ \mathbf{e}_-^\dagger\mathbf{e}_+ & \mathbf{e}_-^\dagger\mathbf{e}_- \end{pmatrix} = \begin{pmatrix} 1 & 0 \\ 0 & 1 \end{pmatrix} \tag{4.83}$$

$$\mathbf{T}_r'\mathbf{T}_r^{-1} = \begin{pmatrix} \mathbf{e}_+^{\dagger\prime}\mathbf{e}_+ & \mathbf{e}_+^{\dagger\prime}\mathbf{e}_- \\ \mathbf{e}_-^{\dagger\prime}\mathbf{e}_+ & \mathbf{e}_-^{\dagger\prime}\mathbf{e}_- \end{pmatrix} = \mathbf{e}_+^{\dagger\prime}\mathbf{e}_- \begin{pmatrix} 0 & 1 \\ -1 & 0 \end{pmatrix} = -\frac{ma'k}{\omega^2}\begin{pmatrix} 0 & 1 \\ -1 & 0 \end{pmatrix} \tag{4.84}$$

Applying the (4.84) to the $\mathbf{Z}$ equation (4.77) one gets

$$\mathbf{Z}' = \begin{pmatrix} \alpha(\vec{\mathbf{k}},\eta) \\ \beta(\vec{\mathbf{k}},\eta) \end{pmatrix} = \frac{ma'k}{\omega^2}\begin{pmatrix} 0 & -e^{-2i\int\omega \mathrm{d}\eta} \\ e^{2i\int\omega \mathrm{d}\eta} & 0 \end{pmatrix}\mathbf{Z}, \tag{4.85}$$

where $\mathbf{Z}^\dagger\mathbf{Z} = |\alpha|^2 + |\beta|^2 = 1$. The α and β are the same as the Bogoliubov coefficients (4.64). This means that the initial condition is given by

$$\mathbf{Z}(\vec{\mathbf{k}},\eta_0) = \begin{pmatrix} 0 \\ 1 \end{pmatrix} \tag{4.86}$$

Rewriting $\mathbf{u}$ in terms of $\mathbf{Z}$

$$\mathbf{u} = \mathbf{T}_r^{-1}\begin{pmatrix} e^{i\int\omega \mathrm{d}\eta} & 0 \\ 0 & e^{-i\int\omega \mathrm{d}\eta} \end{pmatrix}\begin{pmatrix} \beta(\vec{\mathbf{k}},\eta) \\ \alpha(\vec{\mathbf{k}},\eta) \end{pmatrix} \tag{4.87}$$

one obtains

$$u_+(\vec{\mathbf{k}},\eta) = \beta(\vec{\mathbf{k}},\eta)\sqrt{1-\frac{ma}{w}}e^{i\int\omega \mathrm{d}\eta} + \alpha(\vec{\mathbf{k}},\eta)\sqrt{1+\frac{ma}{w}}e^{-i\int\omega \mathrm{d}\eta} \quad , \tag{4.88a}$$

$$u_-(\vec{\mathbf{k}},\eta) = \beta(\vec{\mathbf{k}},\eta)\sqrt{1+\frac{ma}{w}}e^{i\int\omega \mathrm{d}\eta} - \alpha(\vec{\mathbf{k}},\eta)\sqrt{1-\frac{ma}{w}}e^{-i\int\omega \mathrm{d}\eta} \quad , \tag{4.88b}$$

[9] The eigen-values are λ and $-\lambda$ because the matrix $\mathbf{M}$ is traceless.

where it is explicit the relation between the fields $u_\pm$ and the parameters α and β. The empty fields are defined when $\alpha = 1$ and $\beta = 0$.

The initial condition for $u_\pm$ correspond to the *positive frequency* solution which is expected for a particle description [43]. The particle creation is related to a negative frequency solution. In the Bogoliubov transformations (4.63), a new creation operator is defined. It depends on time and it is a mixture of operators related to particles and anti-particles in the far past. It means that the definition of vacuum in the far past is different of the one defined today.

Using Hamiltonian (4.56) only for particles when $\eta \to -\infty$, where

$$u_+ = \sqrt{1 + \frac{ma}{\omega}}, \tag{4.89a}$$

$$u_- = -\sqrt{1 - \frac{ma}{\omega}}, \tag{4.89b}$$

it is obtained that

$$\hat{\mathrm{H}}\Big(\hat{a}_l^\dagger(\vec{\mathbf{k}})\,|0\rangle\Big) = E_k\Big(\hat{a}_l^\dagger(\vec{\mathbf{k}})\,|0\rangle\Big) = \sqrt{k^2 + m^2a^2}\Big(\hat{a}_l^\dagger(\vec{\mathbf{k}})\,|0\rangle\Big), \tag{4.90a}$$

$$\hat{\mathrm{H}}\Big(\hat{b}_l^\dagger(\vec{\mathbf{k}})\,|0\rangle\Big) = -E_k\Big(\hat{b}_l^\dagger(\vec{\mathbf{k}})\,|0\rangle\Big) = -\sqrt{k^2 + m^2a^2}\Big(\hat{b}_l^\dagger(\vec{\mathbf{k}})\,|0\rangle\Big). \tag{4.90b}$$

As expected, the initial conditions gives positive energies eigen-values for particles and negative eigen-values for anti-particles.

4.2.2 Inflation

The inflationary scenario, in its most common implementation, comes from a scalar field slowly rolling down its potential [81]. By the time the inflationary quasi-de Sitter phase comes to an end, the universe is still unpopulated by particles. The mechanisms responsible for the particle production in the scenario are the so-called preheating and the reheating processes [82, 83, 84].

The reheating consists of the decay of the inflaton field through oscillations around its minimum. The coupling of the inflaton to bosonic and/or fermionic fields allows its decay to the respective bosons and/or fermions. Each reheating model has its peculiarities [84, 85], but they must lead to the predictions of Big-Bang Nucleosynthesis.

Particle production can be even more efficient considering a phase prior to reheating[10]. Contrary to the narrow parametric resonance of the reheating, a broad resonance can be achieved going beyond perturbative effects on the inflaton field. The preheating phase [82, 85] then opens new channels of decay, boosting the production of particles.

[10] It can also be thought as the first phase of reheating

4.2.3 Bounce

The Wheeler-DeWitt equation for a minisuperspace model of a FLRW geometry in the case where the matter content is a single hydrodinamical fluid with a barotropic equation $p = \lambda\rho$ is given by the equation (2.7b) with no tensorial perturbations

$$i\frac{\partial\Psi_{(0)}(a,T)}{\partial T} = \frac{1}{4}\frac{\partial^2\Psi_{(0)}(a,T)}{\partial\chi^2}, \tag{4.91}$$

where

$$\chi = \frac{2}{3}(1-\lambda)^{-1}a^{3(1-\lambda)/2}, \tag{4.92}$$

a is the scale factor [11] and T is a degree of freedom which plays the role of time. The solution for this equation [86, 87] is given by (2.14)

$$\begin{aligned}\Psi_{(0)}(a,T) &= \left[\frac{8T_b}{\pi\left(T^2+T_b^2\right)}\right]^{1/4}\exp\left\{\left[\frac{-4T_b a^{3(1-\lambda)}}{9\left(T^2+T_b^2\right)(1-\lambda)^2}\right]\right\} \\ &\times \exp\left\{-i\left[\frac{4Ta^{3(1-\lambda)}}{9\left(T^2+T_b^2\right)(1-\lambda)^2}+\frac{1}{2}\arctan\left(\frac{T_b}{T}\right)-\frac{\pi}{4}\right]\right\},\end{aligned} \tag{4.93}$$

which is subject to unitary evolution condition and the normalized initial wave function

$$\Psi_{(0)}^{(i)}(\chi) = \left(\frac{8}{T_b\pi}\right)^{1/4}\exp\left\{-\frac{\chi^2}{T_b}\right\}. \tag{4.94}$$

The generated bohmian trajectory is given by (2.15)

$$\dot{a} = \frac{\partial S}{\partial a}, \tag{4.95}$$

which has the solution

$$a(T) = a_b\left[1+\left(\frac{T}{T_b}\right)^2\right]^{1/[3(1-\lambda)]}, \tag{4.96}$$

which is nonsingular at $T = 0$ and tends to the classical solution for $T \to \pm\infty$.

In terms of usual perfect fluids, radiation dominates for small a, so it will dominate during the bounce. Dust matter dominates far from the bounce, hence it will considered in this work the cases for pure radiation and radiation plus dust matter. The relation between η and of T is, from (1.34a)

$$d\eta = [a(T)]^{3\lambda-1}\,dT. \tag{4.97}$$

For pure radiation ($\lambda = 1/3$), $T = \eta$ and equation (4.96) for this particular case reads

$$a(T) = a_b\sqrt{1+\left(\frac{\eta}{\eta_b}\right)^2}. \tag{4.98}$$

[11] The scale factor behaves like a spatial variable. Theis trajectories will be constructed.

For radiation plus dust matter the scale factor is given by [88]

$$a(\eta) = a_e \left[\left(\frac{\eta}{\eta_*} \right)^2 + 2\frac{\eta_b}{\eta_*} \sqrt{1 + \left(\frac{\eta}{\eta_b} \right)^2} \right], \tag{4.99}$$

where a_e is the scale factor at matter-radiation equality and parameters η_* and η_b are related to the wave-function parameters. It is recovered the case of pure radiation expanding this expression for large η_* and identifying $a_b = 2a_e\eta_b/\eta_*$.

In order to make contact with cosmological data, it is convenient to reparametrize the bounce solutions in terms of observable quantities. The Friedmann equation for radiation and dust matter fluids reads

$$H^2 = H_0^2 \left(\frac{\Omega_{r0}}{a^4} + \frac{\Omega_{m0}}{a^3} \right), \tag{4.100}$$

where H is the Hubble parameter, $\Omega_r = \rho_r/\rho_{\rm crit}$ and $\Omega_m = \rho_m/\rho_{\rm crit}$ are the density parameters for radiation and dust matter, respectively, and $\rho_{\rm crit} = 3H^2/(8\pi G)$ is the critical density. The subscript $_0$ denotes the values observed today. The critical density today is $\rho_{\rm crit0} \approx 10^{-26}$ Kg/m^3.

Far from the bounce scale (large η), where quantum effects are negligible, the Friedmann equation reads

$$H^2 = \frac{4a_e}{\eta_*^2} \left(\frac{a_e}{a^4} + \frac{1}{a^3} \right), \tag{4.101}$$

Comparing Eqs. (4.100) and (4.101), in terms of the comoving Hubble radius as $R_H = 1/(a_0H_0)$ the density parameters today are given by

$$\Omega_{r0} = \frac{a_e}{a_0} \frac{4R_H^2}{\eta_*^2}, \qquad \Omega_{m0} = \left(\frac{a_e}{a_0} \right)^2 \frac{4R_H^2}{\eta_*^2}. \tag{4.102}$$

Expanding the scale factor (4.99) for large η_*, *i*.e., for radiation domination near the bounce and dust matter domination in the far past, the Friedmann equation results

$$H^2 = H_0^2 \Omega_{r0} x^4 \left(1 - \frac{x^2}{x_b^2} \right), \tag{4.103}$$

where $x = a_0/a$ is a redshiftlike variable and, consequently, x_b provides the scale factor where the bounce occurs (apart from a small correction from dust matter density), which is defined by

$$x_b = \frac{R_H}{\eta_b \sqrt{\Omega_{r0}}}. \tag{4.104}$$

Solving equations (4.103) and (4.104) for a_e, η_* and η_b and computing the scale factor at the bounce a_b in terms of theses quantities, one obtains

$$a_e = a_0 \frac{\Omega_{r0}}{\Omega_{m0}}, \qquad \eta_* = 2R_H \frac{\sqrt{\Omega_{r0}}}{\Omega_{m0}}, \qquad \eta_b = \frac{R_H}{x_b \sqrt{\Omega_{r0}}}, \qquad a_b = \frac{a_0}{x_b}. \tag{4.105}$$

In terms of these variables, the bounce curvature scale can be obtained from the four-dimensional Ricci escalar $R = 6a''(\eta)/a^3(\eta)$, which results

$$L_b = \left.\frac{1}{\sqrt{R}}\right|_{\eta=0} = \frac{a_b\eta_b}{\sqrt{6(1+2\gamma_b)}} = \frac{1}{\sqrt{1+2\gamma_b}}\frac{a_0 R_H}{x_b^2\sqrt{6\Omega_{r0}}}, \tag{4.106}$$

where

$$\gamma_b \equiv \frac{\Omega_{m0}}{4x_b\Omega_{r0}} \tag{4.107}$$

is the ratio of the dust matter and radiation density at the bounce. The bounce scale factor x_b, which appears explicitly in the Friedmann equation, must be constrained by physical conditions. The first condition is that the bounce curvature scale must be larger that the Planck length, $L_b > L_p$, which sets an upper bound on x_b. This bound is relevant since the Wheeler-DeWitt equation should be a valid approximation for any fundamental quantum gravity theory only at scales not so close to the Planck length. Using $H_0 = 70$ [Km s^{-1} Mpc^{-1}], $a_0 R_H/L_p \approx 8\times 10^{60}$, which sets

$$x_b \lesssim \frac{\sqrt{8}10^{30}}{(6\Omega_{r0})^{1/4}} \approx 2\times 10^{31}. \tag{4.108}$$

This result is obtained for $\gamma_b \ll 1$, where one assumes the bounce energy scale must be larger than at the start of nucleosynthesis (≈ 10 MeV). Here it were assumed that Ω_{r0} should not be smaller than its usual value $\Omega_{r0} = 8\times 10^{-5}$, and we used the cosmic microwave background radiation temperature value $T = 2.7\ K$. This assumption in the energy scale set a second condition $x_b \gg 10^{11}$, which gives a lower bound in the bounce scale factor. Therefore, it is obtained the constraint

$$10^{11} \ll x_b \lesssim 2\times 10^{31}. \tag{4.109}$$

In the case where dust matter is taken into account, assuming the value $\Omega_{m0} = 3\times 10^{-1}$, from the range of x_b one obtains the following interval for γ_b:

$$3.7\times 10^{-29} \lesssim \gamma_b \ll 7.5\times 10^{-9}. \tag{4.110}$$

The small values of γ_b make it explicit that the dust matter fluid dominates only in the far past, whereas the radiation fluid dominates near the bounce scale.

Some of the bounce parameters introduced above appear explicitly in the equations of motion of fermions in the Friedmann background with bouncing. For this reason, it is convenient to introduce some new parameters in terms of the current ones to be used in these equations in the following sections, which are defined by

$$\bar{\eta} = \frac{\eta}{\eta_b}, \qquad \bar{k} = k\eta_b, \qquad r_b = ma_b\eta_b. \tag{4.111}$$

In terms of these parameters, the scale factor, Eq. (4.99), for radiation and dust matter can be written as

$$a(\bar{\eta}) = a_b \left(\gamma_b \bar{\eta}^2 + \sqrt{1 + \bar{\eta}^2} \right), \tag{4.112}$$

whereas the case of pure radiation ($\Omega_{m0} = 0$, *i*.e., $\gamma_b = 0$) it reduces to

$$a(\bar{\eta}) = a_b \sqrt{1 + \bar{\eta}^2}. \tag{4.113}$$

Finally, it is relevant to notice from Eq. (4.106) that $L_b \approx a_b \eta_b$, which leads to

$$r_b \approx \frac{L_b}{m}, \tag{4.114}$$

where $1/m$ can be identified with the Compton length of the massive particle.

In the following subsection it is introduced the equations of motion for fermions for Universes dominated by dust matter and radiation and by pure radiation.

4.2.4 Equations

The equations of motion in the reciprocal space for the variables $u_{k,\pm}(\eta)$, equations (4.51), that parametrize the Dirac fermion evolution in the FLRW background in terms of the variables (4.111) read

$$\frac{d^2 u_{\bar{k},\pm}(\bar{\eta})}{d\bar{\eta}^2} + \left[\bar{k}^2 + \frac{r_b^2}{a_b^2} a(\bar{\eta})^2 \pm i \frac{r_b}{a_b} \frac{da(\bar{\eta})}{d\bar{\eta}} \right] u_{\bar{k},\pm}(\bar{\eta}) = 0, \tag{4.115}$$

where initial conditions for $u_{k,\pm}(\eta)$ for (4.49), in the new variables read

$$u_{\bar{k},\pm}(\bar{\eta}_0) = \sqrt{1 \pm \frac{r_b a(\bar{\eta}_0)}{a_b \omega(\bar{\eta}_0)}} e^{i\phi}. \tag{4.116}$$

In the special case where the universe matter content is a radiation fluid, the scale factor is given by Eq. (4.113) and equation (4.115), resulting in

$$\frac{d^2 u_{\bar{k},\pm}(\bar{\eta})}{d\bar{\eta}^2} + \left[\bar{k}^2 + r_b^2 \left(1 + \bar{\eta}^2 \right) \pm \frac{i r_b \bar{\eta}}{\sqrt{1 + \bar{\eta}^2}} \right] u_{\bar{k},\pm}(\bar{\eta}) = 0. \tag{4.117}$$

These equations have no analytical solutions in terms of known functions and need to be solved numerically. It is worth to mention that their asymptotic limits ($\bar{\eta} \to \pm\infty$) have solutions in terms of parabolic cylinder functions [52]. These same special functions give analytical results for the Fourier modes of a scalar field in the same background, which have similar equations except for the absence of the complex term in the square brackets.

In the case when the energy fluid content is radiation and dust matter, the scale factor is given by Eq. (4.112) and Eq. (4.115), yielding

$$\frac{d^2 u_{\bar{k},\pm}(\bar{\eta})}{d\bar{\eta}^2} + \left[\bar{k}^2 + r_b^2 \left(\gamma_b \bar{\eta}^2 + \sqrt{1 + \bar{\eta}^2} \right)^2 \pm i r_b \bar{\eta} \left(2\gamma_b + \frac{1}{\sqrt{1 + \bar{\eta}^2}} \right) \right] u_{\bar{k},\pm}(\bar{\eta}) = 0. \tag{4.118}$$

These equations have no analytical solution as well, and are solved numerically. Asymptotically analytical solution are also no longer available.

Once the solutions for $u_{\bar{k},\pm}(\bar{\eta})$ are obtained, the occupation number $|\beta_k(\eta)|^2$ for each mode k can be obtained from Eq. (4.64). The occupation number is a function of the rescaled conformal time $\bar{\eta}$, and converges to a constant. We will see that for some momenta and masses, $|\beta_k(\eta)|^2$ exhibits a peak near the bounce and oscillates until it stabilizes to a constant value for some $\bar{\eta} = \bar{\eta}_*$, where particle prodution becomes negligible. This constant value behaves as an asymptotic state[12], and represents the particle creation. Thefefore, for $|\beta_k(\eta)|^2$ evaluated at $\bar{\eta} = \bar{\eta}_*$, one obtain the particle number $|\beta_{\bar{k}}|^2$, where the time variable is suppressed and write in the new parameters (4.111).

In terms of the parameters defined in (4.111), we obtain that

$$n = \frac{1}{\pi^2 a^3 \eta_b^3} \int_0^\infty d\bar{k}\bar{k}^2 |\beta_{\bar{k}}|^2, \tag{4.119}$$

$$\Delta\rho = \frac{1}{\pi^2 a^4 \eta_b^4} \int_0^\infty d\bar{k}\bar{k}^2 |\beta_{\bar{k}}|^2 \omega_{\bar{k}}, \tag{4.120}$$

where $\omega_{\bar{k}} = \sqrt{\bar{k}^2 + r_b^2 a^2/a_b^2}$.

4.3 Numerical Integration

4.3.1 Fermion masses and bounce depth

For the fermion production during the bounce,we will focus on two types of neutrinos: the standard model neutrinos, m_ν and right-handed heavy Majorana neutrinos m_R, inspired by the see-saw mechanism and possible leptogenesis scenarios. It will also be taken into account the production of fermions with mass of order of neutrons.

The neutron mass is known for decades, and its value to the decimal place is 939.6MeV. Most recent measurements of the SM neutrino masses[13] give only upper limits to its value, of about 10^{-2} eV. For the right-handed neutrinos, there is a larger range of values to work with.

Different realizations of leptogenesis [89, 90] and SM-extensions [91] provide a whole range of scales for the right-handed neutrino masses. A model independent analysis of the leptogensis together with the upper bound on SM-neutrino masses gives us the lower bound on their mass to be 10^9GeV [92]. Considering Grand Unification Theories,

[12] In [4], one obtains analytically particle production between two asymptotic states, which are adiabatic vacua

[13] In the Standard Model, to be precise, the neutrinos are massless. We're referring to massive light neutrinos as SM ones to the sake of simplicity.

the mass of the massive neutrino could even reach values of their scale, of the order of $10^{15\sim18}$ GeV [72].

As the Majorana neutrino in question is a sterile one (interacts only with gravity), it can also be treated as a Dark Matter candidate [93], which in turn gives us different constraints, in accordance to how the DM model is constructed. In general, the scale for DM candidates is of order of KeV or MeV, despite being allowed to reach the GUT scale mass as previously mentioned [94, 95]. Basically, different applications of the neutrinos results in mass ranges of their own. For our model, the massive neutrinos would only represent a fraction of the Dark Matter, considering that the contracting universe already has most of this component already in place.

Different ranges of masses will be tested. The efficiency of production of the fermions is expected to be related to their masses, as well as to the depth of the bounce. This trial and error approach will give us the most efficient particle production from the pairs of fermion mass and bounce depth.

The bounce scale is relevant since it shows how gravity is strong during the bounce phase. It is responsible for the aforementioned deviation from the Minkowski spacetime. The stronger the curvature, the more it is expected the curved spacetime effects to be felt – as particle production. The bounce scale is present at the expression of r_b, which is $r_b = mL_b$. The value of r_b is usually small, even for the heavier SM particles. Starting with a deeper bounce, i.e. closer to the Planck scale, with $L_b = 10^3 L_P$, and picking the Higgs boson, $m_H = 125$ GeV, its value would be of the order 10^{-15}. For the order of the magnitude of the masses presented above, r_b could be evaluated between 10^1 and 10^{-29}. Shallower bounces would mean a higher value of r_b, up to 6 orders of magnitude.

4.3.2 Results

In this section it is shown some numerical results for the creation of neutral fermionic particles in a radiation dominated quantum bounce. Information about particle creation is obtained from the behavior of the Bogoliubov coefficient β_k, which is non-zero when particles are created. From the definition of particle number density, Eq. (4.120), the relevant physical quantity is the integrand, from which it is obtained the density of created particles for each mode k. It is performed a numerical analysis of this integrand in the logarithmic scale.

In figures 16 and 17 it is plotted the behavior of the Bogoliubov coefficient β_k for each mode k for the production of neutrinos and neutrons, respectively. For each case, the solid and dashed curves represent the choices $x_b = 10^{24}, 10^{30}$, respectively. The neutrinos masses are not precisely known, but have the upper limit ≤ 0.12 eV [96]. It is chosen $m_\nu \approx 0.1$ eV for our calculations. On the other hand, the neutron mass is well know, so

we consider $m_n \approx 1$ GeV.

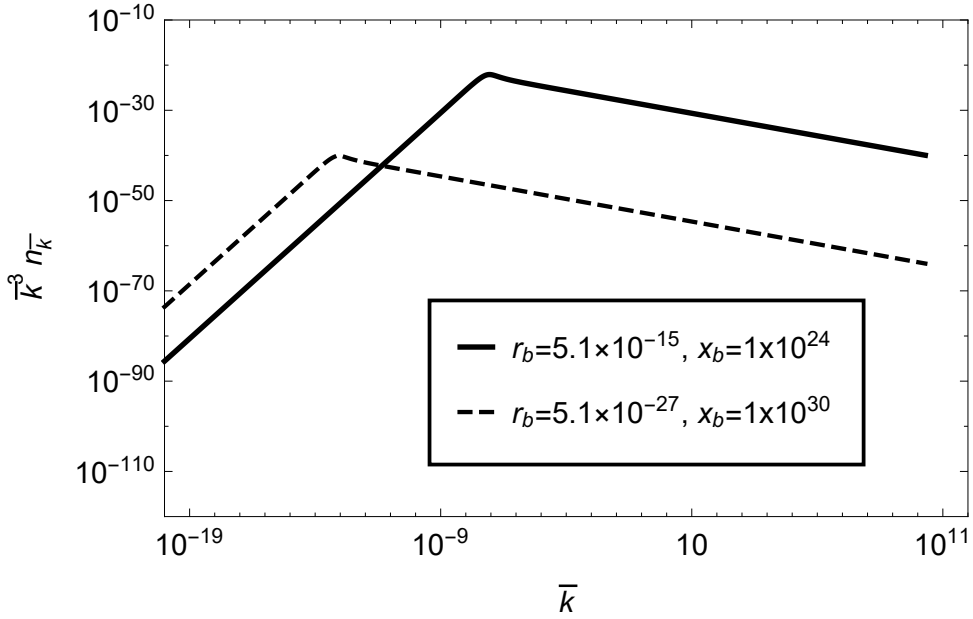

Figure 16 – The Bogoliubov coefficients for the neutrino mass 10^{-4} GeV for the representative choices $x_b = 10^{24}$ ($r_b = 5.1 \times 10^{-15}$) and $x_b = 10^{30}$ ($r_b = 5.1 \times 10^{-27}$) given by solid and dashed lines, respectively.

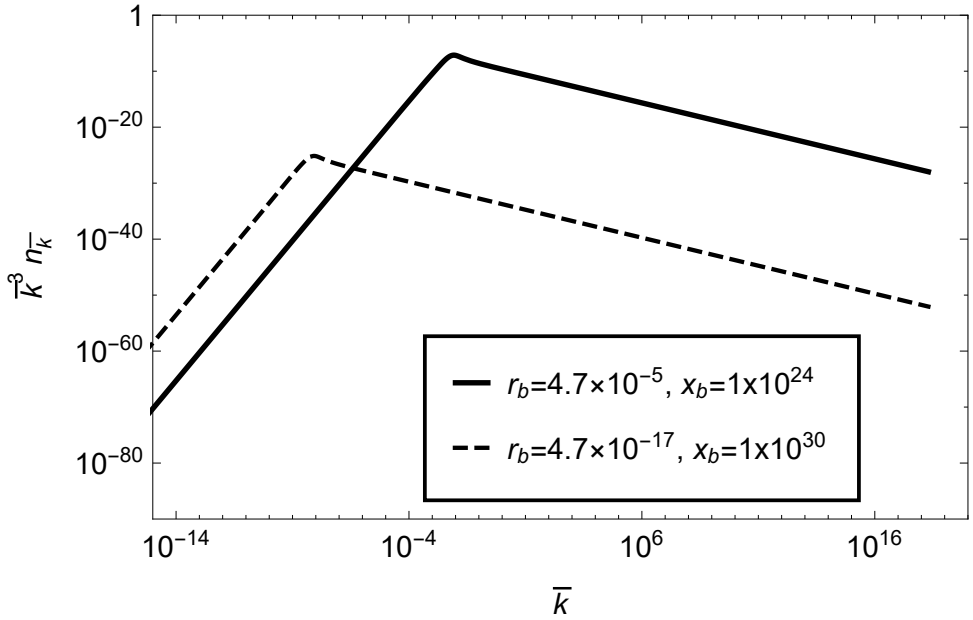

Figure 17 – The Bogoliubov coefficients for the neutron mass 1 GeV for the representative choices $x_b = 10^{24}$ ($r_b = 4.7 \times 10^{-5}$) and $x_b = 10^{30}$ ($r_b = 4.7 \times 10^{-17}$) given by solid and dashed lines, respectively.

In addition to neutrino and neutrons masses, it is also considered heavier neutrinos. In figure 18 it is plotted the behavior of the Bogoliubov coefficient β_k for each mode k for the production of heavy neutrinos masses $1, 10^3, 10^6$ GeV for the specific choice $x_b = 10^{30}$, whereas in figure 19 it is plotted the density parameter $\Omega_{\nu_{\rm h}} = \rho_{\nu_{\rm h}}/\rho_{\rm crit0}$ normalized by x^3

for heavy neutrinos as a function of m_{ν_h} for the same x_b value. In comparison to figures 16 and 17, it is chosen only the value $x_b = 10^{30}$ because, from figure 19, it gives a relevant range ($m_{\nu_h} \lesssim 5 \times 10^7$ GeV) for which $\Omega_{\nu_h} \lesssim 10^{-2}$ today ($x = 1$). For the choice $x_b = 10^{24}$, however, $\Omega_{\nu_h} \lesssim 10^{-2}$ is obtained only for $m_{\nu_h} \lesssim 1$ TeV.

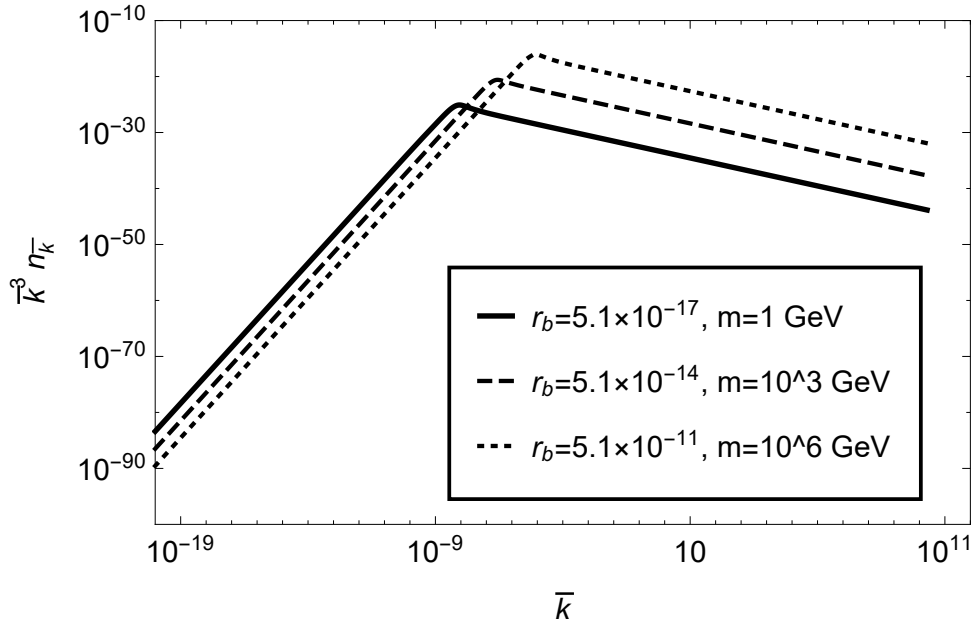

Figure 18 – The Bogoliubov coefficients for the neutrino masses 1 GeV, 10^3 GeV, and 10^6 GeV for the representative choice $x_b = 10^{30}$ given by solid, dashed and dotted lines, respectively.

The particle number density n is a time dependent quantity. In order to obtain particle creation due to the quantum bounce, it is taken as an initial condition some $\eta = \eta_i$

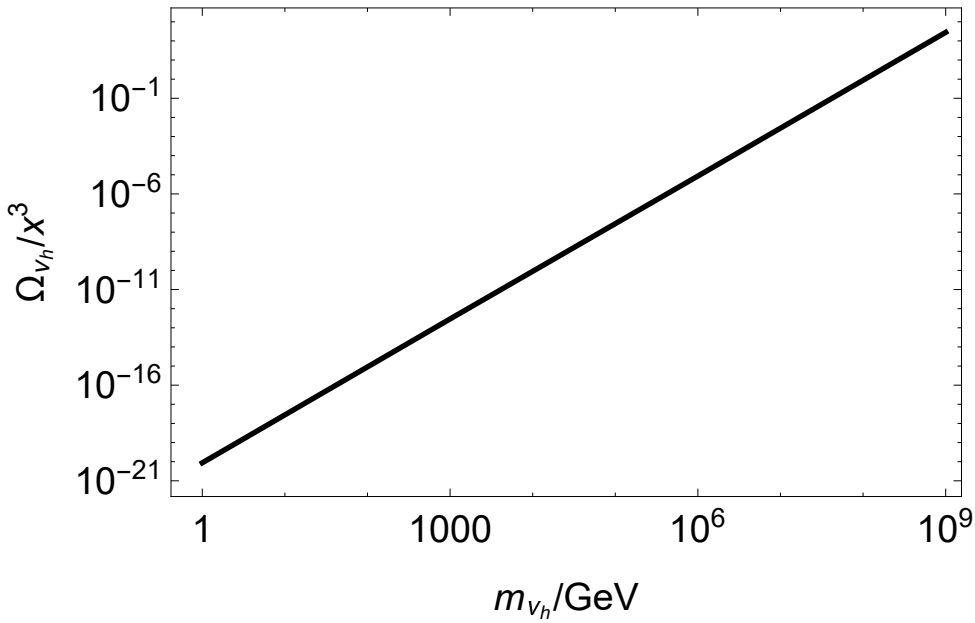

Figure 19 – The density parameter $\Omega_{\nu_h} = \rho_{\nu_h}/\rho_{\text{crit0}}$ for heavy neutrinos normalised by x^3 as a function of m_{ν_h} for the representative choice $x_b = 10^{30}$.

in the far past ($\eta \to -\infty$) such that $\beta_k \approx 0$ and evolve the system to some ($\eta \to \infty$), where β_k stabilizes to a constant value, which means that particles are no further produced. In order words, it is captured the region near the bounce instant which gives a relevant particle production density.

Despite any analytical solution for β_k was not obtained, it is possible to numerically integrate it for all values of k modes and give approximations for n and $\Delta\rho$, Eqs. (4.119) and (4.120), respectively, in terms of the definition $x = a_0/a$ and the new variables (4.111). In the calculation of n, it was computed the integral numerically, which gives a number, and the expression outside the integral is proportional to $x_b^3 x^3$, then $n \propto x_b^3 x^3$. For each choice of x_b, $n \propto x^3$ and, finally, n for $x = 1$ gives the particle density today. In the calculation of $\Delta\rho$, there is a also a dependence on the frequency $\omega_{\bar{k}}$, which results $\omega_{\bar{k}} = \sqrt{\bar{k}^2 + r_b^2 x_b^2/x^2}$. Evaluating $\Delta\rho$ today, i.e., when $x = 1$, the frequency reads $\omega_{\bar{k}} = \sqrt{\bar{k}^2 + r_b^2 x_b^2}$. For all cases it was considered in the analysis the values of momenta for which particle production is most relevant, $\bar{k}_{\text{peak}}$, are much smaller than $r_b x_b$. Therefore, it is possible to approximate $\bar{k} \ll r_b x_b$ (i.e., $k \ll ma$) in $\omega_{\bar{k}}$, which implies $\omega_k \to r_b x_b$ (similar to a limit of large a). Thus, the particles created by the quantum bounce are non-relativistic today. From the non-relativistic approximation

$$\Delta\rho \approx mn. \tag{4.121}$$

For a visualization of this non-relativistic behavior, Table 1 shows the momenta k_{peak} and k_* for each case of figures 16, 17 and 18, which are, respectively, the momenta for which particle creation is most relevant and the momenta $k = r_b x_b/x$ in the value which separates relativistic and non-relativistic behavior. Finally, from $\Delta\rho$ it is straightforward to obtain the density parameter $\Omega = \Delta\rho/\rho_{\text{crit}0}$.

For neutrinos and neutrons

$$n_\nu \approx 5 \times 10^{-41} x^3 \text{ cm}^{-3} \ , \quad n_n \approx 4 \times 10^{-26} x^3 \text{ cm}^{-3}. \tag{4.122}$$

$$\Delta\rho_\nu \approx 8 \times 10^{-69} x^3 \text{ g/cm}^3 \ , \quad \Delta\rho_n \approx 8 \times 10^{-50} x^3 \text{ g/cm}^3. \tag{4.123}$$

$$\Omega_\nu \approx 8 \times 10^{-40} x^3 \ , \quad \Omega_n \approx 8 \times 10^{-21} x^3. \tag{4.124}$$

For the heavy neutrinos

$$n_{\nu_{\text{h}},\text{m}=10^{11}\text{GeV}} \approx 1 \times 10^{-9} x^3 \text{ cm}^{-3} \ , \quad n_{\nu_{\text{h}},\text{m}=1 \text{ GeV}} \approx 5 \times 10^{-26} x^3 \text{ cm}^{-3}. \tag{4.125}$$

The results for n, $\Delta\rho$ and Ω revealed a negligible dependence on the bounce depth x_b for both neutrinos and neutrons. For this reason, for both choices of x_b it is presented single results n_i, $\Delta\rho_i$ and Ω_i, where $i = \nu, n$.

The energy density results represent dust-like fluids, for which $\rho = mn$. The density parameters results show that for both cases the energy density of created particles is much smaller than the current critical density.

Comparing the results of particle creation, Eqs. (4.122), with figures 16 and 17, it is noticed that although particle creation is stronger for specific k modes in each case, numerical integration for over all k modes reveals that the total production is the same for each choices of r_b (i.e., x_b) for each type of particle as already mentioned.

4.4 Conclusion

In this chapter, it was discussed the creation of non-charged fermions due to minimal coupling with gravity. Numerical results were found to Universes filled only with radiation, even though it is not expected a huge difference with Universes filled with others fluids, since the major creation of particles occur in the radiation era. The range of particle density calculated is not enough to explain all fermionic matter present in the Universe [71, 97]. Different from [71, 72], where the creation of particle occur due to phase transitions, the number of particle by logarithm of frequency is smooth, and less intense. Although it is not possible to explain the amount of fermionic matter, a heavy fermion with a stronger coupling with gravity like [98] could explain why there is more particles than anti-particles in the Universe. This is measured by the Baryon Asymmetry of the Universe (BAU) [97] given by

$$\begin{aligned} \eta = \left.\frac{N_B - N_{\bar{B}}}{N_\gamma}\right|_{T=3K} &\simeq 10^{-10} \\ &\lesssim 10^{-10}\left(\frac{n}{4.11\times 10^{13}\mathrm{cm}^{-3}}\right). \end{aligned} \tag{4.126}$$

For the calculated particles, only the heaviest one could be responsible for such process. This will be the subject of future investigations.

Bibliography

1 PETER, P.; Pinto-Neto, N. Cosmology without inflation. *Phys. Rev. D*, American Physical Society, v. 78, n. 6, p. 063506, set. 2008. 1, 19

2 VITENTI, S. D. P.; Pinto-Neto, N. Large adiabatic scalar perturbations in a regular bouncing universe. *Physical Review D*, v. 85, n. 2, jan. 2012. ISSN 1550-7998, 1550-2368. 1

3 BACALHAU, A. P.; Pinto-Neto, N.; VITENTI, S. D. P. Consistent scalar and tensor perturbation power spectra in single fluid matter bounce with dark energy era. *Physical Review D*, v. 97, n. 8, abr. 2018. ISSN 2470-0010, 2470-0029. 1

4 CELANI, D. C. F.; Pinto-Neto, N.; VITENTI, S. D. P. Particle creation in bouncing cosmologies. *Physical Review D*, v. 95, n. 2, jan. 2017. ISSN 2470-0010, 2470-0029. 1, 40, 43, 48, 50, 70

5 BERGERON, H. et al. Singularity avoidance in a quantum model of the Mixmaster universe. *Phys. Rev. D*, American Physical Society, v. 92, n. 12, p. 124018, 2015. 1, 33

6 ALMEIDA, C. R. et al. Three examples of quantum dynamics on the half-line with smooth bouncing. *Annals of Physics*, v. 392, p. 206–228, maio 2018. ISSN 0003-4916. 1, 25

7 BESSADA, D. et al. Stochastic background of relic gravitons in a bouncing quantum cosmological model. *Journal of Cosmology and Astroparticle Physics*, v. 2012, n. 11, p. 054–054, nov. 2012. ISSN 1475-7516. 1, 36, 47

8 Pinto-Neto, N.; SCARDUA, A. Detectability of primordial gravitational waves produced in bouncing models. *Physical Review D*, v. 95, n. 12, jun. 2017. ISSN 2470-0010, 2470-0029. 2

9 GÖDEL, K. An Example of a New Type of Cosmological Solutions of Einstein's Field Equations of Gravitation. *Reviews of Modern Physics*, v. 21, n. 3, p. 447–450, jul. 1949. 6

10 GOURGOULHON, E. 3+1 Formalism and Bases of Numerical Relativity. mar. 2007. 6

11 WALD, R. M. *General Relativity*. 1984 edition. ed. Chicago: University Of Chicago Press, 1984. ISBN 978-0-226-87033-5. 6

12 KERR, R. P. Gravitational Field of a Spinning Mass as an Example of Algebraically Special Metrics. *Physical Review Letters*, v. 11, n. 5, p. 237–238, set. 1963. 7

13 ZHANG, F. *The Schur Complement and Its Applications*. [S.l.]: Springer Science & Business Media, 2005. ISBN 978-0-387-24271-2. 7

14 SELIGER, R. L.; WHITHAM, G. B. Variational principles in continuum mechanics. *Proceedings of the Royal Society A: Mathematical, Physical and Engineering Sciences*, The Royal Society, v. 305, n. 1480, p. 1–25, May 1968. 10

15 SCHUTZ, B. F. *A First Course in General Relativity*. Edição: 2. Cambridge ; New York: Cambridge University Press, 1 de julho de 2009. ISBN 978-0-521-88705-2. 10

16 WEINBERG, S. *Cosmology*. Oxford ; New York: Oxford University Press, USA, 28 de abril de 2008. ISBN 978-0-19-852682-7. 10, 12

17 SCHUTZ, B. F. Perfect Fluids in General Relativity: Velocity Potentials and a Variational Principle. *Physical Review D*, v. 2, n. 12, p. 2762–2773, dez. 1970. ISSN 0556-2821. 10

18 TAUB, A. H. General Relativistic Variational Principle for Perfect Fluids. *Physical Review*, v. 94, n. 6, p. 1468–1470, jun. 1954. ISSN 0031-899X. 10

19 LEMOS, N. A. *Mecânica Analítica*. Edição: 2ª. São Paulo: Livraria da Física, 1 de janeiro de 2007. ISBN 978-85-88325-24-1. 12

20 PETER, P.; PINHO, E.; Pinto-Neto, N. Tensor perturbations in quantum cosmological backgrounds. *Journal of Cosmology and Astroparticle Physics*, v. 2005, n. 07, p. 014–014, jul. 2005. ISSN 1475-7516. 13

21 MUKHANOV, V. *Physical Foundations of Cosmology*. 1. ed. [S.l.]: Cambridge University Press, 2005. ISBN 978-0-521-56398-7. 14, 33, 39

22 BICEP2 et al. BICEP2 I: Detection Of B-mode Polarization at Degree Angular Scales. p. 19, mar. 2014. 14

23 ALI, S. T.; ENGLIS, M. Quantization methods: A Guide for physicists and analysts. *Rev. Math. Phys.*, v. 17, p. 391–490, 2005. 17

24 FRIEDMAN, A. On the Curvature of space. *Zeitschrift für Physik*, v. 10, n. 1, p. 377–386, 1922. [Gen. Rel. Grav.31,1991(1999)]. 18

25 de Sitter, W. On Einstein's Theory of Gravitation and its Astronomical Consequences. Third Paper. *Monthly Notices of the Royal Astronomical Society*, v. 78, n. 1, p. 3–28, nov. 1917. ISSN 0035-8711. 18

26 LEMAITRE, G. A Homogeneous Universe of Constant Mass and Growing Radius Accounting for the Radial Velocity of Extragalactic Nebulae. *Annales de la Societe scientifique de Bruxelles A*, v. 47, n. 8, p. 49–59, 1927. [Gen. Rel. Grav.45,no.8,1635(2013)]. 18

27 LIVIO, M. Mystery of the missing text solved. *Nature*, Nature Publishing Group, a division of Macmillan Publishers Limited. All Rights Reserved. SN -, v. 479, n. 479i, p. 171 EP–, 2011. Comment. 18

28 HUBBLE, E. A relation between distance and radial velocity among extra-galactic nebulae. *Proceedings of the National Academy of Sciences*, v. 15, n. 3, p. 168–173, mar. 1929. ISSN 0027-8424, 1091-6490. 18

29 TOLMAN, R. C. On the Theoretical Requirements for a Periodic Behaviour of the Universe. *Physical Review*, v. 38, n. 9, p. 1758–1771, nov. 1931. ISSN 0031-899X. 18

30 RINDLER, W. Visual Horizons in World-Models. *General Relativity and Gravitation*, v. 34, n. 1, p. 133–153, jan. 2002. ISSN 0001-7701, 1572-9532. 18

31 DICKE, R. H. *Gravitation and the Universe: Robert H. Dicke, Jayne Lectures for 1969*. [S.l.]: Pa., American philosophical Society, 1970. 18

32 NOVELLO, M.; BERGLIAFFA, S. P. Bouncing cosmologies. *Physics Reports*, v. 463, n. 4, p. 127–213, 2008. ISSN 0370-1573. 18, 19

33 BATTEFELD, D.; PETER, P. A critical review of classical bouncing cosmologies. *Physics Reports*, v. 571, p. 1–66, 2015. ISSN 0370-1573. A critical review of classical bouncing cosmologies. 18, 19

34 NOVELLO, M.; SALIM, J. M. Nonlinear phothons in the Universe. *Physical Review D*, D20, p. 377–383, 1979. 18

35 MELNIKOV, V. N.; ORLOV, S. V. Nonsingular cosmology as a quantum vacuum effect. *Physics Letters A*, v. 70, n. 4, p. 263–265, mar. 1979. ISSN 0375-9601. 18

36 GUTH, A. H. Inflationary universe: A possible solution to the horizon and flatness problems. *Physical Review D*, v. 23, n. 2, p. 347–356, jan. 1981. 19

37 CAI, Y.-F. et al. Nonsingular cosmology with a scale-invariant spectrum of cosmological perturbations from Lee-Wick theory. *Physical Review D*, American Physical Society, v. 80, n. 2, p. 023511, jul. 2009. ISSN 1550-7998. 19

38 PETER, P.; PINHO, E. J. C.; Pinto-Neto, N. Noninflationary model with scale invariant cosmological perturbations. *Phys. Rev. D*, American Physical Society, v. 75, n. 2, p. 023516, jan. 2007. 19

39 TURNER, M. S. Detectability of inflation-produced gravitational waves. *Physical Review D*, American Physical Society, v. 55, n. 2, p. R435–R439, jan. 1997. ISSN 0556-2821. 19, 48

40 WANDS, D. Duality invariance of cosmological perturbation spectra. *Physical Review D*, American Physical Society, v. 60, n. 2, p. 023507, jun. 1999. 19

41 FINELLI, F.; BRANDENBERGER, R. Generation of a scale-invariant spectrum of adiabatic fluctuations in cosmological models with a contracting phase. *Physical Review D*, American Physical Society, v. 65, n. 10, p. 103522, maio 2002. ISSN 0556-2821. 19

42 NOVELLO, M.; BERGLIAFFA, S. E. P. Bouncing cosmologies. *Physics Reports*, v. 463, n. 4, p. 127–213, jul. 2008. ISSN 03701573. 19

43 GREINER, W.; REINHARDT, J.; BROMLEY, D. A. *Field Quantization*. 1st ed 1996. 2nd printing 1997 edition. ed. [S.l.]: Springer, 1997. ISBN 978-3-540-78048-9. 19, 58, 65

44 LEMOS, N. A. Radiation-dominated quantum Friedmann models. *Journal of Mathematical Physics*, v. 37, n. 3, p. 1449, 1996. ISSN 00222488. 19, 21

45 GAZEAU, J.-P. *Coherent States in Quantum Physics*. 1 edition. ed. Weinheim : Chichester: Wiley-VCH, 2009. ISBN 978-3-527-40709-5. 19, 23

46 PINHO, E. J. C.; Pinto-Neto, N. Scalar and vector perturbations in quantum cosmological backgrounds. *Physical Review D*, v. 76, n. 2, p. 023506, jul. 2007. 20

47 NETO, N. P. *Teorias E Interpretacoes Da Mecanica Quantica*. [S.l.]: Livraria da Física, 2010. ISBN 978-85-7861-056-2. 22

48 Pinto-Neto, N.; SANTOS, G.; STRUYVE, W. Quantum-to-classical transition of primordial cosmological perturbations in de Broglie–Bohm quantum theory. *Physical Review D*, v. 85, n. 8, abr. 2012. ISSN 1550-7998, 1550-2368. 22

49 Pinto-Neto, N.; SANTOS, G.; STRUYVE, W. Quantum-to-classical transition of primordial cosmological perturbations in de Broglie-Bohm quantum theory: The bouncing scenario. *Physical Review D*, v. 89, n. 2, jan. 2014. ISSN 1550-7998, 1550-2368. 22

50 MAIER, R. et al. Bouncing models with a cosmological constant. *Physical Review D*, v. 85, n. 2, p. 023508, jan. 2012. 23

51 MAGNUS, W.; OBERHETTINGER, F. *Formulas and Theorems for the Special Functions of Mathematical Physics*. First american edition edition. [S.l.]: Chelsea Pub. Co, 1949. 29, 30

52 GRADSHTEYN, I. S.; RYZHIK, I. M. *Table of Integrals, Series and Products, Corrected and Enlarged Edition*. New York: Academic Press, 1980. ISBN 978-0-12-294760-5. 29, 30, 69

53 BERGERON, H. et al. Smooth big bounce from affine quantization. *Physical Review D*, v. 89, n. 8, p. 083522, abr. 2014. 30

54 WEBER, J. Gravitational Radiation. *Physical Review Letters*, v. 18, n. 13, p. 4, 1967. 35

55 QUINTIN, J. et al. Evolution of cosmological perturbations and the production of non-Gaussianities through a nonsingular bounce: Indications for a no-go theorem in single field matter bounce cosmologies. *Phys. Rev. D*, American Physical Society, v. 92, n. 6, p. 063532, set. 2015. 36

56 ADE, P. A. R. et al. iPlanck/i 2015 results. *Astronomy & Astrophysics*, EDP Sciences, v. 594, p. A20, out. 2016. ISSN 0004-6361. 36

57 ABBOTT, B. P. et al. Observation of Gravitational Waves from a Binary Black Hole Merger. *Phys. Rev. Lett.*, American Physical Society, v. 116, n. 6, p. 061102, fev. 2016. 36, 37

58 MAGGIORE, M. Gravitational wave experiments and early universe cosmology. *Physics Reports*, v. 331, n. 6, p. 283–367, jul. 2000. ISSN 03701573. 15, 36, 43

59 THRANE, E.; ROMANO, J. D. Sensitivity curves for searches for gravitational-wave backgrounds. 36

60 COLLABORATION, L. S.; COLLABORATION, V. Searching for stochastic gravitational waves using data from the two colocated LIGO Hanford detectors. *Physical Review D*, American Physical Society, v. 91, n. 2, p. 022003, jan. 2015. 36, 47, 48

61 GIOVANNINI, M. Stochastic backgrounds of relic gravitons: A theoretical appraisal. *PMC Physics A*, v. 4, n. 1, p. 1, 2010. ISSN 1754-0410. 36

62 ZELDOVICH, Y. B. A Hypothesis, Unifying the Structure and the Entropy of the Universe. *Monthly Notices of the Royal Astronomical Society*, v. 160, n. 1, p. 1P–3P, out. 1972. ISSN 0035-8711. 36, 37

63 de Haro, J.; CAI, Y. F. An extended matter bounce scenario: Current status and challenges. 2015. ISSN 15729532. 39

64 de Haro, J.; AMORÓS, J. Viability of the matter bounce scenario in Loop Quantum Cosmology from BICEP2 last data. *Journal of Cosmology and Astroparticle Physics*, IOP Publishing, v. 2014, n. 08, p. 025–025, ago. 2014. ISSN 1475-7516. 39

65 Wilson-Ewing, E. The matter bounce scenario in loop quantum cosmology. *Journal of Cosmology and Astroparticle Physics*, IOP Publishing, v. 2013, n. 03, p. 026–026, mar. 2013. ISSN 1475-7516. 39

66 SENDRA, I.; SMITH, T. L. Improved limits on short-wavelength gravitational waves from the cosmic microwave background. *Physical Review D*, American Physical Society, v. 85, n. 12, p. 123002, jun. 2012. ISSN 1550-7998. 48

67 JHANGIANI, V. Geometric significance of the spinor Lie derivative. I. *Foundations of Physics*, v. 8, n. 5-6, p. 445–462, jun. 1978. ISSN 0015-9018, 1572-9516. 49, 52

68 BASSETT, B. A.; TSUJIKAWA, S.; WANDS, D. Inflation dynamics and reheating. *Reviews of Modern Physics*, American Physical Society, v. 78, n. 2, p. 537–589, 2006. ISSN 00346861. 50

69 HAWKING, S. W. Black hole explosions? *Nature*, Nature Publishing Group, v. 248, n. 5443, p. 30–31, 1974. ISSN 00280836. 50

70 UNRUH, W. G. Notes on black-hole evaporation. *Physical Review D*, American Physical Society, v. 14, n. 4, p. 870–892, 1976. ISSN 05562821. 50

71 GIUDICE, G. F. et al. Production of massive fermions at preheating and leptogenesis. *Journal of High Energy Physics*, v. 1999, n. 08, p. 014–014, ago. 1999. ISSN 1029-8479. 50, 75

72 PELOSO, M.; SORBO, L. Preheating of massive fermions after inflation: Analytical results. *Journal of High Energy Physics*, v. 2000, n. 05, p. 016–016, maio 2000. ISSN 1029-8479. 50, 71, 75

73 MORADI, S. Creation of Scalar and Dirac Particles in Asymptotically Flat Robertson-Walker Spacetimes. *International Journal of Theoretical Physics*, Springer US, v. 47, n. 11, p. 2807–2818, 2008. ISSN 0020-7748. 50

74 WELDON, H. A. Fermions without vierbeins in curved space-time. *Physical Review D*, v. 63, n. 10, p. 104010, abr. 2001. 51

75 WILLMORE, T. J. The Definition of Lie Derivative. *Proceedings of the Edinburgh Mathematical Society*, v. 12, n. 01, p. 27, jun. 1960. ISSN 0013-0915, 1464-3839. 52

76 ARMINJON, M.; REIFLER, F. Equivalent Forms of Dirac Equations in Curved Space-times and Generalized de Broglie Relations. *Brazilian Journal of Physics*, v. 43, n. 1-2, p. 64–77, jan. 2013. ISSN 0103-9733. 54

77 BRILL, D. R.; WHEELER, J. A. Interaction of Neutrinos and Gravitational Fields. *Reviews of Modern Physics*, v. 29, n. 3, p. 465–479, jul. 1957. ISSN 0034-6861. 54

78 CHAPMAN, T. C.; LEITER, D. J. On the generally covariant Dirac equation. *American Journal of Physics*, v. 44, n. 9, p. 858–862, set. 1976. ISSN 0002-9505, 1943-2909. 54

79 PAL, P. B. Representation-independent manipulations with Dirac matrices and spinors. mar. 2007. 59

80 BIRRELL, N. D.; DAVIES, P. C. W. *Quantum Fields in Curved Space*. Reprint edition. Cambridge: Cambridge University Press, 1984. ISBN 978-0-521-27858-4. 62

81 LYTH, D. H.; RIOTTO, A. Particle physics models of inflation and the cosmological density perturbation. *Physics Reports*, v. 314, n. 1, p. 1–146, 1999. ISSN 0370-1573. 65

82 KOFMAN, L.; LINDE, A.; STAROBINSKY, A. A. Reheating after Inflation. *Phys. Rev. Lett.*, American Physical Society, v. 73, n. 24, p. 3195–3198, dez. 1994. 65

83 KOFMAN, L.; LINDE, A.; STAROBINSKY, A. A. Towards the theory of reheating after inflation. *Phys. Rev. D*, American Physical Society, v. 56, n. 6, p. 3258–3295, set. 1997. 65

84 AMIN, M. A. et al. Nonperturbative dynamics of reheating after inflation: A review. *International Journal of Modern Physics D*, v. 24, n. 01, p. 1530003, 2015. 65

85 ALLAHVERDI, R. et al. Reheating in Inflationary Cosmology: Theory and Applications. *Annual Review of Nuclear and Particle Science*, v. 60, n. 1, p. 27–51, 2010. 65

86 Acacio de Barros, J.; Pinto-Neto, N.; Sagioro-Leal, M. A. The causal interpretation of dust and radiation fluid non-singular quantum cosmologies. *Physics Letters A*, v. 241, p. 229–239, maio 1998. 66

87 ALVARENGA, F. G. et al. Quantum cosmological perfect fluid models. *Gen. Rel. Grav.*, v. 34, p. 651–663, 2002. 66

88 Pinto-Neto, N.; SANTINI, E. S.; FALCIANO, F. T. Quantization of Friedmann cosmological models with two fluids: Dust plus radiation. *Phys. Lett.*, A344, p. 131–143, 2005. 67

89 TRODDEN, M. Baryogenesis and leptogenesis. *eConf*, C040802, p. L018, 2004. 70

90 DREWES, M. et al. Testing the low scale seesaw and leptogenesis. *Journal of High Energy Physics*, v. 2017, n. 8, p. 18, ago. 2017. ISSN 1029-8479. 70

91 MOHAPATRA, R. N.; Senjanovi ć, G. Neutrino Mass and Spontaneous Parity Nonconservation. *Phys. Rev. Lett.*, American Physical Society, v. 44, n. 14, p. 912–915, abr. 1980. 70

92 DAVIDSON, S.; IBARRA, A. A lower bound on the right-handed neutrino mass from leptogenesis. *Physics Letters B*, v. 535, n. 1, p. 25–32, 2002. ISSN 0370-2693. 70

93 DODELSON, S.; WIDROW, L. M. Sterile neutrinos as dark matter. *Phys. Rev. Lett.*, American Physical Society, v. 72, n. 1, p. 17–20, jan. 1994. 71

94 BERTONE, G.; HOOPER, D.; SILK, J. Particle dark matter: Evidence, candidates and constraints. *Physics Reports*, v. 405, n. 5, p. 279–390, 2005. ISSN 0370-1573. 71

95 ARCADI, G. et al. The waning of the WIMP? A review of models, searches, and constraints. *The European Physical Journal C*, v. 78, n. 3, p. 203, mar. 2018. ISSN 1434-6052. 71

96 MERTENS, S. Direct Neutrino Mass Experiments. *J. Phys. Conf. Ser.*, v. 718, n. 2, p. 022013, 2016. 71

97 CANETTI, L.; DREWES, M.; SHAPOSHNIKOV, M. Matter and antimatter in the universe. *New Journal of Physics*, IOP Publishing, v. 14, n. 9, p. 095012, 2012. ISSN 1367-2630. 75

98 ANTUNES, V.; BEDIAGA, I.; NOVELLO, M. Gravitational mechanism for baryogenesis in the cosmological QCD phase transition. 2016. 75